

**STRUCTURAL ANALYSES AND ASSESSMENT
OF HISTORICAL ÇARDAK CARAVANSERAI IN
DENİZLİ**

**A Thesis Submitted to
the Graduate School of Engineering and Sciences of
İzmir Institute of Technology
in Partial Fulfillment of the Requirements for the Degree of**

MASTER OF SCIENCE

in Civil Engineering

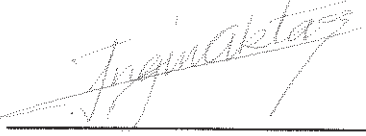
**by
Esra ŞAHİN**

July 2019

İZMİR

We approve the thesis of Esra ŞAHİN

Examining Committee Members:



Assoc. Prof. Dr. Engin AKTAŞ
Department of Civil Engineering, İzmir Institute of Technology

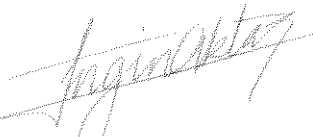


Assoc. Prof. Dr. İbrahim Serkan MISİR
Department of Civil Engineering, Dokuz Eylül University

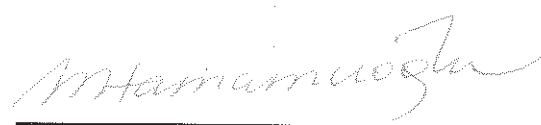


Assoc. Prof. Dr. Emre ERCAN
Department of Civil Engineering, Ege University

16/July/2019



Assoc. Prof. Dr. Engin AKTAŞ
Supervisor,
Department of Civil Engineering
İzmir Institute of Technology



Assoc. Prof. Dr. Mine TURAN
Co-Supervisor,
Department of Architectural Restoration
İzmir Institute of Technology



Prof. Dr. Şebnem ELÇİ
Head of the Department of Civil
Engineering

Prof. Dr. Aysun SOFUOĞLU
Dean of the Graduate School of
Engineering and Sciences

ACKNOWLEDGMENTS

I would like to express my deep appreciation, gratitude and thanks for my advisor Assoc. Prof. Dr. Engin AKTAŞ, Department of Civil Engineering, Izmir Institute of Technology and my co-advisor Assoc. Prof. Dr. Mine TURAN, Department of Architectural Restoration.

I would like to thank to Research Assistants Ertuğrul Türker UZUN and Kutay YÜCETÜRK from Department of Civil Engineering, Izmir Institute of Technology for their supports in modeling and analyses of the structure.

I would also like to thank to Istanbul Esenyurt University for their contributions to my thesis study.

Throughout my education, I would like to express my special thanks to my parents who have always supported me with their financial and moral support.

ABSTRACT

STRUCTURAL ANALYSES AND ASSESSMENT OF HISTORICAL ÇARDAK CARAVANSERAI IN DENİZLİ

The assessment of historical masonry structures are significant in terms of transferring our cultural heritage to future generations. The conservation of these masonry structures is possible through investigating problems and their causes with tools such as structural modeling and analyses. In this study, the structural modeling and analyses of a historical masonry structure was aimed. Çardak caravanserai in Denizli was chosen as the case study since it has preserved its authenticity and integrity.

In this scope, the software used for modeling and structural analyses was SAP2000 v20.2 commercial finite element software. For modeling, frame elements were used in the columns and shell elements were used in the other structural elements. Self-weight analysis, modal analysis and response spectrum analysis were conducted in terms of the assessment. The self-weight analysis was made under dead load. The analysis indicated the current state of the structure. In modal analysis, free vibration periods, mode shapes and mass participation ratios of the structure were determined. In response spectrum analysis, according to Turkish Siesmic Design Code 2018, mode integration method was used as linear calculation method. In this analysis, the khan was evaluated under the dead load and earthquake loads in the x and y directions. The structural elements that exceed the compressive, tensile and shear strength were identified as hot spots and recommendations on the further investigations on these critical points of the structure were presented.

ÖZET

DENİZLİ'DE BULUNAN TARİHİ ÇARDAK KERVANSARAYININ YAPI ANALİZİ VE DEĞERLENDİRİLMESİ

Tarihi yığma yapıların değerlendirilmesi kültürel mirasımızın gelecek nesillere aktarılması açısından önem taşır. Bu yığma yapıların korunması ise yapıda mevcut problemlerin ve sebeplerinin yapısal modelleme ve analizler gibi araçlarla irdelenmesi ile mümkün olmaktadır. Bu çalışmada, bir tarihi yığma yapının modellenmesi ve analizleri hedeflenmiştir. Özgünlüğünü ve bütünselliğini korumuş olan; Denizli'de bulunan, Çardak kervansarayı örnek yapı olarak seçilmiştir.

Bu kapsamda, modelleme ve yapısal analizler için kullanılan yazılım SAP2000 v20.2 ticari sonlu elemanlar analiz ve tasarım yazılımıdır. Modelleme için kolonlarda çubuk elemanlar, diğer yapı elemanlarında ise kabuk elemanlar kullanılmıştır. Değerlendirme için kendi ağırlığı altında analiz, modal analiz ve davranış spektrumu analizi yapılmıştır. Kendi ağırlığı altında analiz ölü yük altında yapılmıştır. Bu analiz yapının mevcut durumunu göstermiştir. Modal analizde, yapının serbest titreşim periyotları, mod şekilleri ve kütle katılım oranları belirlenmiştir. Davranış spektrumu analizinde, Deprem Yönetmeliği 2018'e göre, doğrusal hesaplama yöntemi olarak mod birleştirme yöntemi kullanılmıştır. Çardak han ölü yük ve x ve y yönündeki deprem yükleri altında değerlendirilmiştir. Basınç, çekme ve kayma gerilmelerini aşan yapı elemanları bölgeleri kritik noktalar olarak gösterilmiştir ve bu noktalar ile ilgili daha detaylı irdeleme yapabilmek için öneriler sunulmuştur.

TABLE OF CONTENTS

AKNOWLEDGMENTS.....	iii
ABSTRACT	iv
ÖZET	v
TABLE OF CONTENTS	vi
LIST OF FIGURES	viii
LIST OF TABLES.....	xvi
CHAPTER 1. INTRODUCTION.....	1
1.1. Aim and Method.....	3
1.2. Content.....	4
CHAPTER 2. THEORETICAL FRAMEWORK	5
2.1. Masonry as Structure	5
2.2. Material Characteristics of Masonry Structures	6
2.3. Masonry Structures In Terms of Mechanical Behaviour.....	7
2.3.1. Compressive Strength of Masonry	8
2.3.2. Tensile Strength of Masonry	8
2.3.3. Shear Strength of Masonry	9
2.4. Condition Assessment	9
2.4.1. Destructive Test Methods.....	9
2.4.2. Non-Destructive Test Methods.....	9
2.4.3. In-Situ Test Methods	10
2.5. Finite Element Method for Masonry Walls.....	11
2.5.1. Micro Modeling.....	12
2.5.2. Macro Modeling	12
2.5.3. Meso Modeling.....	18
CHAPTER 3. DESCRIPTION OF ÇARDAK KHAN.....	19
3.1. Location	19
3.2. Mass and Facade Characteristics	21
3.3. Spatial Characteristics	22
3.3.1. Courtyard	22
3.3.2. Shelter	23
3.4. Structural Elements.....	24

3.4.1. Superstructural Elements	25
3.4.2. Walls and Buttresses	28
3.4.3. Floor and Staircase	31
3.4.4. Foundations	33
3.5. Architectural Elements	34
3.5.1. Portal.....	34
3.5.2. Pilasters and Ornamentation.....	36
3.5.3. Water Spouts.....	37
3.6. Current Structural Condition	37
CHAPTER 4. HISTORICAL RESEARCH	40
4.1. Historic Developments	40
4.2. Caravanserai as a Building Type	40
4.2.1. Terminology	40
4.2.2. Positioning	41
4.2.3. Function	42
4.2.4. Architectural Characteristics	42
4.2.5. Structural Characteristics.....	42
4.2.6. Typology.....	44
4.3. Historic Evaluation of Çardak Caravanserai	45
4.3.1. Inscription Panel of Çardak Khan.....	47
4.3.2. Donor	48
4.3.3. Documentary Value	49
CHAPTER 5. MODELING AND ANALYSES OF ÇARDAK CARAVANSERAI....	52
5.1. Modeling of Çardak Caravanserai with SAP2000.....	52
5.2. Determination of The Material Properties of The Structure.....	56
5.3. Load Cases.....	58
5.4. The Assessment and Results of Structural Analyses	60
5.4.1. Self-Weight Analysis.....	60
5.4.2. Modal Analysis.....	68
5.4.3. Response Spectrum Analysis.....	73
5.4.3.1. Results of Response Spectrum Analysis.. ..	76
CHAPTER 6. CONCLUSIONS AND RECOMMENDATIONS.....	96
REFERENCES	98

LIST OF FIGURES

<u>Figure</u>	<u>Page</u>
Figure 2.1. Mortar joint between the compressed earth blocks and bond.	6
Figure 2.2. Compressive test and stress-strain curve of the brick	7
Figure 2.3. Finite element method	12
Figure 2.4. Modeling technique for masonry structure.....	12
Figure 2.5. Micro modeling	12
Figure 2.6. Masonry failure mechanisms (a) joint tensile cracking; (b) joint slipping; (c) unit direct tensile cracking; (d) unit diagonal tensile cracking; (e) masonry crushing	16
Figure 2.7. Suggested modeling strategy. Units (u), which are expanded in both directions by the mortar thickness, are modeled with continuum elements. Mortar joints (m) and potential cracks in the units are modeled with zero-thickness interface elements	17
Figure 2.8. Masonry sample and macro modeling.....	17
Figure 2.9. The Hoffman type and experimental results	17
Figure 2.10. A Hill type yield surface and Rankine type yield surface	17
Figure 2.11. The Hill type yield surface	17
Figure 2.12. The Rankine type yield surface	17
Figure 2.13. Meso modeling or simplified micro modeling	18
Figure 3.1. Çardak caravanserai in Denizli as viewed from the east.....	19
Figure 3.2. Location of Çardak Khan	20
Figure 3.3. Seljuk caravanserais and caravan roads in Anatolia.....	20
Figure 3.4. Çardak caravanserai and its environs, site plan.....	21
Figure 3.5. Ground floor plan, restitution	22
Figure 3.6. The Ground floor plan	23
Figure 3.7. The central gallery as viewed from the east.	24
Figure 3.8. The northern gallery of the caravanserai as viewed from the west.	25
Figure 3.9. Roof plan of the caravanserai, restitution.....	26
Figure 3.10. Vault and arch profile types, reflected ceiling plan	26
Figure 3.11. Vault and arch profile types	27
Figure 3.12. The stairs leading to the terrace roof	28

<u>Figure</u>	<u>Page</u>
Figure 3.13. Wall types	29
Figure 3.14. The caravanserai as viewed from its southeast.....	30
Figure 3.15. The interior walls of the service spaces at the north.	31
Figure 3.16. Stair detail.....	32
Figure 3.17. The staircase at the southeast corner of the shelter.	32
Figure 3.18. The foundations under the interior walls.....	33
Figure 3.19. Foundation detail	33
Figure 3.20. The portal of the shelter.....	34
Figure 3.21. The eastern elevation of the shelter	35
Figure 3.22. The east (entrance) elevation of the portal	35
Figure 3.23. The interior view of the portal of the shelter	36
Figure 3.24. Geometric ornamentation of the entrance portal (left), the bullhead pattern at the central gallery (right).....	36
Figure 3.25. The water spout at the north (left) and waterspout detail (right).....	37
Figure 3.26. Detail of wall connection from southeast.....	37
Figure 3.27. Condition classes illustrated on the ground floor plan	39
Figure 4.1. Kırkgöz khan, base plan	43
Figure 4.2. Aksaray Sultan khan (left), Alara khan (right), reconstruction plans.....	45
Figure 4.3. Çardak castle and Maymun mountain as viewed from Han-abad.....	46
Figure 4.4. The inscription panel of Çardak caravanserai	477
Figure 4.5. The leon figures and the inscription panel of Çardak khan.....	48
Figure 5.1. View of columns and external walls of the model	54
Figure 5.2. View of the model without external walls and roof	54
Figure 5.3. View of the model without roof	55
Figure 5.4. Front view of shell model of Çardak caravanserai	55
Figure 5.5. Back view of shell model of Çardak caravanserai	56
Figure 5.6. Determination of load distributed over the area	59
Figure 5.7. Normal and shear stresses on shell element	60
Figure 5.8. The displacement of Çardak khan in Z direction under self-weight (mm) ..	61
Figure 5.9. The displacement of Çardak khan in Y direction under self-weight (mm)..	61
Figure 5.10. Normal stresses S11 developed under self-weight (10^{-3} MPa)	62

<u>Figure</u>	<u>Page</u>
Figure 5.11. Back side of normal stresses S11 developed under self-weight(10^{-3} MPa)	62
Figure 5.12. View of arches, columns and interior walls of normal stresses, S11 developed under self-weight (10^{-3} MPa).....	63
Figure 5.13. Detail of arches on xz plane at y = +5 m axis for normal stresses, S11 under self-weight.....	63
Figure 5.14. Detail of arches and vaults on yz plane at x = +5 m axis for normal stresses, S11 under self-weight	64
Figure 5.15. Detail of arches on xz plane at y = +2.5 m axis for normal stresses, S22 under self-weight	64
Figure 5.16. Detail of arches and vaults on yz plane at x = +2.5 m axis for normal stresses, S22 under self-weight	64
Figure 5.17. Normal stresses S22 developed under self-weight (10^{-3} MPa)	65
Figure 5.18. Back side of normal stresses S22 developed under self-weight(10^{-3} MPa)	65
Figure 5.19. View of arches, columns and interior walls of normal stresses S22 developed under self-weight (10^{-3} MPa).....	66
Figure 5.20. Shear stresses S12 developed under self-weight (10^{-3} MPa).....	66
Figure 5.21. Back side of shear stresses S12 developed under self-weight (10^{-3} MPa) .	67
Figure 5.22. View of arches, columns and interior walls of shear stresses S12 developed under self-weight (10^{-3} MPa).....	67
Figure 5.23. Detail of arches on xz plane at y = +2.5 m axis for shear stresses, S12 under self-weight.....	68
Figure 5.24. Detail of arches and vaults on yz plane at x = +2.5 m axis for shear stresses, S12 under self-weight	68
Figure 5.25. Deformed shape of 1. dominant mode (T = 0.199 sec.).....	70
Figure 5.26. Deformed shape of 2. dominant mode (T = 0.171 sec.).....	70
Figure 5.27. Deformed shape of 3. mode (T = 0.159 sec.).....	70
Figure 5.28. Deformed shape of 4. mode (T = 0.146 sec.).....	71
Figure 5.29. Deformed shape of 5. mode (T = 0.137 sec.).....	71
Figure 5.30. Deformed shape of 6. mode (T = 0.134 sec.).....	71
Figure 5.31. Deformed shape of 7. mode (T = 0.132 sec.).....	72
Figure 5.32. Deformed shape of 8. mode (T = 0.129 sec.).....	72
Figure 5.33. Deformed shape of 9. mode (T = 0.125 sec.).....	72

<u>Figure</u>	<u>Page</u>
Figure 5.34. Deformed shape of 10. mode (T = 0.124 sec.)	73
Figure 5.35. Horizontal elastic design spectrum.....	74
Figure 5.36. The seismic load pattern in x and y direction.....	75
Figure 5.37. Response spectrum function	75
Figure 5.38. The vertical displacement in Z direction under Dead+Ex+0.3Ey load combination	76
Figure 5.39. The vertical displacement of back side in Z direction on yz plane at x = +15 m axis under Dead+Ex+0.3Ey load combination.....	77
Figure 5.40. The vertical displacement of arches in Z direction on xz plane at y = +2.5 m axis under Dead+Ex+0.3Ey load combination	77
Figure 5.41. The vertical displacement of section in Z direction on yz plane at x = +2.5 m axis under Dead+Ex+0.3Ey load combination	77
Figure 5.42. The displacement in X direction under Dead+Ex+0.3Ey load combination.....	78
Figure 5.43. The displacement of back side in X direction of the section on yz plane at x = +15 m axis under Dead+Ex+0.3Ey load combination	78
Figure 5.44. The displacement of arches in X direction on xz plane at y = +2.5 m axis under Dead+Ex+0.3Ey load combination	79
Figure 5.45. The displacement of section in X direction on yz plane at x = +2.5 m axis under Dead+Ex+0.3Ey load combination	79
Figure 5.46. Normal stresses S11 due to spectral excitation under Dead+Ex+0.3Ey load combination (MPa)	80
Figure 5.47. Normal stresses S11 except vaults due to spectral excitation under Dead+Ex+0.3Ey load combination (MPa).....	80
Figure 5.48. Normal stresses S11 of back side on yz plane at x = +15 m axis under Dead+Ex+0.3Ey load combination	81
Figure 5.49. Normal stresses S11 of arches on xz plane at y = +2.5 m axis under Dead+Ex+0.3Ey load combination	81
Figure 5.50. Normal stresses S11 of section on yz plane at x = +2.5 m axis under Dead+Ex+0.3Ey load combination	81
Figure 5.51. Normal stresses S22 under Dead+Ex+0.3Ey load combination (10^{-3} MPa).....	82

Figure

Page

Figure 5.52. Normal stresses S22 except vaults under Dead+Ex+0.3Ey load combination (10⁻³ MPa) 82

Figure 5.53. Normal stresses S22 of back side on yz plane at x = +15 m axis under Dead+Ex+0.3Ey load combination 83

Figure 5.54. Normal stresses S22 of arches on xz plane at y = +2.5 m axis under Dead+Ex+0.3Ey load combination 83

Figure 5.55. Normal stresses S22 of section on yz plane at x = +2.5 m axis under Dead+Ex+0.3Ey load combination 83

Figure 5.56. Shear stresses S12 under Dead+Ex+0.3Ey load combination (10⁻³ MPa) 84

Figure 5.57. Shear stresses S12 except vaults under Dead+Ex+0.3Ey load combination (10⁻³ MPa) 84

Figure 5.58. Shear stresses S12 of back side on yz plane at x = +15 m axis under Dead+Ex+0.3Ey load combination 85

Figure 5.59. Shear stresses S12 of arches on xz plane at y = +2.5 m axis under Dead+Ex+0.3Ey load combination 85

Figure 5.60. Shear stresses S12 of section on yz plane at x = +2.5 m axis under Dead+Ex+0.3Ey load combination 85

Figure 5.61. The vertical displacement in Z direction under Dead+Ey+0.3Ex load combination 86

Figure 5.62. The vertical displacement in Z direction of back side on yz plane under Dead+Ey+0.3Ex load combination 86

Figure 5.63. The vertical displacement in Z direction of arches on xz plane at y = +2.5 m axis Dead+Ey+0.3Ex load combination 87

Figure 5.64. The vertical displacement in Z direction of section on yz plane at x = +2.5 m Plane axis under Dead+Ey+0.3Ex load combination 87

Figure 5.65. The displacement in Y direction under Dead+Ey+0.3Ex load combination 88

Figure 5.66. The displacement of back side in Y direction on yz plane under Dead+Ey+0.3Ex load combination 88

Figure 5.67. The displacement of arches in Y direction on xz plane at y = +2.5 m axis under Dead+Ey+0.3Ex load combination 89

<u>Figure</u>	<u>Page</u>
Figure 5.68. The displacement in Y direction of the section on yz plane at x = +2.5 m axis Dead+Ey+0.3Ex load combination	89
Figure 5.69. Normal stresses S11 under Dead+Ey+0.3Ex load combination (10 ⁻³ MPa).....	90
Figure 5.70. Normal stresses S11 except vaults under Dead+Ey+0.3Ex load combination (10 ⁻³ MPa)	90
Figure 5.71. Normal stresses, S11 of back side on yz plane under Dead+Ey+0.3Ex load combination.....	91
Figure 5.72. Normal stresses, S11 of arches on xz plane at y = +5 m under Dead+Ey+0.3Ex load combination	91
Figure 5.73. Normal stresses, S11 of section on yz plane at x = +5 m axis under Dead+Ey+0.3Ex load combination	91
Figure 5.74. Normal stresses, S22 under Dead+Ey+0.3Ex load combination (MPa)	92
Figure 5.75. Normal stresses, S22 except vaults under Dead+Ey+0.3Ex load combination (MPa).....	92
Figure 5.76. Normal stresses S22 of back side on yz plane under Dead+Ey+0.3Ex load combination.....	93
Figure 5.77. Normal stresses, S22 of main exterior wall on xz plane at y = +12.5 m axis under Dead+Ey+0.3Ex load combination	93
Figure 5.78. Normal stresses, S22 of section on yz plane at x = +5 m axis under Dead+Ey+0.3Ex load combination	93
Figure 5.79. Shear stresses, S12 under Dead+Ey+0.3Ex load combination (10 ⁻³ MPa)	94
Figure 5.80. Shear stresses, S12 except vaults under Dead+Ey+0.3Ex load combination (10 ⁻³ MPa)	94
Figure 5.81. Shear stresses, S12 of back side on yz plane under Dead+Ey+0.3Ex load combination.....	95
Figure 5.82. Shear stresses, S12 of arches on xz plane at y = +5 m axis under Dead+Ey+0.3Ex load combination	95
Figure 5.83. Shear stresses, S12 of section on yz plane at x = +5 m axis under Dead+Ey+0.3Ex load combination	95

LIST OF TABLES

<u>Table</u>	<u>Page</u>
Table 5.1. Mechanical characteristics of masonry wall materials	57
Table 5.2. Strength values for stone masonry	58
Table 5.3. Load Combinations	59
Table 5.4. The periods and mass participation ratios for the first ten modes	69

CHAPTER 1

INTRODUCTION

Masonry construction technique is among the oldest building techniques of the world. Some of the world's most significant masonry structures are the Egyptian Pyramids, the Colosseum in Rome, India's Taj Mahal and the Great Wall of China (O'Sullivan, 2016). The use of masonry has two reasons. Firstly, the material of masonry such as brick and stone can be found easily. Secondly, manpower is supported by gravity, while constructing a masonry structure (Şen, 2006: 1). The main components of historical masonry structures are walls, domes, vaults, arches, and pillars. The secondary components can be classified as buttresses, ties, floors and stairs (Gedik, 2008: 3).

The compressive strength of a masonry structure is high, but it has low tensile strength. This case indicates that masonry structures are very vulnerable under tensile stresses.

The analysis and modeling of the historical masonry structures require tough and profound investigations. Because the general behavior of such structures depends on a great number of factors such as the behavior of singular walls, soil properties, rigidity and material properties (Calderoni, Ghersi et al., 1994: 227). These factors vary in the structures. However, these difficulties are eliminated by three dimensional modeling of masonry structures. Micro, macro and meso modeling methods are widely used as modeling techniques. Macro modeling is preferred since it is easier to think of composite material by homogenizing the masonry building elements (Kocaman, Kazaz et al., 2008: 42).

In the literature, many studies on modeling and analyses of historical masonry structures are available. Few of those studies have been mentioned below.

Teomete (2004). In the master's thesis called "Finite Element Modeling of Historical Masonry Structures; Case Study: Urla Kamanlı Mosque", the modeling of historical masonry structures was investigated by using the finite element method. The linear and non-linear analyses of the structure were conducted by the use of LUSAS software. As a result of the analyses, it was asserted that there are cracks on the east and west walls of the structure.

Kuruşcu (2005). In the master's thesis called "The Analysis of Masonry Structures", the modeling techniques for masonry structures were presented by being surveyed the problems in numerical analysis. Also, the parametric study was conducted by being developed the isotropic damage model of masonry structures. The study was compared with numerical analysis method.

Şen (2006). In the master's thesis called "Modeling and Analysis of The Historical Masonry Structures", The three dimensional finite element model and linear elastic analysis of the structure were carried out using the program SAP2000. Consequently, it was determined that the structure is not at risk in terms of seismic action. However, the dome is critical because of the formed crack locations.

Betti and Vignoli (2007). In the study called "Modeling and Analysis of a Romanesque Church under Earthquake Loading: Assessment of Seismic Resistance", the three dimensional finite element model, linear and non-linear static and dynamic analyses of the church were conducted using the computer program ANSYS. Consequently, the stresses and the strains of the structure were compared. It was determined that the church is at risk due to the cracks in the walls. Also, the techniques for repairing and strengthening were presented so as to evaluate the seismic cases.

Roca, Cervera et al. (2010). In the study called "Structural Analysis of Masonry Historical Constructions, Classical and Advanced Approaches", the plastic analysis, limit analysis, elastic linear analysis, simplified modeling, finite element method based on macro modeling, discontinuous models and micro modeling, non-linear finite element method and discrete element method were investigated in order to evaluate the different approaches.

Özdemir (2018). In the master's thesis called "Computer Aided Analysis of Historic Structures; Example of Patara Antique City Theater Stage Structure", The structural modeling and analyses were performed using the program SAP2000. Macro modeling was preferred as the modeling technique. As a result of the analysis, the weaknesses of the building were determined and some precautions were proposed. Also, the comments were made about the earthquake behavior of the structure.

In this thesis, a masonry structure, *Çardak* Caravanserai in Denizli, dated to the 13th century has been investigated. The caravanserai was constructed in 1230 by the Seljuk regent *Esedüddin Ayaz bin Abdullah Eş-Şihabi* (the inscription panel as cited in Uzunçarşılı 1929; Bakırer 1996; Pektaş 2007) during *Alaeddin Keykubad* period. *Çardak*

Khan is now located in the town of Çardak which is 55 km to the east of Denizli. It is also known as *Han-abad*.

1.1. Aim and Method

The purpose of the study is to analyze structural characteristics and behavior of Çardak Khan and form an understanding of issues and challenges on the structure's integrity that could serve later as a guide in proposing structural intervention strategies. A historical research on the caravanserai building type, archive research on the caravanserai itself, comparative study with similar structures of its period, and literature research on behavior of masonry structures are conducted to have a solid understanding before proceeding with the analysis. This study does not involve with material characterization on the constituents of the materials used in the structure, but rather using the information in the literature some assumptions are made on the properties of the materials used. SAP2000 commercial software is chosen as the tool for structural analysis. A finite element model is generated in SAP2000 software to perform linear elastic static and modal analysis. Behavior of the structure under self weight and response of the structure to seismic demand is investigated using response spectrum analysis. The locations which are challenged most under the defined loading conditions using the structural model are evaluated. The current condition and issues observed at the site of caravanserai has been evaluated with perspective of structural analysis.

In summary, this study would serve as a basis in determining the structural deficiencies and proposing reasonable intervention approaches. The most important aspects of the study are architectural and structural methods. In terms of architecture, the facade and spatial characteristics, architectural and structural elements and current structural conditions were examined. However, structural methods are needed to determine the elements of the caravanserai that are under risk. Therefore, the three dimensional finite element model was created. Macro modeling was preferred as modeling technique in order to make the masonry structure simpler. Self-weight, modal and response spectrum analyses were conducted to conclude the risk condition of the structure. According to the results of the analysis, some suggestions were made in conservation of the structure.

1.2. Content

Firstly, the study of literature, aim, method and content are presented. The previous studies on historical masonry structures are briefly mentioned. In the second chapter, definition of masonry structures, their material characteristics, mechanical behavior and assessment techniques, finite element method on masonry walls, macro, micro and meso modeling are explained. The advantages and disadvantages of masonry structures, the durability of the material, the compressive, tensile and shear strength of masonry structures and the basic test methods for detecting the current condition of the structures are elucidated. Furthermore, finite element method and modeling approaches are presented depending on the literature. In the third chapter, the case study monument, Çardak Khan, is described. Its location, mass and facade characteristics, spatial characteristics, architectural and structural characteristics and current structural condition are explained. Superstructures, walls, buttresses, floor, staircase and foundations known as structural characteristics and portal, ornamentations and water spouts known as architectural characteristics are described with the restitution plans and profile types. According to the current structural condition, structural failures such as collapse and material deterioration are mostly observed on the courtyard of the caravanserai. Fourthly, historical research on the building itself and on the building type, typology and function of the khan are presented. Also, according to the architectural and structural characteristics, the importance of the caravanserai among the others and its documentary value are specified. In the fifth chapter, the modeling process and structural analysis of Çardak caravanserai are presented. Modeling technique, frame and shell elements used in the structure are described in detail. Material properties are taken from literature. Load cases and combinations are formed. Structural elements under risk are determined with the help of static and dynamic analyses. Finally, results are discussed and conclusive remarks and recommendations are formed.

CHAPTER 2

THEORETICAL FRAMEWORK

Masonry structures are structures that consists of load bearing system which are made out of brick, stone or tile or a combination of these materials. Masonry construction is one of the oldest building methods. In this chapter, the definition of masonry structures, characteristics of their material, their mechanical behaviour and techniques used for their condition assessment are presented.

2.1. Masonry as Structure

Masonry construction technique is an old technique which is still in use. It is seen in historic mosques, churches, synagogues, madrasahs, tombs, khans, and caravanserais of Anatolia.

The most significant feature of masonry construction is its simplicity. Others are the durability, solidity, versatility, sound absorption and aesthetics (Lourenco, 1996: 1).

There are advantages and disadvantages of the masonry structures.

Advantages of masonry structures are listed below:

- Utilization of masonry material can increase the thermal mass of a building.
- Masonry structures are heat resistant, therefore, they provide good fire protection.
- Masonry structures have a practical life more than five hundred years as compared to thirty to one hundred years for structures of steel or reinforced concrete.

Disadvantages of masonry structures are listed below:

- Extreme weather causes degradation of masonry wall surfaces because of frost damage.
- Masonry must be constructed on a strong foundation to avoid settlement and cracking (Hendry, Sinha et al., 2004: 1).

2.2. Material Characteristics of Masonry Structures

Masonry structures include mortar and units such as bricks, blocks, adobes, ashlar and irregular stones (Lourenco, 2002: 301). Mortar is a material used in masonry construction to fill the gaps between the bricks and blocks and bonds units together to present a collective behavior of the elements of the masonry structure member (Figure 2.1). The main purpose of the use of mortar is to link structural units with each other. Also, the mortar helps to distribute the loads on the structural elements and it protects the structure against external influences (Satongar, 1994: 22). The mortar emerged with the use of brick and adobe as construction material. In Romans period, lime mortar came into use for the first time. In Seljuk and Ottoman architecture, khorasan mortar was used (Saraç, 2003: 36).

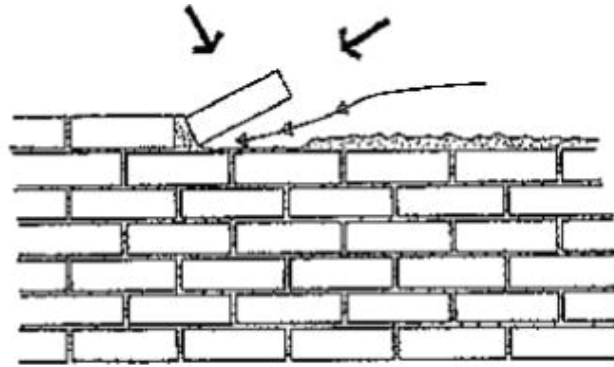


Figure 2.1. Mortar joint between the compressed earth blocks and bond

(Source: Guillaud et al., 1985: 22)

Brick is construction material obtained by boiling clay at high temperature. It is known that the brick was used before the Roman period (Yılmaz, 2006: 17). The modulus of elasticity and the tensile strength of the brick are low. Also, it is widely used because of its cheapness and ease of construction. The compressive test and stress-strain curve of the brick are given below (Figure 2.2).

Stone called mass rock has widespread use in building construction since ancient times. It is used as rubble, rough, fine or cut stone (VGM, 2006: 53). The compressive strength of the stone is high and its tensile strength is low. So, it is used without tensile stress on arch, vault, dome and columns (Dabanlı, 2008: 24). One of the most important properties that control the durability of the stone is that it has hollow and impermeable material (Dabanlı, 2008: 26).

Wood is a material, which is found extensively in nature despite of the fact that it has short lived (Gedik, 2008: 5). Compressive, tensile and bending strength of the wood are high. Accordingly, it was used as slab and tie elements in historical masonry structures, residential structures and architectural details (Yılmaz, 2006: 18).

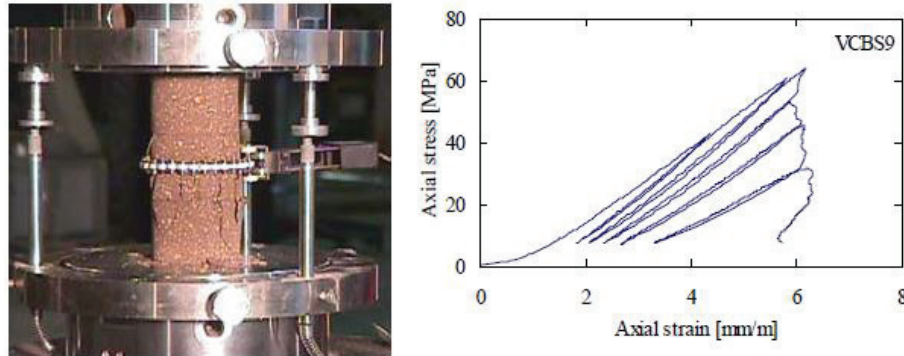


Figure 2.2. Compressive test and stress-strain curve of the brick

(Source: Dabanlı, 2008: 24)

The characteristics which have an impact on the load bearing capacity of masonry are compressive strength, tensile strength, shear strength, durability, thermal expansion, water absorption coefficient and the mortar (Ünay, 2002: 6).

Since the masonry is anisotropic, brittle and non-homogeneous, a rather complex behavior expected from masonry structures. Except for this, masonry construction is so strong in terms of compression, whereas poor in terms of tension (Gedik, 2008: 3). There are three different failure modes, nominally; tensile cracking, shear failure and compressive crushing.

2.3. Masonry Structures in terms of Mechanical Behaviour

The essential requirement of structural elements is their sufficient strength and stiffness. Material properties determine the limit of stress that the material can resist and consists the stress rating which can be applied prior to deformation. The strength and stiffness for several material change according to the condition of loading. Stresses comprise of compressive, tensile and shear stress inside element in many aspects. Generally, deformations do not increase on an steady rate. Therefore, the stress and stiffness in masonry structure elements change according to deformation ratio.

2.3.1. Compressive Strength of Masonry

Masonry structure elements are considered as a composite material. The factors affecting compressive strength of masonry structure elements are geometry, type, shape, strength and water absorption capacity of unit element; mixing ratio of mortar, moisture content and deformation manner.

Masonry structure elements are usually under the thumb of compressive stress due to the structural forms. Compressive strength is determined by testing the results of unit element (Saygılı, 2014: 3). Mortar indicates softer than brick and stone and it expands laterally more than the others, because these materials are different elastic characteristics (Gedik, 2008: 8). However, compressive strength of the unit elements such as bricks are very close to the compressive strength of the unit element. The more rigid and massive irregular elements in which the stone is generally used as the unit element. The compressive strength of the masonry structural element is more effective than the type and thickness of the mortar connecting the unit elements and the compressive strength of the unit element reduces the effect of the element on overall resistance (Ünay, 2002).

2.3.2. Tensile Strength of Masonry

Masonry structure element is a considerably brittle material and it usually carries a high risk of abrupt tensile fractures. Especially, tensile stresses are more likely to occur on bending elements such as dome, arch, vault and pendant in historical masonry structures (Gedik, 2008: 9). Diagonal tensile stresses occur due to shear stresses in elements such as walls and columns. Due to moisture and heat changes, deformations such as elongation and shortening also cause significant tensile stresses.

Considering the more practical use of the masonry structural elements, the tensile stresses due to bending are more important than the axial tensile stresses. Because in historical buildings, the elements that are directly affected by axial tensile stresses are rarely encountered. The researches revealed that tensile strength due to bending in the elements of the masonry building was directly related to the moisture content of the unit element, the density of the mortar and the unit element surface texture. As the thickness of the mortar provides more strength, the tensile strength of the material increases (Ünay, 2002).

2.3.3. Shear Strength of Masonry

The shear stress of the masonry structural elements depends on the connection between the mortar and the unit element (Gedik, 2008: 10). Although the mechanism between the unit element and the mortar is not fully understood, it is affected by the physical and chemical properties of the mortar and stone and mortar. In addition to compressive and tensile fractures, the structural elements are often in danger of shear fractures (Ünay, 2002).

2.4. Condition Assessment

It is known that historical masonry structures are heterogeneous materials that are comprised of units and joints. Analysis of the structures must be realised in relation with the material properties. However, historical structures are unrenovable sources, so their testing methods should be decided very carefully. There are three basic approaches for determining the current condition of the structures;

- Destructive Test Methods
- Non-Destructive Test Methods
- In-Situ Test Methods

2.4.1. Destructive Test Methods

Destructive test methods are characterised by taking a sample in the laboratory. The samples should be taken out the lowest possible damage. In addition, number of the samples should be as little as possible (Gedik, 2008: 11). The aims of the test are to determine the chemical, physical and mechanical properties of the historical masonry structures and to find its decay and the durability (Şen, 2006).

2.4.2. Non Destructive Test Methods

Non destructive test methods do not directly find the properties such as strength and stiffness. Thus, there is rarely relationship between the non-destructive test methods

and physical characteristics of the masonry (Şen, 2006: 7). Infrared thermography, tomographic imaging, ultrasonic velocity testing and sonic velocity testing, surface penetrating radar, rebound hammer, metal location, stress wave transmission and impact-eco are the non-destructive test methods which are applied to masonry constructions (Şen, 2006: 8).

Infrared Thermography Testing: Infrared thermography testing is applied to find the voids, cracks and wet location. This testing method affects in wide range where components are moving, difficult to survey or damaged to contact (Usamentiaga, Veregas et al., 2014: 12320).

Tomographic Imaging: It is used to determine the internal properties such as voids, cracks and deteriorations by the ultrasonic stress wave velocity measurements (Saygılı, 2014: 13).

Ultrasonic Velocity Testing and Sonic Velocity Testing: These testing methods allow void locations and masonry damages to determine (Şen, 2006: 8).

Surface Penetrating Radar Testing: In this testing method, the internal deterioration in walls, voids locations with high salt content and moisture content are examined by using the wave energy (Şen, 2006: 8).

Rebound Hammer: This technique determines the variations in masonry structures and compressive strength of masonry (Saygılı, 2014: 12).

Metal Location: It has been used to locate metal elements embedded in masonry structures (Şen, 2006: 7).

Stress Wave Transmission: Hazards in masonry structures and voids are determined by the stress wave transmission (Şen, 2006: 7).

Impact-Eco: This technique, which is used to identify the variations in masonry structures by the wave echoes, is conducted to find the depth of the different cracks and to characterize the morphology on rubble stone (Saygılı, 2014: 12).

2.4.3. In-Situ Test Methods

In-situ test methods which is known as in-place test methods are utilized instead of destructive test methods. They give information on the engineering properties which are not directly used of the non-destructive test methods. The test may give reasonable conclusions for condition assessment. In addition, flatjack methods, dynamics

monitoring, pull-out test, thermography test and sonic tests are stated as the in-situ test methods (Teomete, 2004: 5-7).

Flatjack Methods: This test method includes the determination of the magnitude of vertical compressive stress, masonry stress exposed to compression and the measurement of in-situ compression response (Şen, 2006: 9). In this method, determining the stress level and the modulus of elasticity of masonry structures may be purposed (Crocì, 1998: 71).

Dynamics Monitoring: This testing method detects the natural vibrations on the structures, mode shapes and modal frequencies of the building and mechanical behavior of masonry walls (Binda et al., 2000: 208).

Put-out Test: This approach uncovers the tensile and shear strength of structural elements (Teomete, 2004: 6).

Thermography Test: Using the thermography test method, the asset of different materials, the cavities, moisture, the presence of water and heating system are explored (Binda et al., 2000: 214).

Sonic Tests: The voids and cracks in structural elements, the injection technique on the wall and its morphology can be obtained by the use of sonic tests (Binda et al., 2000: 215).

2.5. Finite Element Method on Masonry Walls

The finite element method (FEM) is a numerical technique for engineering problems. These engineering problems include deformation and stress analyses of aircraft, automotive, building and bridge structures, fluid flow, seepage, field analysis of heat flux and so on (Teomete, 2004: 17). Most of these processes are expressed by using partial differential equations. Finite element method cuts a structure into several elements. Then reconnects elements at “nodes” as if nodes were pins or drops of glue that hold elements together (Figure 2.3). This process results in a set of simultaneous algebraic equations. Detailed information on finite element method is available in Chandrupatla and Belegundu (1991), Zienkiewicz and Taylor (1987), and Bathe (1982). There are three different approaches in masonry structures: micro modeling, macro modeling and meso modeling as shown in Figure 2.4 (Lourenco, 2002: 301-319).

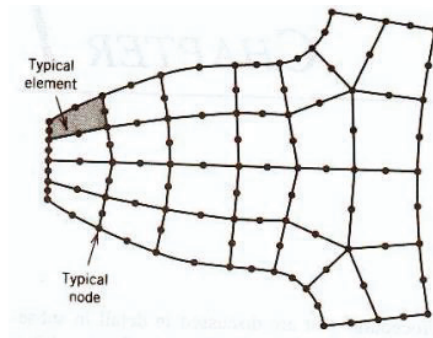


Figure 2.3. Finite element method

(Source: Weck and Kim, 2004: 6)

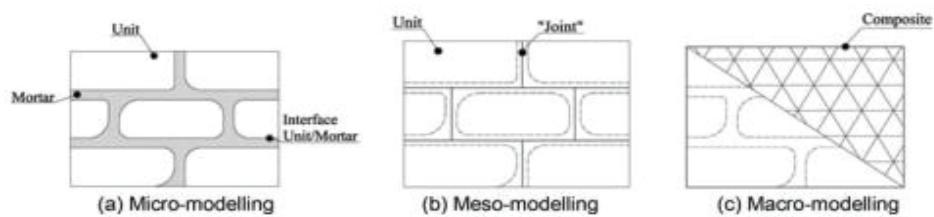


Figure 2.4. Modeling technique for masonry structure

(Source: Lourenco, 2002: 301)

2.5.1. Micro Modeling

Micro modeling, known as heterogeneous modeling, is modeled by separately incorporating materials forming the masonry wall. In this modeling technique, units like brick, stone and the mortar are modeled separately. In addition, the interface areas of these elements are included in the model. This modeling ensures the material discretization (Figure 2.5).

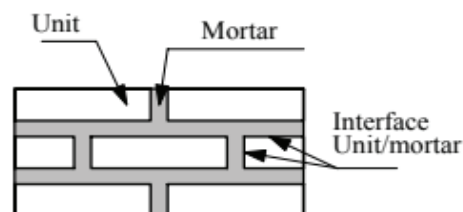


Figure 2.5. Micro modeling

(Source: Lourenco, 1996: 12)

Micro modeling is one of the most significant methods in terms of understanding the behavior of masonry. By using micro models, the different failure mechanisms can be regarded (Figure 2.6). Lourenco characterized the different failure mechanisms of masonry;

- Cracking of the joints.
- At low values of normal stress, sliding along the bed or head joints.
- In direct tension cracking of the units.
- At values of normal stress enough to develop friction in the joints, diagonal tensile cracking of the units.
- Under high values of normal stress due to the mortar dilatancy, splitting of units in tension (Lourenco, 1996: 43).

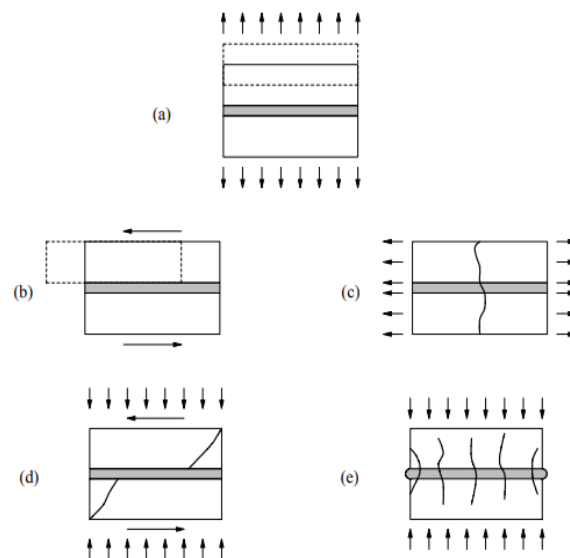


Figure 2.6. Masonry failure mechanisms (a) joint tensile cracking; (b) joint slipping; (c) unit direct tensile cracking; (d) unit diagonal tensile cracking; (e) masonry crushing
(Source: Lourenco, 1996: 44)

In addition, all damage is concentrated in the weak joints and in potential pure tensile cracks in the units placed vertically in the middle of each unit (Lourenco, 1996: 43). The interface elements, which are modelled as potential crack, are utilized to model potential cracks in the units (Teomete, 2004: 20). Therefore, it is known that the interface elements are inelastic cases (Figure 2.7).

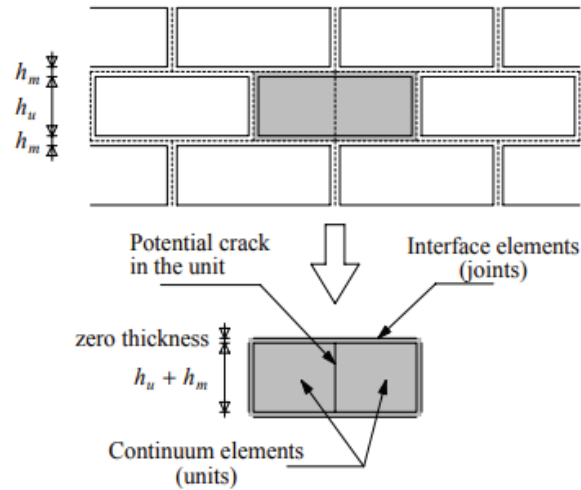


Figure 2.7. Suggested modeling strategy. Units (u), which are expanded in both directions by the mortar thickness, are modeled with continuum elements. Mortar joints (m) and potential cracks in the units are modeled with zero-thickness interface elements
 (Source: Lourenco, 1996: 45)

A lot of experiments were done for micro modeling. The test results are close to each other. Elaborated information about the tests, micro modeling can be obtained at (Lourenco, 1996: 46).

Berto et al. (2005) investigated the behavior of masonry prisms under axial compression by using micro modeling approach. So, mortar, strong brick and strong mortar properties were drawn conclusion.

Ural and Doğangün (2007) showed that the cracks which are come into existence in masonry walls are in the interface of the mortar and the masonry unit by the approach.

Mandilora et al. (2012) developed the bed joint mortar by truss elements in micro modeling approach.

Sattar (2013) observed masonry elements as bed joints in horizontal elements and head joints in vertical elements by the use of micro modeling method.

2.5.2. Macro Modeling

When the analysis of masonry structures has been investigated, all these structures could not be performed using micro model because of a great number of constituents. Macro modeling can be utilized for modeling all masonry structures, in which a relation

between average stresses and strains in the composite material is established (Lourenco, 1996: 123).

This modeling strategy does not distinguish between individual units and joints. However, masonry is treated as a homogeneous anisotropic continuum as shown in Figure 2.8.

Macro modeling strategy is defined by the material homogenization. Many researchers present their ideas on this subject. Especially, three dimensional modeling is proposed to investigate masonry walls subjected to out-of-plane actions for homogenization (Cecchi and Sab, 2002: 715-746). Thanks to three dimensional modeling, the bending stiffness of masonry structure is defined easier. After the model was obtained, the effects of joints sizes and the effects of ratio deformability of mortar were consider.

The simplified homogenized procedure was investigated the buckling behavior of slender unreinforced masonry walls (Milani et al., 2013: 98-120). Furthermore, the study based on the finite element homogenization technique emphasized the significance on the determination of the out of plane flexural facade (Casolo and Milani, 2013: 330-351).

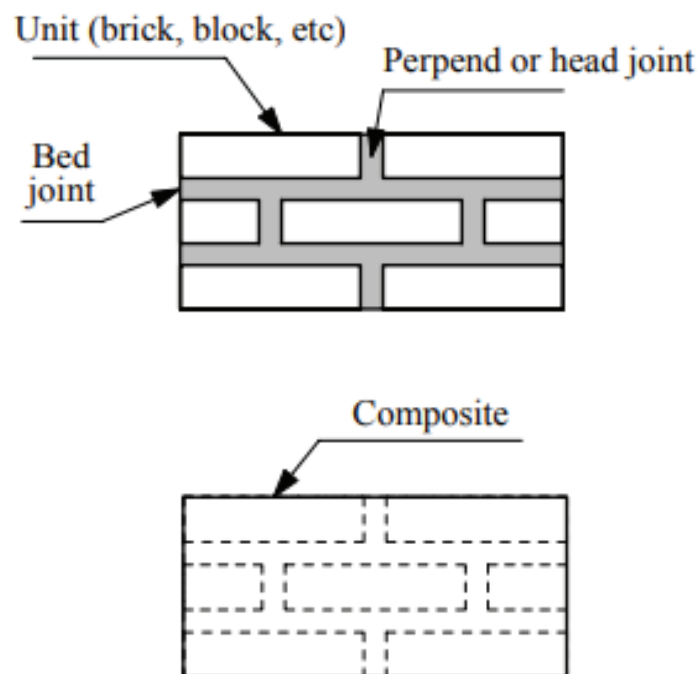


Figure 2.8. Masonry sample and macro modeling

(Source: Lourenco, 1996: 12)

The analysis of historical masonry structures used in a macro-modeling should be done with describing a material in terms of all stress state. There are two different approaches for the macro-modeling of masonry. The first one can be defined as the material behavior with a single yield criterion (Lourenco, 1996: 125). When investigated, the Hoffman yield criterion is very flexible (Figure 2.9). However, its masonry experimental values have an inadmissible fit. In addition, the yield criterion does not indicate the tensile strength in uniaxial behavior (Lourenco, 1996: 125).

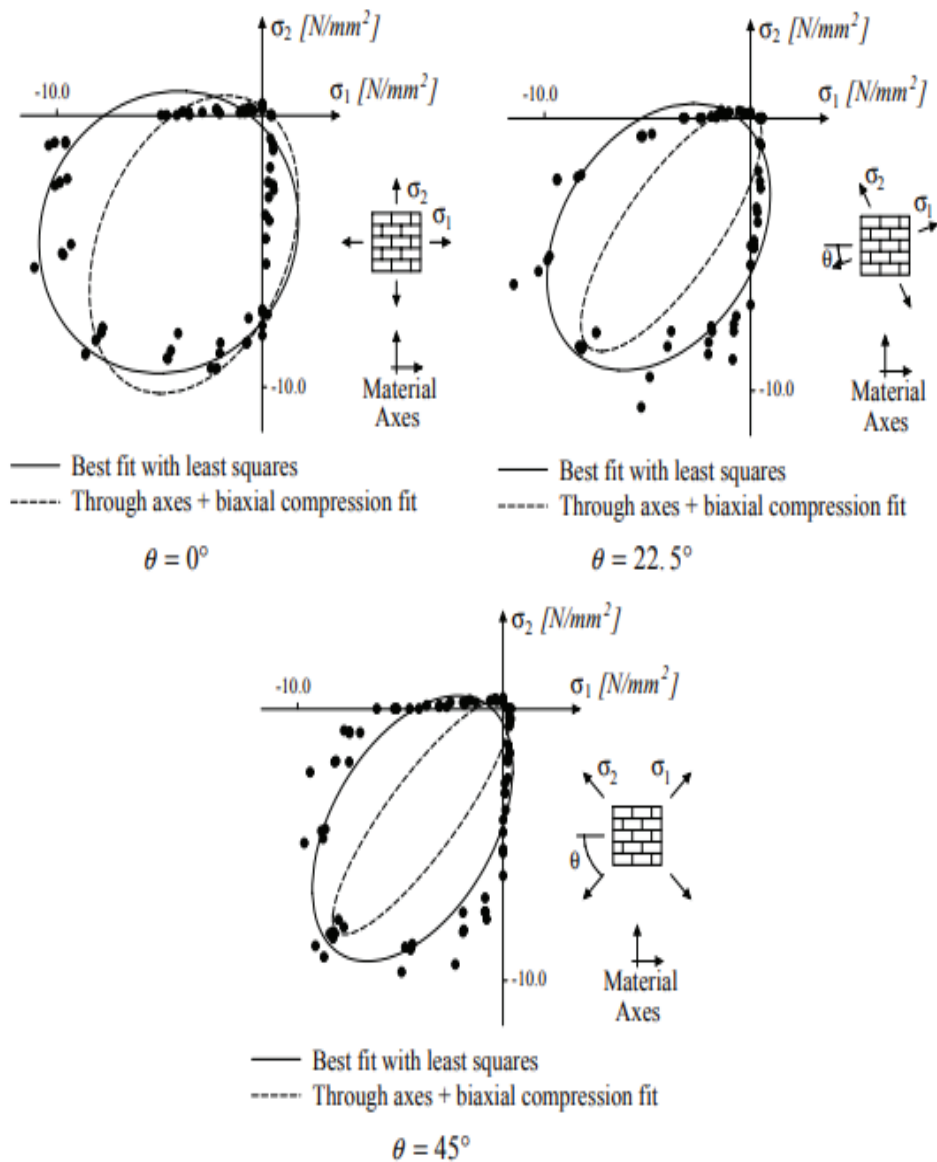


Figure 2.9. The Hoffman type and experimental results

(Source: Lourenco, 1996: 124)

This approach comprises of the conventional formulations to define orthotropic behavior. The orthotropic material behavior is described a Hill type yield criterion and a Rankine type yield criterion (Figure 2.10). The Hill type yield criterion is compression and the Rankine type yield criterion is also tension (Figure 2.11-12).

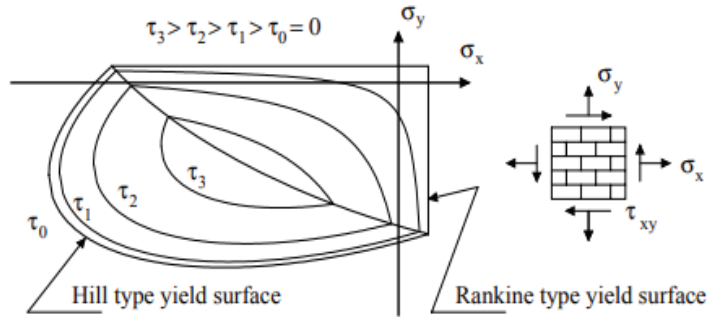


Figure 2.10. A Hill type yield surface and Rankine type yield surface

(Source: Lourenco, 1996: 126)

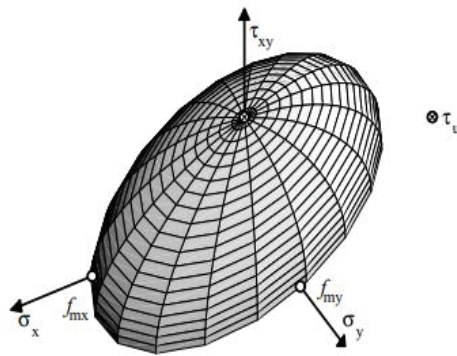


Figure 2.11. The Hill type yield surface

(Source: Lourenco, 1996: 133)

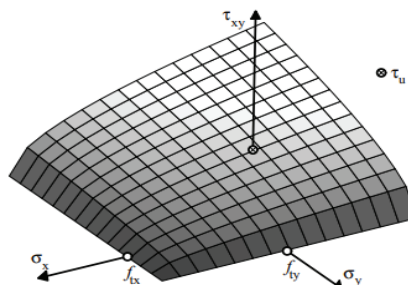


Figure 2.12. The Rankine type yield surface

(Source: Lourenco, 1996: 129)

2.5.3. Meso Modeling

In this modeling approach, the mortar and two unit-mortar interfaces is in an average interface while the units are expanded so as to keep the same geometry. Therefore, masonry is a set of elastic blocks.

In meso modeling called the simplified micro modeling, beside units like brick and stone which occur the masonry structure, the surfaces in which these elements touch each other are modeled (Figure 2.13). However, the mortar connecting the units is not included as a separate element in the model.

In simplified micro modeling method, while brick unit forming the masonry wall is geometrically modeled, the simplification is done for mortar. For this purpose, the mortar connecting the units is accomplished by incorporating contact elements into the model. Contact formation between two objects are common case in engineering analysis. Contact problem, connected by contact formation and disappearance between objects and increase and decrease of rigidity due to too much change, is a complex non-linear problem.

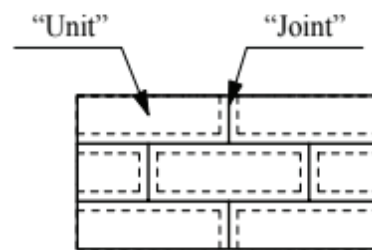


Figure 2.13. Meso modeling or simplified micro modeling

(Source: Lourenco, 1996: 12)

Chaimoon and Attard (2006) used meso modeling approach in triangle finite elements for finding the behavior of masonry walls in the event of shear and compression breakage.

Ural and Doğangün (2009) investigated that the masonry units were split from each other since they were widened as much as half of the mortar thickness in meso modeling technique.

CHAPTER 3

DESCRIPTION OF ÇARDAK KHAN

Location of Çardak khan, mass and facade characteristics, spatial characteristics, structural elements, architectural elements and current structural condition are presented in this chapter.



Figure 3.1. Çardak caravanserai in Denizli as viewed from the east

3.1. Location

Çardak caravanserai is located in Çardak province, which is 55 km to the east of the city center of Denizli, and 300 m to the north of the Denizli-Afyon highway.



Figure 3.2. Location of Çardak Khan

(Source: Google maps)

The old caravan route passed from the south of the khan. This caravan road was utilized largely throughout history. It connected the Aegean Region to Central Anatolia. The ancient Roman road from Ephesus to Pamphylia and the Byzantine road from Konya, Beyşehir, and Eğirdir to Laodicea and Ayasuluk (Ephesus) passed by Han-abad (Yavuz, 2007: 134-135).



Figure 3.3. Seljuk caravanserais and caravan roads in Anatolia

(Source: Bektaş, 1999: Map VI)

The present entrance to the khan is from a secondary road, *Han Street*, at its east.

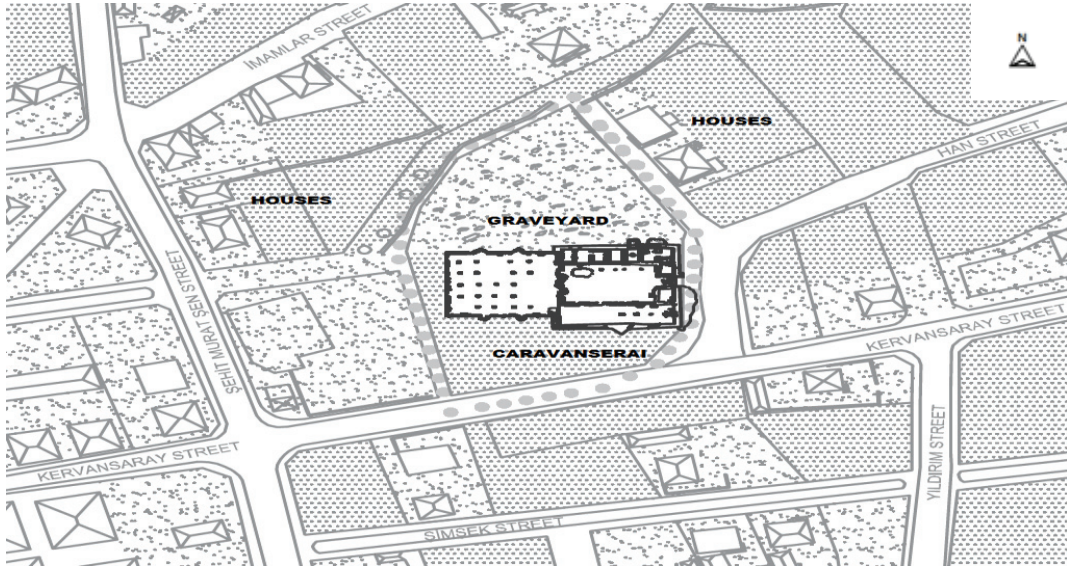


Figure 3.4. Çardak caravanserai and its environs, site plan

(Source: Bayram et al., 2017)

3.2. Mass and Facade Characteristics

The caravanserai situated in east-west direction is composed of a rectangular courtyard (32.27 m in length, 31.16 m in width) with building ruins and a prismatic shelter (29.23 m in length, 26 m in height) entered from the courtyard. The entrance to the courtyard is from a portal ruin at the center of the east side.

Entrance facade of the courtyard (25.87 m in width, 4.80 m in height) is composed of a portal ruin at its center and blind facades at its two sides. The entrance facade of the shelter has another portal (2.97 m in length, 3.41 m in height) at its center and cylindrical buttresses at its two sides.

The southern facade of the composition is composed of a high and blind wall (29.23 m in width, 3.70 m in height) supported with two polygonal buttresses at the west, and the ruins of the courtyard wall (3.77 m in weight, 2.50 m in height) at the east. There are two water spouts, which are U formed stone channels, close to the top portion of the high wall for draining rain water down the terrace roof of the shelter.

The western facade of the courtyard (32.20 m in width and 1.85 m in height) is composed of the portal of the shelter at its center (5.62 m in height), and two cylindrical buttresses (5.27 m in height) at the sides.

The western facade of the composition does not have any buttress.

The northern facade of the composition is composed of a high and blind wall (29.5 m in width, 4.60 m in height) supported with two triangular buttresses at the west, and the ruins of the courtyard wall (2.87 m in length) at the east. There are three water spouts or their remains / traces close to the top portion of the high wall.

3.3. Spatial Characteristics

The building is composed of open and closed spaces at present. These parts refer to the courtyard and the ruins surrounding it, and the shelter, respectively.

3.3.1. Courtyard

The open courtyard is entered through a portal. Service spaces surround the courtyard. The entry to the courtyard is roughly at the center of the east wall of the courtyard.

The courtyard portal was demolished.

The ruins on the northern part of the courtyard comprehend various functions such as the bath, kitchen, storage, workshop, staff room and iwan (Bayram et al., 2017). The ruin at the east of the courtyard and juxtaposing the entrance is the masjid. The arcaded ruin at the east is the resting band for animals and people (Figure 3.5).

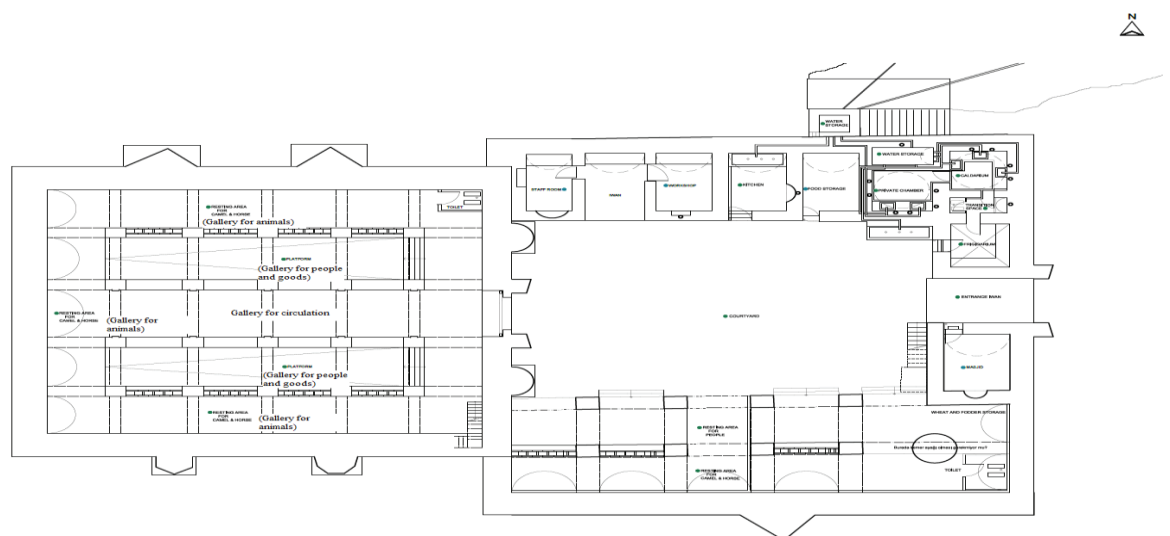


Figure 3.5. Ground floor plan, restitution

(Source: Bayram et al., 2017)

3.3.2. Shelter

The shelter, which is at the west of the courtyard, is a vaulted structure composed of a single space. The length of the shelter is 29.23 m and its width is 26 m (Figure 3.6). It has five barrel vaulted galleries at east-west direction. Pierced walls separate the galleries from each other. The central gallery is relatively higher (height: 5.40 m), and the height of the vaults decende from the center to the sides (height: 4.60 m) (Figure 3.7). There are non-load bearing walls in between the galleries. These low wall remains belong to the original platforms for housing people and goods. The shelter is very dim, since illumination is provided from the small ventilation holes (diameter: 70 cm) at the vaults. The portal is the only opening at ground level. There is a staircase at the southeast corner providing connection with the terraced roof.

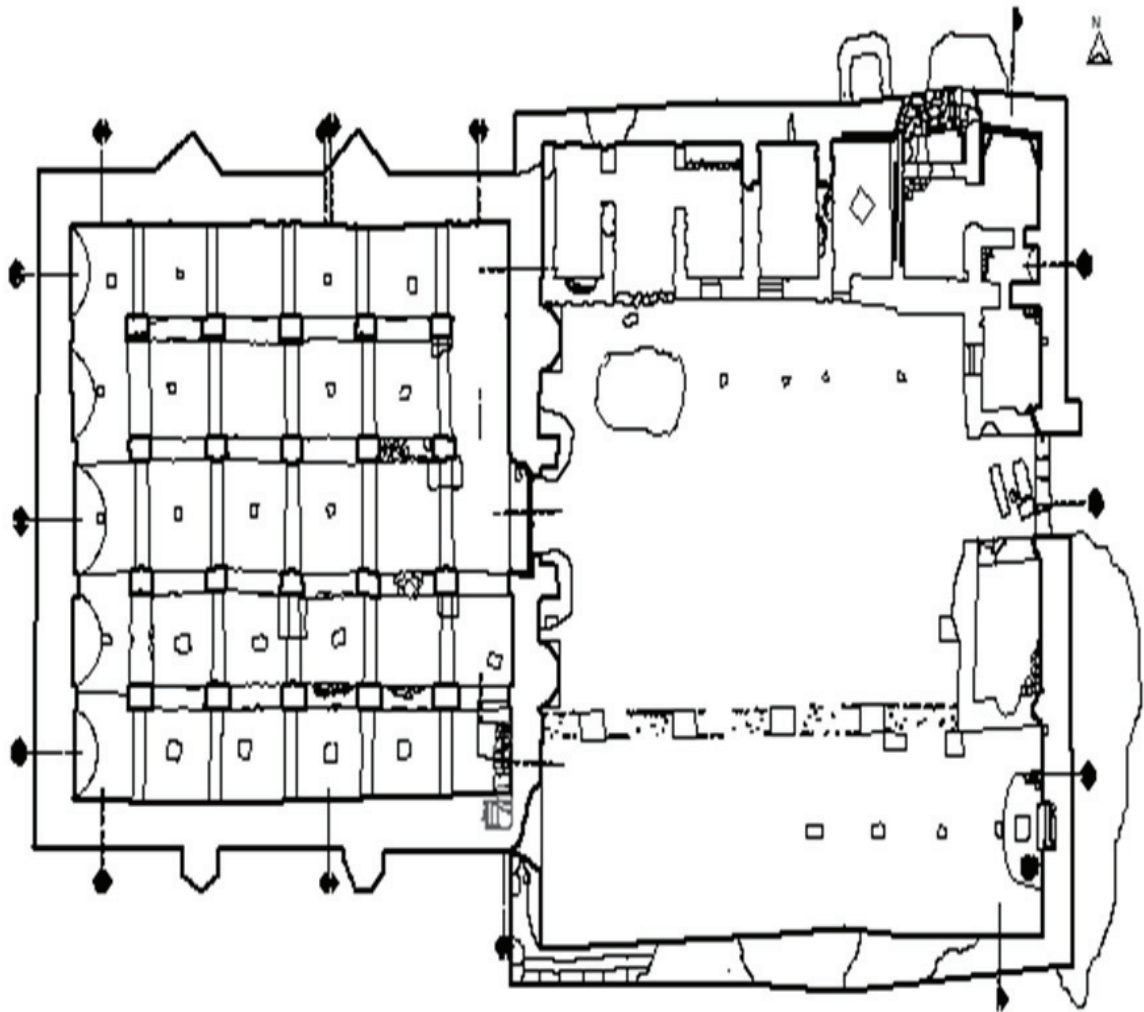


Figure 3.6. The ground floor plan
(Source: Bayram et al., 2017)



Figure 3.7. The central gallery as viewed from the east

3.4. Structural Elements

Structural elements are superstructural elements, walls and buttresses, floor and staircase, and foundations. In this section, these elements will be explained.

3.4.1. Superstructural Elements

Superstructural elements consist of vaults (Figure 3.8), arches, the squinch remain and a concrete slab.



Figure 3.8. The northern gallery of the caravanserai as viewed from the west

The barrel vaults of the shelter are located in east-west direction (Figure 3.9). The spanning distance at the center is 4.50 m, while it diminishes to 3.58 m and 1.97 m in the vaults at its north, and 3.06 m and 1.50 m in the vaults its south, respectively. Their heights are 3.10 m, 3.11 m, 3.37 m, 3.14 m and 2.98 m respectively from the north to the south. Their profiles are double centered and pointed (Figure 3.10). They are out of rubble stone put together with lime mortar. At their exterior, earthen finishing is observed. There are ventilation holes along the key stones of the vaults. Just under the springing line of the vaults, the construction holes are still observable.

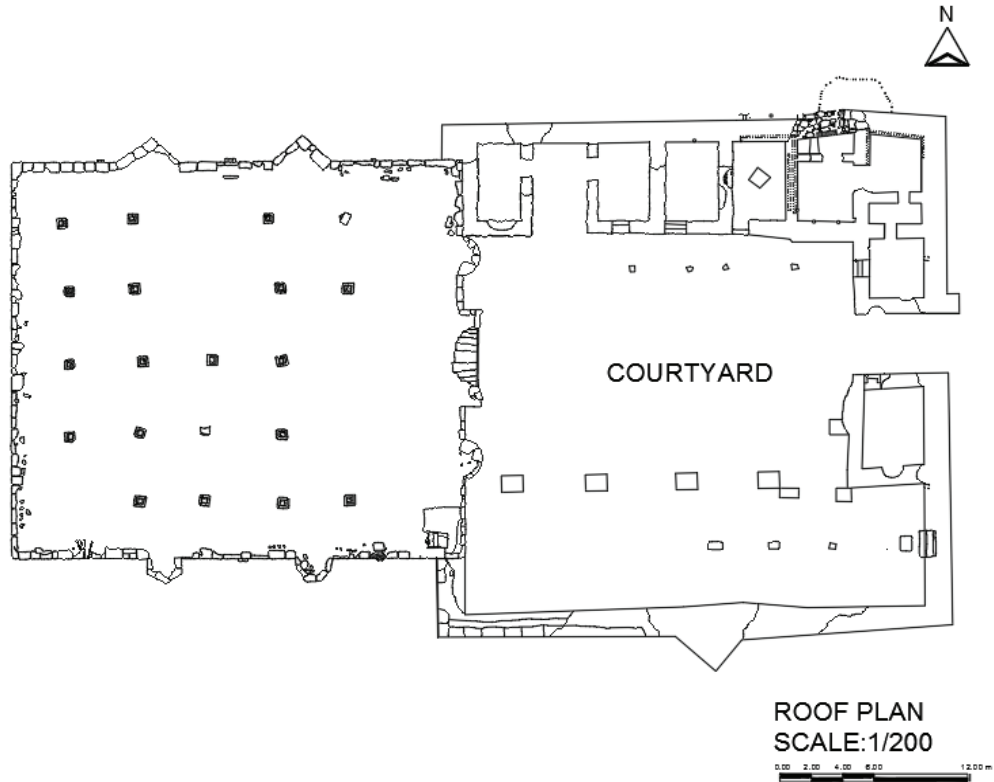


Figure 3.9. Roof plan of the caravanserai, restitution
(Source: Bayram et al., 2017)

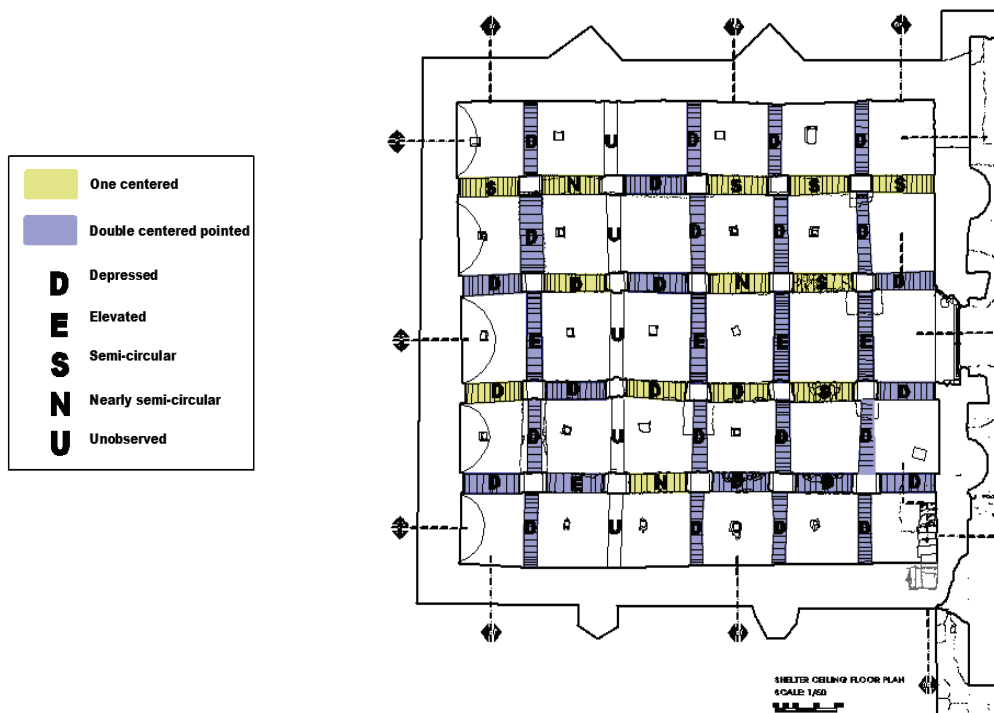


Figure 3.10. Vault and arch profile types, reflected ceiling plan
(Source: Bayram et al., 2017)

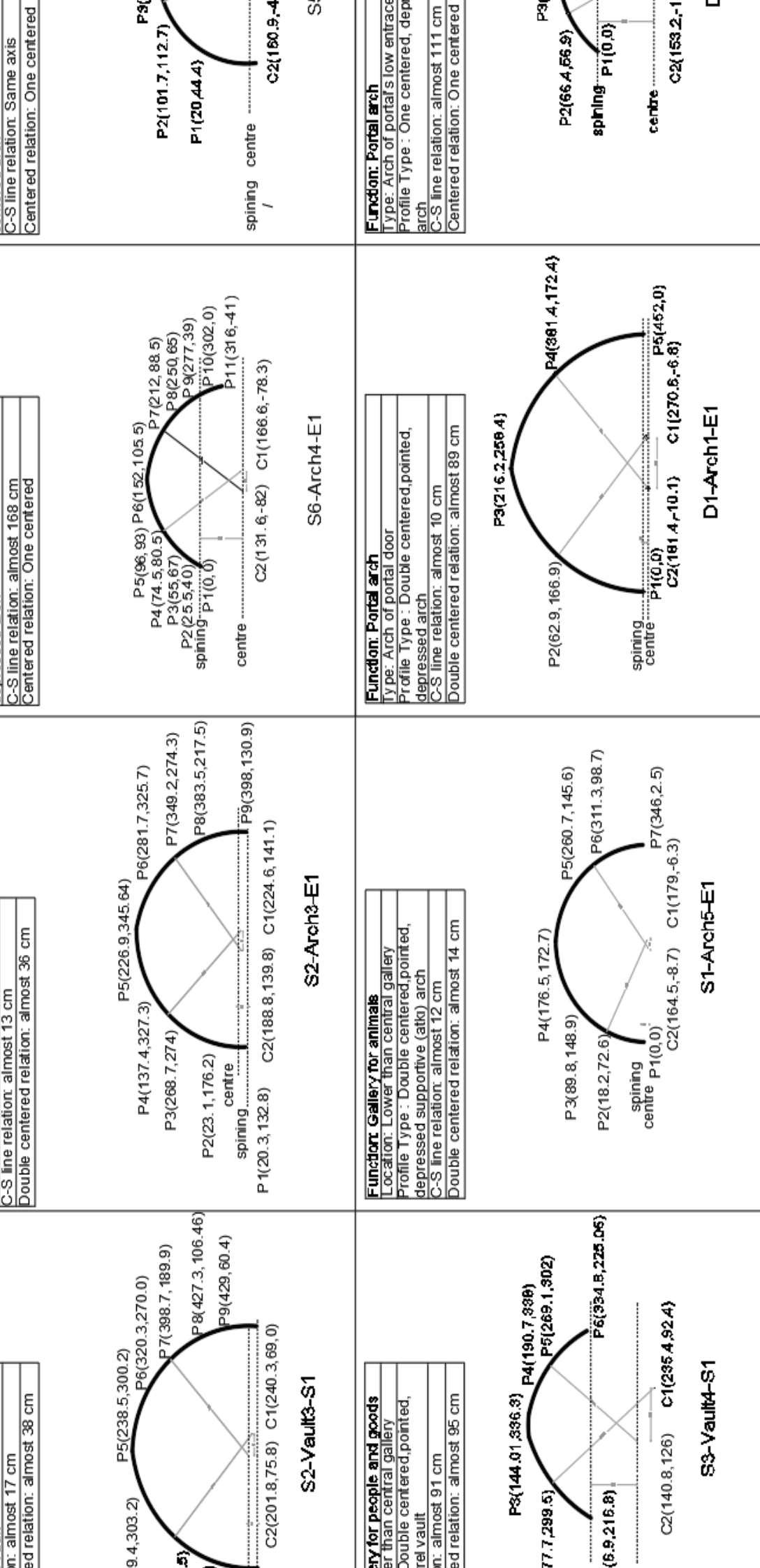


Figure 3.1.1. Vault and arch profile types

(Source: Bayram et al., 2017)

Each vault is supported with five reinforcing arches distributed evenly. Their voussoirs are out of cut stone and lime mortar. The thickness of the extrados is approximately 60.00 cm, while that of the intrados is approximately 90.00 cm.

The four interior load bearing walls in east-west direction are pierced with pointed arches that are either one or two centered. The spanning distances vary between 0.70 m and 3.71 m. Their heights are approximately 1.80 m and 1.92 m from the northern gallery to the south, respectively.

The arch of the door at the portal of the shelter is one centered, pointed and depressed. The spanning distance and height are 2.71 m and 2.66 m, respectively.

The squinch remain is at the bath section at the northeast of the courtyard. It is out of brick put together with lime mortar.

The concrete slab is an additional structural element observed over the stairs leading to the terrace roof at the southeast corner of the shelter (Figure 3.12).



Figure 3.12. The stairs leading to the terrace roof

3.4.2. Walls and Buttresses

The load-bearing exterior walls of the shelter are continuous walls. The eastern and southern ones that used to be observed from the old caravan route are out of well-cut stone at their outer surface, rough cut stone at inner surface and rubble stone and lime mortar in between (Figure 3.13). The western and northern walls that were designed as rear facades are out of relatively low quality cut stone at their outer surfaces, rough cut stone at inner surface and rubble stone in between. The widths of northern and southern walls carrying the loads of the vaults are 1.80 m and 2.20 m, respectively. The widths of

the western and eastern walls carrying their own loads are 1.40 m and 1.70 m, respectively.

Courtyard Walls

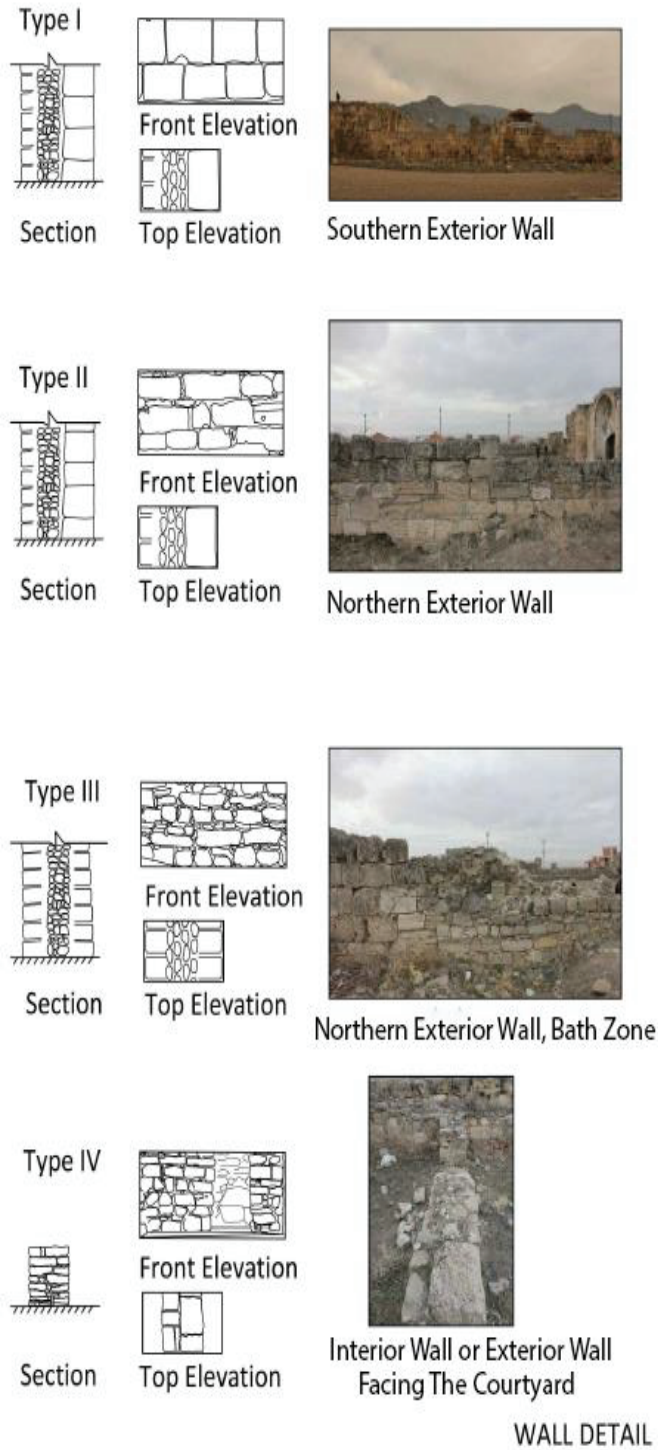


Figure 3.13. Wall types

(Source: Bayram et al., 2017)

These walls are supported with buttresses from their exteriors, excluding the western one. There are two buttresses distributed evenly at each facade. Their forms are triangular (width: 375 cm, projection: 24 cm, height: 3.68 m), circular (width: 193 cm, projection: 110 cm, height: 5.27 m) and polygonal (width: 213 cm, projection: 121 cm, height: 4.80 m) starting from the north in clockwise order.



Figure 3.14. The caravanserai as viewed from its southeast

The interior load bearing wall of the shelter (Figure 3.14), which are pierced with arches, are cut stone at their both surfaces. Their sections are unobserved. Their widths are 85 cm and 87.5 cm from the north to the south. The surfaces facing the central gallery are decorated with pilasters and animal figures.

The non-load bearing walls at the interior belong to the original platforms for resting of people. At present, they define two u forms at the second and fourth galleries from the north to the south. They are single layered and out of rubble stone and lime mortar. Their widths are the same as the related load bearing wall.

As the construction joints reveal, the service spaces around the courtyard were constructed after the completion of the shelter walls. Nevertheless, their techniques are very similar. Thus, there is not a period difference.

The load-bearing exterior walls of the service spaces around the courtyard are also continuous and three layered. The difference in the elaboration of front and rear facades

is visible here as well. They are well cut stone and relatively low quality cut stone at the outer surfaces of the front and rear facades, respectively. The interior surfaces are rough cut stone and the cores are rubble stone and lime mortar. Only at the middle portion of the northern wall, which corresponds to the bath ruins, a different technique is observed: rough cut stone at both surfaces, and rubble stone and lime mortar in between. There is a triangular buttress (width: 229 cm, projection: 30 cm, height: 170 cm) supporting the southern wall. The widths are 104, 106, 110 and 105 cm, starting from the north in clockwise order. They are all partially collapsed and the maximum height observed is 1.85 m at the courtyard wall.

The interior load bearing wall of the service spaces around the courtyard are rough cutstone and single layered (Figure 3.15). Their widths vary between 1.20 m and 2.40 m. They have lost almost all of their third dimension: maximum height is 215 cm.



Figure 3.15. The interior walls of the service spaces at the north

3.4.3. Floor and Staircase

The ground of the shelter is screed at present. As the sampling excavations reveal, original rubble stone and compacted earth are present underneath the intervention layer (Figure 3.16). The courtyard is covered with debris in general.

The staircase (Figure 3.17) at the southeast corner of the shelter links the interior to the terrace roof. It is L formed; the lower portion is parallel to the eastern wall (width 35 cm, length 1.05 m), the upper portion is parallel to the southern wall (width 32 cm, length 1.25 m). The stairs are out of cut stone block, each approximately 30 cm in height.

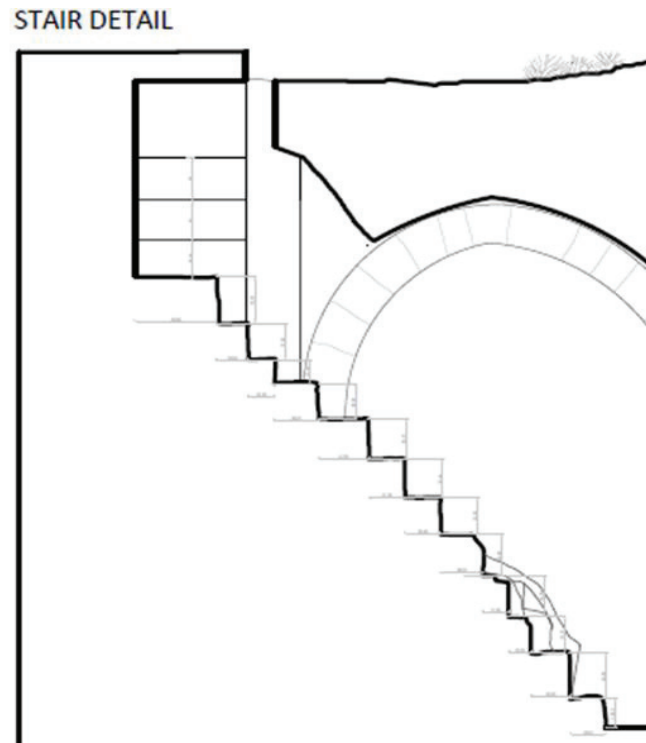


Figure 3.16. Stair detail

(Source: Bayram et al., 2017)



Figure 3.17. The staircase at the southeast corner of the shelter

3.4.4. Foundations

As the sampling excavations reveal, the foundations continue underneath the interior walls (non-load bearing walls) of the shelter (Figure 3.18) and the interior walls of the service spaces (Figure 3.19). They are out of rubble stone.

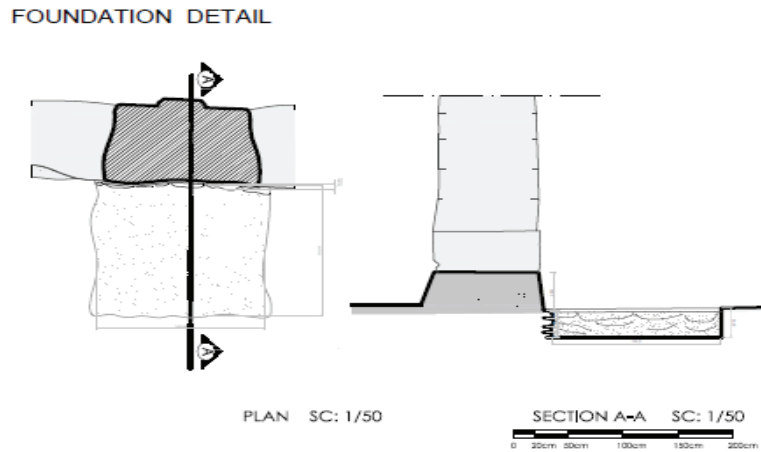


Figure 3.18. Foundation detail, partial plan and transverse section from a gallery
(Source: Bayram et al., 2017)



Figure 3.19. The foundations under the interior walls in the service spaces at the north

3.5. Architectural Elements

The architectural elements of the building refer to non-structural elements enriching the architectural organization. They consist of a portal, lightwells, water spouts, a lampholder, pilasters and ornamentations in the shelter; and a portal, niches, a furnace, terracotta pipes at the service spaces.

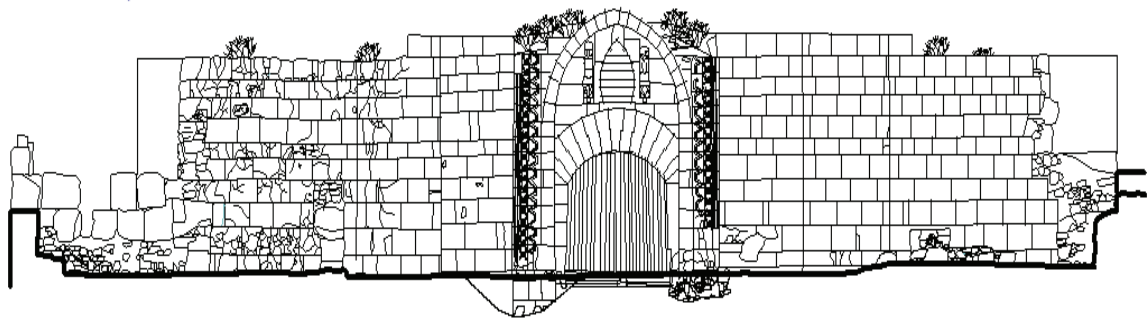
3.5.1. Portal

There are two portals: providing access to the courtyard and the shelter. The courtyard portal at the center of the eastern facade spans 3.88 m and has lost its third dimension. There are well cut stones scattered around the opening probably belonging to the lost portal. At the threshold, there is a trace of a hinge pin (Figure 3.20).

The portal of the shelter (width: 6.20 m, total height: 1.20 m) is at the center of the eastern side. It is a gateway projecting (372 cm) towards the courtyard. It is composed of a central opening (width: 0.85 m, height maximum: 1.50 m) crowned with a depressed arch, an inscription panel enriched with two lion figures at its sides and a pointed arch at the very top. The sides comprehend geometric decoration. The structure is part of the eastern load bearing wall of the shelter. The inscription panel is marble, the lions are carved out of stone blocks. The door double leafed. The void (93 cm in length, 35 cm in height) of the timber support of the leaves extent 195 cm and 185 cm, in northern and southern directions, respectively.



Figure 3.20. The portal of the shelter



EAST PORTAL ELEVATION
SCALE:1/100

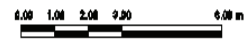
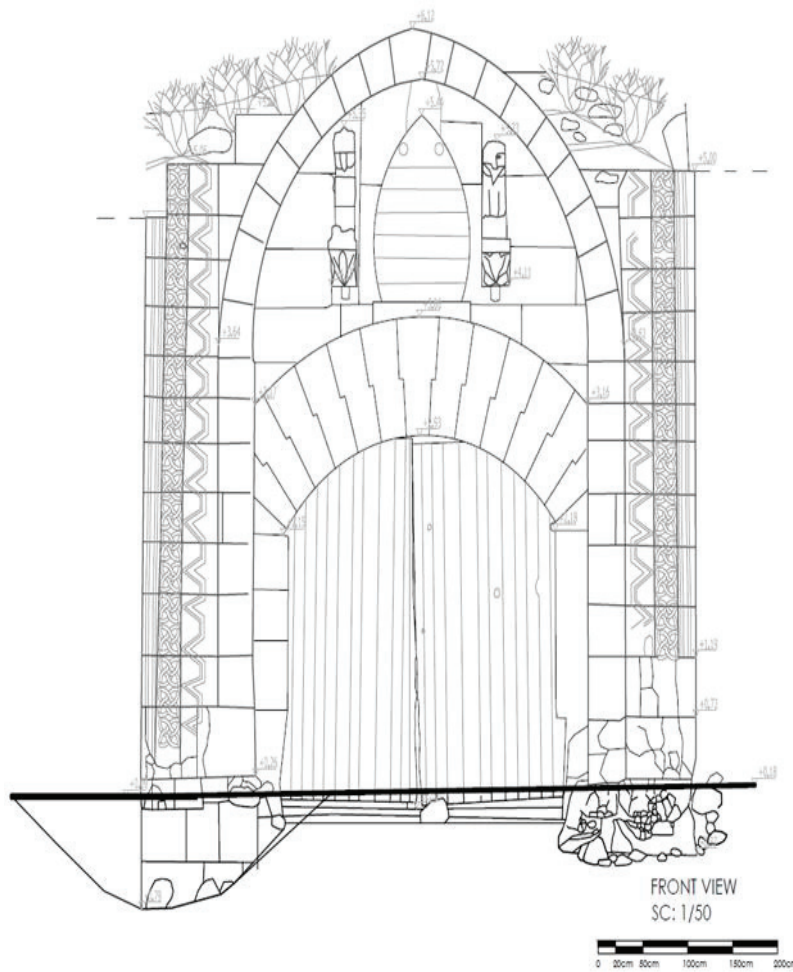


Figure 3.21. The eastern elevation of the shelter

(Source: Bayram et al., 2017)



FRONT VIEW
SC: 1/50



Figure 3.22. The east (entrance) elevation of the Portal

(Source: Bayram et al., 2017)

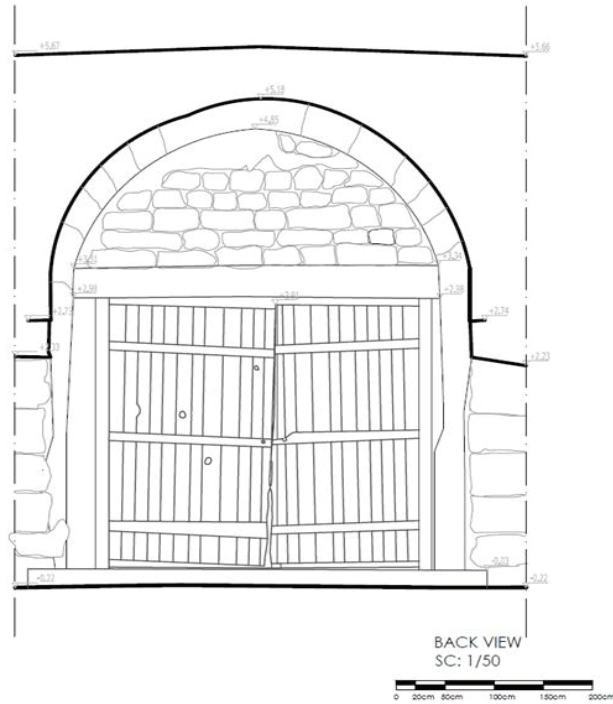


Figure 3.23. The interior elevation of the portal of the shelter

(Source: Bayram et al., 2017)

3.5.2. Pilasters and Ornamentation

There are geometric and figural decoration at Han-Abad. Some figural ornamentations are found at the hall of the shelter. These are bull head and figures. Geometric decoration and lion figures are on the portal of the shelter, which are symmetrically designed (Section: 3.5.1).



Figure 3.24. Geometric ornamentation of the entrance portal (left), the bullhead pattern at the central gallery (right)

3.5.3. Water Spouts

The terrace roof of the shelter is the highest along the axis of the central gallery and lowest at the northern and southern sides. So, the water spouts are at northern and southern sides to direct rain water gathering at the roof to the ground. Three spouts at each side are placed evenly. Each projects 15 cm from its wall and is 30 cm in width, 40 cm in height. They are all carved out of stone blocks.

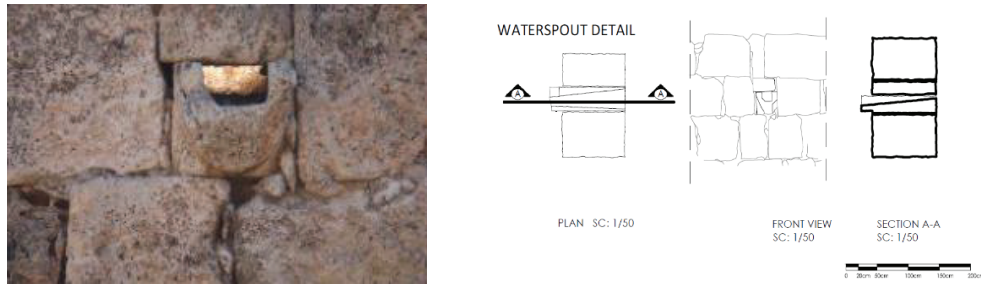


Figure 3.25. The water spout at the north (left) and waterspout detail (right)

3.6. Current Structural Condition

Structural failures include total collapse, partial collapse, out of plumb, joint discharge and loss of material. Total collapse is seen in service spaces in the courtyard. So, they have become open to climatic conditions.

Partial collapse is at the northeast and southeast corners of the shelter (Figure 3.26). Probably, the villagers took the stones and emptied the wall corners. These collapses have given way to the formation of cracks. Damage caused by collapse at the corners affects the load bearing carrying capacity and durability of the structure.

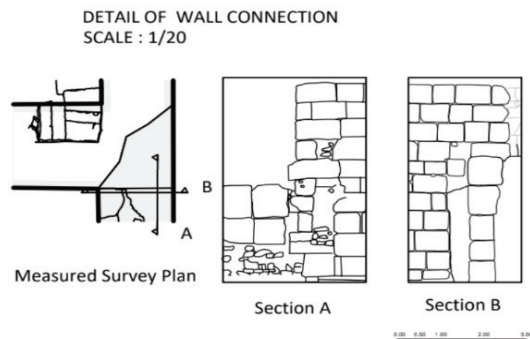


Figure 3.26. Detail of wall connection from southeast

(Source: Bayram et al., 2017)

The western wall of the shelter is out of plumb. The wall is turning outward. Especially, in the second gallery from the north, this is seen at the highest degree.

In case of joint discharge, the stones are separated from each other with the effect of the slightest earthquake or in heavy rain, and the structural element collapses. It is seen in the service space walls of the shelter, in the northeast and southeast corners of the shelter and at the upper elevation of the outer walls of the shelter. It is due to weathering and inappropriate material intervention.

Loss of material is the loss of pieces of stone and mortar materials. Thus, the integrity of the structural element is under risk. It is at the upper elevations of the outer walls of the shelter and the bottom of the shelter walls. The risks of the loss of material are structural vulnerability against earthquakes.

On the other hand, material deterioration includes disintegration, crumbling, minor cracks, discoloration and biological growth.

When the conservation condition of the monument is interpreted in terms of the distribution of structural failures and material deterioration (UNI EN 16096, 2012: 10-13), three condition classes are recorded (Bayram et al., 2017; Figure 3.27). The red zones are condition class 3: major structural failures such as collapse and widespread material deterioration are seen. The elements in these zones require urgent intervention. Preventive conservation measures should be taken. The yellow zones are condition class two: only local structural failures such as out of plumbness and partial collapse are seen; but there is widespread material deterioration. There is risk of loss of historic building elements in short term. So, preventive supportive structure design and partial reconstruction should be considered. The blue zones are condition class 1: there is no structural failure, but there is widespread material deterioration. These are the least risk zones. Nevertheless, preventive conservation measures should be developed against weathering.

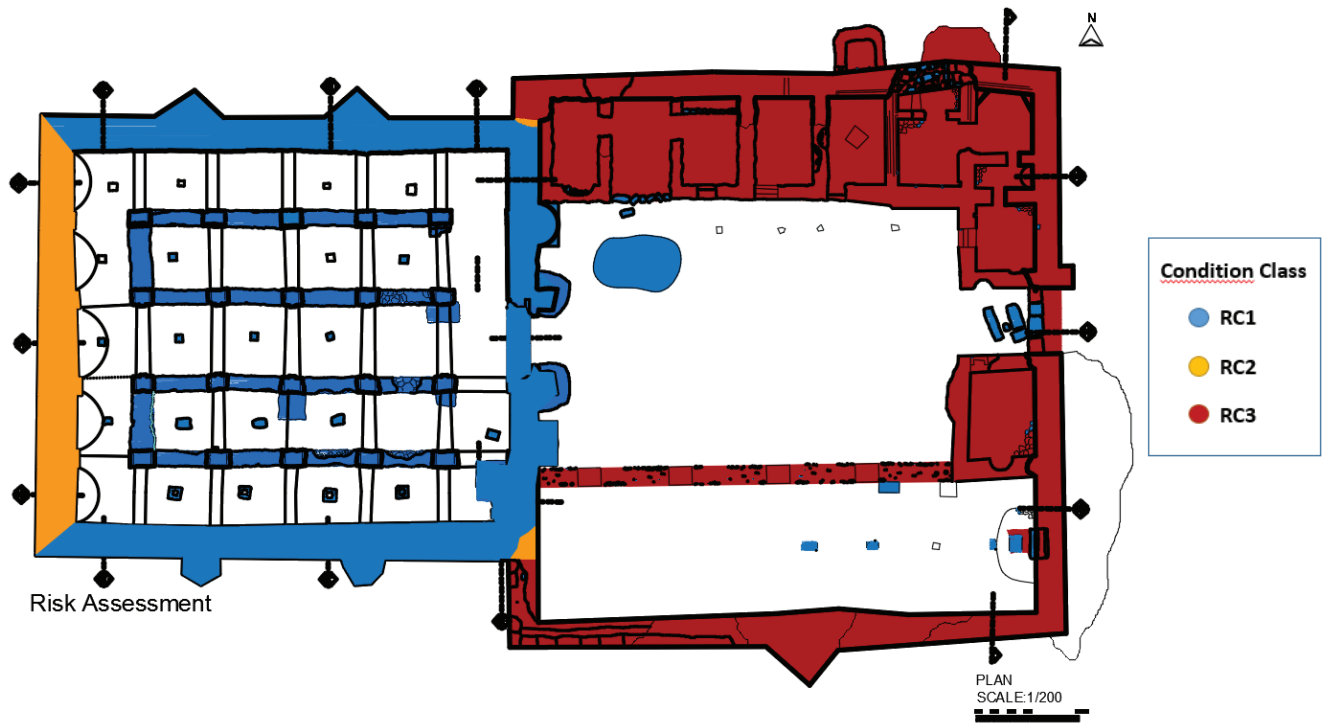


Figure 3.27. Condition classes illustrated on the ground floor plan

(Source: Bayram et al., 2017)

CHAPTER 4

HISTORICAL RESEARCH

Historic developments in Seljukid Anatolia, the history of Çardak caravanserai, positioning of the caravanserai and its functions, architectural characteristics of the caravanserai building type and the related terminology are presented in this chapter.

4.1. Historic Developments

The development of trade in Anatolia was hindered due to the continuous disagreement between the Christians and the Muslims during Byzantine empire period. So, the trade activity was made extensively outside the borders of Anatolia. Seljuks conquered the most significant export and import ports of Anatolia. They gave significance to security of the caravan routes in order to support international trade. Therefore, Anatolia became a bridge for trade between east and west until the end of the 12th century (Kutlu, 2009: 1).

4.2. Caravanserai as a Building Type

In this section, terminology, positioning, functions, architectural characteristics, structural characteristics and typology are presented.

4.2.1. Terminology

Han-abad is described as a ribat in its foundation charter (Kutlu, 2009: 27). A ribat is an Arabic term for a small fortification as built along a frontier during the first years of the Muslim conquest of North Africa to house military volunteers, called the *murabitun*. These fortifications later served to protect commercial routes, and as centers for isolated Muslim communities. Generally, ribat referred to the guard duty at a frontier outpost in order to defend *dar al-Islam*, the one who performs ribat is called *murabit*. Ribats were first seen in the 8th century, the word “*ribat*” in its abstract refers to voluntary

defense of Islam, which is why ribats were originally used to house those who fought to defend Islam in *jihad*. They can also be referred to by other names such as *khanqah*, most commonly used in Iran, and *tekke*, most commonly used in Turkey (Schimmel, 1975: 231-232).

The most important establishments which were built against Turkish raids were “Rabat”s or “Ribat”s (Yalçiner, 1997: 999). This term refers to guarding bases or stations on the borders of early Islamic states (Akalın, 2002: 299). The word “Caravanserai” derives from Persian. The meaning of word is “the protector”. The establishment where caravans were settled are called “Caravanserai”. For these buildings, the word “Han” which is of Turkish origin is used too (Yavuz, 1997).

According to Fuat Köprülü (1942), the caravanserai is related to “Ribat”. The origins of these buildings find idea of “*Cihad*” in the muslimism. The ribats were constructed by the Muslims and they were seen as “Fortress”. The ribats which were the danger of battle and at the great centers supplied hospitality to the poors which came from foreign countries.

Osman Turan (1964) asserts that the ribats which lost their military importance were used as caravanserai. At the same time, he agreed with Fuat Köprülü’s opinions.

Oktay Aslanapa (1960) mentions that the Karahan, Gazne and Gread Seljuk ribats were the origins of Anatolia Seljuk caravanserais.

According to Kurt Müller (1920), the Roman Castrum is the origins of the caravanserais.

In conclusion, in the light of all the facts mentioned above caravanserai is called as “*Han-abad*” by local people. The name of the caravanserai changes according to functions. These functions are military, social and commercial. For instance, *Ribat* utilizes in military function. Apart from that, the word could change in the origin of language. For the sake of example, “*Han*” is of Turkish original word. As for *Çardak* word, it may derive from nearby castle.

4.2.2. Positioning

The caravanserais were established at nine hours intervals considering the travel time of camels, donkeys and horses to supply a secure accommodation place for the travellers, animals and goods (Yavuz, 1997: 84).

4.2.3. Function

Caravanserais could serve commercial, military, social and diplomatic functions. The security on the roads was indispensable for development of trade. The caravanserais were used as shelter for the army. During the wars, these buildings were used for hiding weapons and foods. It is seen that they were also utilized as prisons for the soldiers of the enemy during the battles. In the visits of the neighbouring states, the khans supplied hospitality to the foreign people (Fersan, 1974: 49).

4.2.4. Architectural Characteristics

The fundamental functions of the caravanserais are safety and shelter, which are represented in the durability of the building. So, Seljuk-era caravanserais always had shelter sections and frequently courtyards (Yavuz, 1997: 84; Kutlu, 2009: 29). Shelter covers goods, animals and people. There are people and goods on the platforms. Animals also live in galleries. Galleries can be as many as 1, 2, 3 and 5. There is no window. The openings called oculi are located in the top cover, where the light is filtered. The courtyard area comprises of the courtyard and surrounding spaces. These spaces served functions such as bakery, bath, masjid facilities, horseshoes, repair parts and fountain.

4.2.5. Structural Characteristics

Structural elements of a caravanserai are its superstructure, walls, ground and foundations. There are also some decorative elements.

Superstructure consists of vaults and arches, and also domes. The highest vaults and arches are in the middle gallery. They are low on the edges. This situation is observed in Çardak khan and other caravanserais.

The vaults are seen as barrel in caravanserais. Even though each band is a barrel vault whose width varies between 4 and 7 meters in most of the caravanserais, the platform band and the stable band are a single barrel vault in Şarafsa and Kırkgöz khan, reaching 13 m in width (Yavuz, 1997: 85; Figure 4.1).

The arches consist of finely cut stones in Çardak khan. The same technique is seen as Alara khan, Tuzhisarı Sultan khan, Alay khan, Evdir khan and Tercan khan.

Caravanserais enriched with limited domes are Sarı khan, Karatay khan, Eshab-ı Kehf khan, Alay khan, Öresin khan, Sultan khan, Sadettin khan and Sultandağ İshaklı khan. For instance, there are two high vaults in the middle and a dome at the center in Öresin khan (Yavuz, 1997: 89). In Çardak, there is no dome in the shelter, but only at the bath zone.

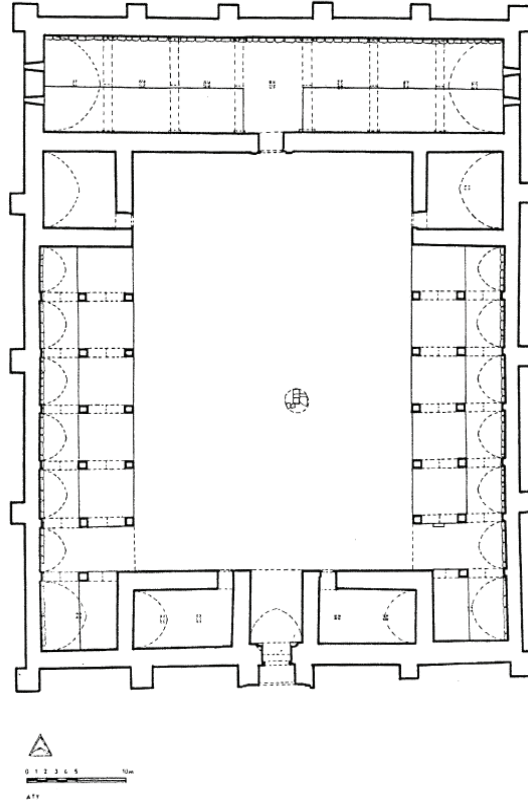


Figure 4.1. Kırkgöz khan, base plan

(Source: Yavuz, 1997: 83)

All caravanserais possess blind and thick walls. The walls of the shelter in most caravanserais are thicker than those in the courtyard. This is seen in Kırkgöz khan, Obruk khan, Kayseri Sarı khan and Hekim khan (Yavuz, 1992: 255) as well as in Çardak khan. The outer walls of the khan are strong and there are no windows. Kayseri Sarı khan, Eli Kesik khan, Kızılören khan, Ishaklı khan and Evdir khan can be given as examples (Yavuz, 1992: 255). Çardak Khan has no windows as well.

The thick exterior walls at the two sides of the shelter are supported by buttresses in most of the caravanserais in order to cope with the lateral load of the vaults running

parallel to the side walls. However, some caravanserais do not have buttresses. The khans without buttress are Altınapa khan, Arğıt khan, Kuruçeşme khan, Eli Kesik khan, İshaklı khan and Deve khan (Yavuz, 1992: 255). Form of the buttresses are the same along the same facade in most cases. However, those of Çardak khan are different at the side walls. Buttresses may be present at some walls, and unresent at others in some caravanserais. This unevenness is seen in Alara khan, Hekim khan, Kırkgöz Khan, Kayseri Sarı khan, Obruk khan, and also in Çardak. The buttresses are common in courtyard sections to strengthen the image of sturdiness.

The exterior surfaces of the continuous walls are constructed of finely cut stones. The interior surfaces of the continuous walls are rubble stones. There is rubble stone and lime mortar in between. This technique is seen in the following caravanserais: Alara khan, Tercan khan, Kızılören khan, Tuzhisarı Sultan khan, and also in Çardak. Pierced walls have rough cut stone at both surfaces with lime mortar. This technique is seen in the following caravanserais: Tuzhisarı Sultan khan, Zıvarık khan, Kargı khan and also in Çardak.

The ground has rubble stone, earth and compacted earth. Akhan, Susuz khan, Ağzıkara khan, Öresin khan (Yavuz, 1992: 261) and also Çardak can be given as example.

The roofs of the caravanserais, which can be accessed by staircases, are usually for observation and defense (Yavuz, 1997: 84). The roof covering is compacted earth, e.g. Alara Khan, Kesikköprü Khan and Çardak Khan.

Decorative elements in Seljuk caravanserais are geometric ornamentation or figured ornamentation. Figured ornaments are observed in Akhan, Karatay khan, Sarı Khan, Çeşnigirhan, Dokuzun Derbent khan (Beyazıt, 2002: 82) and also in Çardak. Evdir khan, Alay khan (Beyazıt, 2002: 82) and Çardak Khan can be given as examples for geometric ornamentation. There is bull, fish and bucket ornaments in Çardak khan and inscription and two lion figures on its portal.

4.2.6. Typology

Erdmann's classification is based on presence or absence of a courtyard (Erdmann, 1961: 21-24). He has clasified caravanserais as khans with a closed section only, and with a closed section and a courtyard by him. Yavuz considers the shelter as the basis of her classification, since it is a must for a caravanserai (Yavuz, 1997: 81). She

considers two parameters: the number of galleries and spatial organization manner. Tuzhisar Sultan khan and Mama Hatun caravanserai are single galleried examples. In terms of spatial organization, two types are determined as additive and concentric organisations. Aksaray Sultan khan, Kırkgöz khan, Akhan and Sarı khan are examples of additive organisation (Yavuz, 1997: 88; Figure 4.2). This design is much more common compared to the concentric one. Mama Hatun Caravanserai, Eshab-ı Khef khan, Sevserek khan and Alara Khan can be given as examples for concentric organisation (Yavuz, 1997: 88; Figure 5.3).

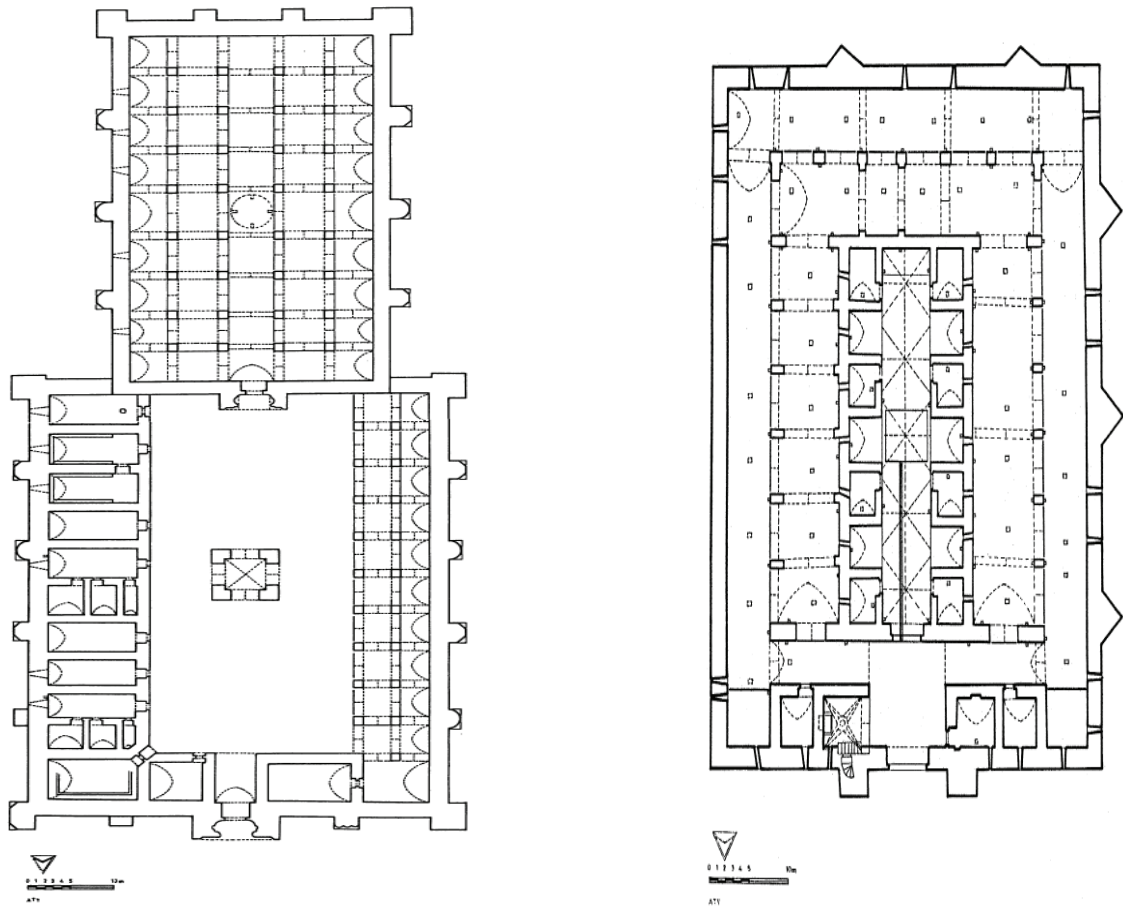


Figure 4.2. Aksaray Sultan khan (left), Alara khan (right), reconstruction plans

(Source: Yavuz, 1997: 85-88)

4.3. History of Çardak Caravanserai

Çardak caravanserai was built by *Esedüddin Ayaz bin Abdullah Eş-Şihabi* in 1230 during *Alaeddin Keykubad* period. It continued to be used during the *Beylik* and *Ottoman*

periods. Han-abad (Çardak Khan) was in use for cereal storage during World War 1 (1914-1918) and the Turkish War of Independence (1920-1922) (Kutlu, 2009: 26). Shortly after that, the local people used it as a sheepfold (Uzunçarşılı, 1929: 210). It was restored in the 1920s.

Çardak caravanserai was a significant *derbent* for checking the passage between western and central Anatolia at an observation point along a narrow passage between the mountains of Maymun and Söğüt (Kutlu, 2009: 24-25). The Çardak Castle is located near the khan. This castle altered hands several times in the 12th between the Byzantines and the Seljuks. Once upon a time, the Byzantines constructed a castle fortress here as an observation point. According to Whittow (1995), the *spolia* used in the construction of Çardak caravanserai could have stem from the Çardak Castle site.

The structure was also used as a caravanserai during the Ottoman period and was used as a granary during the Turkish War of Independence (Kutlu, 2009: 26). The Han is registered with the decision no. 2024 dated 22.05.1991 of the Regional Board for the Protection of Cultural and Natural Heritage of İzmir II. The excavation carried out between 2006 and 2008 has exposed the layout of the courtyard and revealed that the caravanserai had a mosque and a bath located next to the entrance of the courtyard on the southern and northern sides, respectively. At the northern side of the courtyard, the presence of kitchen and related facilities were recorded. At the southern side of the courtyard, the remains of a porticoe were recorded. The Regional Board for the Protection of Cultural Assets of Aydın was requested to complete the revision of the revised restoration project with the decision no. 3345 dated 22.11.2014. The restoration works started in 2017 and will continue for two years. The caravanserai is currently visited by limited tourists.



Figure 4.3. Çardak castle and Maymun mountain as viewed from Han-abad

4.3.1. Inscription Panel of Çardak Khan

The inscription panel is on the portal of the shelter. It is stated on the inscription panel that *Han-abad* was built in 1230 during the reign of Sultan Aleaddin Keykubat 1 and was commissioned by Esedüddin Ayaz bin Abdullah Eş-Şihabi in Ramadan 627 [July-August 1230] (Pektaş, 2007: 162). Esedüddin Ayaz was the governor of the western frontier centered at Denizli and also mir-ahur of Aleaddin Keykubat (Baykara, 1969: 50). Moreover, he was also known as Atabek Ayaz. *Mir-ahur* who was responsible for the horses of the sultan was a high official (Devellioğlu, 2001: 651).

- 1) It belongs to the Sultan
- 2) This ribat was ordered to be built during the reign of our master (mawlana)
- 3) And our lord (sayyidna), the just sultan Alaal-Dunyawa al-Din Abual-Fath
- 4) Kayqubad b. Kayhusraw, the victor [for] the Commander of the Faithful,
- 5) By the humble servant of our most exalted and noble master (mawlana),
- 6) The rightly guided [one] of the nation, the state and the faith,
- 7) Ayaz b. Abdullah al-Shihabi in the great month of Ramadan of the year 627 (Uzunçarşılı, 1929: 210-212).

السلطاني
امر ببناء هذا الرباط في ايام دولة مولانا
وسيدنا السلطان العادل علاء الدنيا و الدين
ابوالفتح كيقباد بن كيقسرو ناصر أمير المؤمنين
اقل عبده الاجل الاشرف مولانا رشيدالعلمة
والدولة والدين اياز بن عبدالله الشهابي
في شهر المعظم رمضان سنة سبع وعشرين وستة مائه

Figure 4.4. The inscription panel of Çardak caravanserai

(Source: Kutlu, 2009: 26)



Figure 4.5. Two lion figures and the inscription panel of Çardak khan

4.3.2. Donor

The donor of the Çardak Caravanserai, Esedüddin Ayaz bin Abdullah eş-Şihabi was a *mirahur* (*ahır beyi*, veterinerian) of Aleaddin Keykubad and a Seljuk viceroy. He was originally from Syria and was known as Atabek Ayaz. Arab historians, such as Ibn al-Athir and Abu al-Fida, relate that he first served the Artukid Sultan, becoming an influential bureaucrat and even marrying one of the sisters of the sultan. When the sultan died in 1200, he became the Artukid sultan for a short period, but he was dethroned. Knowing that his life was in danger, he accepted the invitation from the Seljuk Sultan Rükneddin 2 Suleyman Shah to come to Konya and to serve the Seljuks. He was invited to supervise important building projects of the Artukids. He worked on the repairs of the fortress of Sinop in 1215 and those of the Alaeddin Mosque in Konya. He was listed on the inscriptions of this important mosque as the supervisor. He employed architects and workmen from Syria for Alaeddin Mosque, and he could have done the same for the Çardak Khan. He later supervised the construction of the citadel walls of Konya. As a result, one of the gates at the southeast of the city was called the “Door of Ayaz”. From 1226 to 1228, he supervised the repairs and renovations of the citadel walls of Antalya with his name appearing once again on the inscriptions. He worked in the royal palace as the last *emir* of Alaeddin Keykubad. It is believed that he died in 1231 and thus, this khan was probably his last project.

4.3.3. Documentary Value

There are common and different characteristics of Çardak caravanserais among other caravanserais. The presence of a high vault at the center and lower ones at its sides is a typical characteristic of caravanserais repeated in Çardak khan as well. Preference of barrel vault is a common characteristic of not only caravanserais, but all building types of Seljuk era (Kuban and Yavuz, 2002: 281). It is recorded in 75 % of the building stock. This is seen in Çardak khan as well. The shelter of Çardak khan is not enriched with a dome, which is seen in some limited examples of the era. The vault profiles may be flat, depressed and semicircular, pointed and with double centers, pointed and with four centers, single or double centered tangent, one to four centered panelled. Stone usage in vaults and arches is common, but brick may also be seen. The most common is double centered and pointed profile in stone constructions. In Çardak, at the central gallery; double centered, pointed and elevated profiles; at the side galleries, double centered, pointed and depressed profiles are seen (Figure 3.10). At the pierced wall along the central gallery, majority of the arches (9 out of 12) are depressed. 5 of them are double centered and pointed, while 7 are one centered. At the pierced wall between the northern galleries, 5 out of 6 profiles are one centered, while one is double centered and depressed. At the pierced wall between the southern galleries, 4 out of 6 profiles are double centered and depressed, 1 double centered and elevated and 1 single centered. Thus; the majority are double centred and pointed as in the rest of the Seljukid monuments.

Presence of a single function underneath a single vault; e.g. resting of travelers or animals, is a general characteristic repeated in Çardak. Generally, lime mortar provides bond between vault stones. The majority of the vault stones do not touch each other, thus, they do not benefit from friction force (Kuban and Yavuz, 2002: 278). Banded barrel vaults are also common. The related arches divide long vaults running over the galleries into pieces. They generally start at ground level. In Çardak, this is the same. The distance between these reinforcing arches is about 4 to 5 meters. In Çardak, it is about 4.5 meters. There are three types of relations observed between the arches and the vaults (Kuban and Yavuz, 2002: 278). The first, which is the most widespread type, is composed of arches juxtaposing the vault at its bottom. This is generally seen in rubble stone vaults. There is only mortar between the vault and the arches. The second is arches partially (15-20 cm) within the vault section. The arches project out of the intrados and make recessment at

the extrados. There is no horizontal connection between the vault and the arches. The third is the arches that perfectly fit into the vault profile. In Çardak Khan, arches juxtapose the bottoms of the vaults. This is the widespread typology, but the section of the superstructure is not fully observed.

The exterior walls have limited voids in all Seljuk building types (Kuban and Yavuz, 2002: 274). They are narrow and long slit windows at the upper portions of the walls. In Çardak Khan, there are no slit windows in the walls. The voids within the interior walls are generally spanned with double centered, pointed arches. This is repeated in Çardak as well. Usage of cut stone at the arches of the pierced walls is a common characteristic seen in Çardak. Doors are generally spanned with depressed arches and there are often relieving arches. In Çardak, the arch of the door within the portal is a one centered, depressed arch. Its relieving arch is spanned with a double centered, depressed arch.

The walls of Seljukid period structures are three leafed: rubble stone and mortar inner core with cut stone, rough cut stone or rubble stone facings at the two sides. The quality of the facing is related with the importance of the spaces. Their thicknesses vary between 0.62 and 2.40 m. The thickness of cut stones are nearly 20 cm. Rectangular cut stones are laid horizontally. Lime mortar is used. Around special elements such as iwans and portals, iron cramps were detected. At the corners of the walls and at the connection portions with the buttresses, wall stones sometimes interlock with each other as in Emdir Khan, exterior walls are generally supported with buttresses (Kuban and Yavuz, 2002: 275, 276). The blind, thick and three leafed walls typical for the period are seen in Çardak as well. The entrance facade and the two exterior facades seen from the road side are cut stone, the other two facades are rough stone.

In general, the shelter walls are thicker than the service space ones (Yavuz, 1992: 255). In Çardak Khan, the thickness of the shelter walls vary between 1.80 and 2.20 meters, the courtyard ones are between 1.40 and 1.70 meters. There are buttresses at the walls that bear the load of the vaults and at the entrance facade as elements symbolising sturdiness; but the variation in their plan organisation throughout the building is peculiar.

The usage of compacted earth over rubble stone at the floor on ground of the shelter is seen in Çardak as in the others. Terrace roofs with earthen covering and utilization of water spouts are typical for the era. The portal makes up the highest portion of the roof and the drainage of the roof is designed together with the interior spatial organisation. The leveling of the voids between the vaults were made with earth or rubble

stone. Ceramic vessels diminishing the weight of the superstructure and relieving vaults perpendicular to the main vaults were also detected. (Kuban and Yavuz, 2002: 279, 280).

Limited usage of geometric and figurative ornamentation is also a common characteristic which Çardak shares with other cases. In service section, most of the stairs are located in the courtyard wall (Yavuz, 1992: 258), but the stairs in Çardak khan are located in the shelter wall. The majority of the stairs are constructed out of cut stone which are consoles from the juxtaposing wall (Yavuz, 1992: 258). However, they are masonry in Çardak khan. The platforms in five-naved shelters are seen in form of U (Yavuz, 1992: 263). In Çardak khan, since there is no trace of the part that will form the middle portion of U, the restitution made in the form of two independent platforms.

As a result, Çardak khan is a document reflecting the structural characteristics of Seljuk period. It repeats majority of the widespread characteristics, but there are a few peculiarities such as the two rectangular platforms, variation in the form of the buttresses, and masonry stairs providing access to the terrace roof.

CHAPTER 5

MODELING AND ANALYSES OF ÇARDAK CARAVANSERAI

It is a challenging task to properly model and analyze masonry structures. Not being homogenous in nature through the structure, constituents presenting anisotropic behavior and showing great variability in the properties and even element basis. Therefore it is hard to capture the behavior. But a general understanding of the overall behavior and in lieu of the results pin pointing the hot spots might be possible. The efforts of creating three dimensional model and conducting structural analyses of these building are presented in this chapter.

5.1. Modeling of Çardak Caravanserai with SAP2000

Generally, historical masonry structures considering different type of members acting together forming a load bearing system such as dome, vault etc. may present some difficulties in generating the masonry finite element models. These challenges include the complexity of load bearing systems and materials of these structures. Moreover, varying cross-section of the load carrying members requires some simplifications and idealization of material and geometry in the mathematical model which adds on to uncertainty (VGM, 2016:136).

In recent years, the investigation of masonry structures with numerical models has become widespread. With the developing computer technology, various approaches and methods related to modeling and analysis of masonry structures have emerged. (Dabanlı, 2008: 50).

Geometric idealizations: It is used to indicate the actual behavior of the building. For the modeling of the geometry of elements such as arches, domes and vaults, elements are composed of linear parts (Dabanlı, 2008: 50).

Material idealization: Material models in the model only considered the linear elastic portion of the materials. Due to the fact that masonry building materials are not homogeneous, composed of brick and mortar, minimum elastic strength and modulus of

overall element is considered for modelling. Thus the overall element is homogenized to a single elastic material.

The three-dimensional model is developed using the architectural plans and sections of the caravanserai, which was drawn in AutoCAD format (Bayram, et al., 2017). Then, the SAP2000 software version 20.2 is used for the modeling of this masonry structure. Before starting the modeling, the grid lines for the structure are determined from the provided drawing plans, and these gridlines served as our basis for structural elements to be models.

In finite element model, frame and shell elements are used in the formation of the model. Frame element is suitable for the modeling of columns, beams Shell element is used in the modeling of wall and dome type members.

The shell elements were divided into finite elements (mesh) of appropriate dimensions to suit the boundary conditions of the elements in the supports. Dividing is performed so that the maximum side length of each unit element was 30 cm. The pin support is defined to the nodes located at the base of the three dimensional model. Dead load is taken as mass source.

Structural elements are considered as thin and thick shell according to their thickness. The most significant difference between thin and thick shell is the inclusion of transverse shear deformation in plate-bending behavior. Thick shells take into account stresses through the thickness on the shell elements and regard shear deformation while thin shells do not. In model, thick shell elements were selected since arches, vaults and walls have thick sections.

In the literature, macro and micro finite element models are shown as modeling techniques of masonry structures. In this thesis, macro modeling technique was used because it is easier and cheaper in terms of computation. In this technique, the units forming the masonry structure are modeled by considering as a single homogenized material (Kömürcü, 2017: 29).

According to the finite element model developed the total weight of the structure is 60560 kN. In addition, the thicknesses of the external wall, internal wall and roof of the structure are considered to be 200 cm, 65 cm and 40 cm, respectively. The three dimensional model views of the structure can be seen in Figures 5.1-5.5.

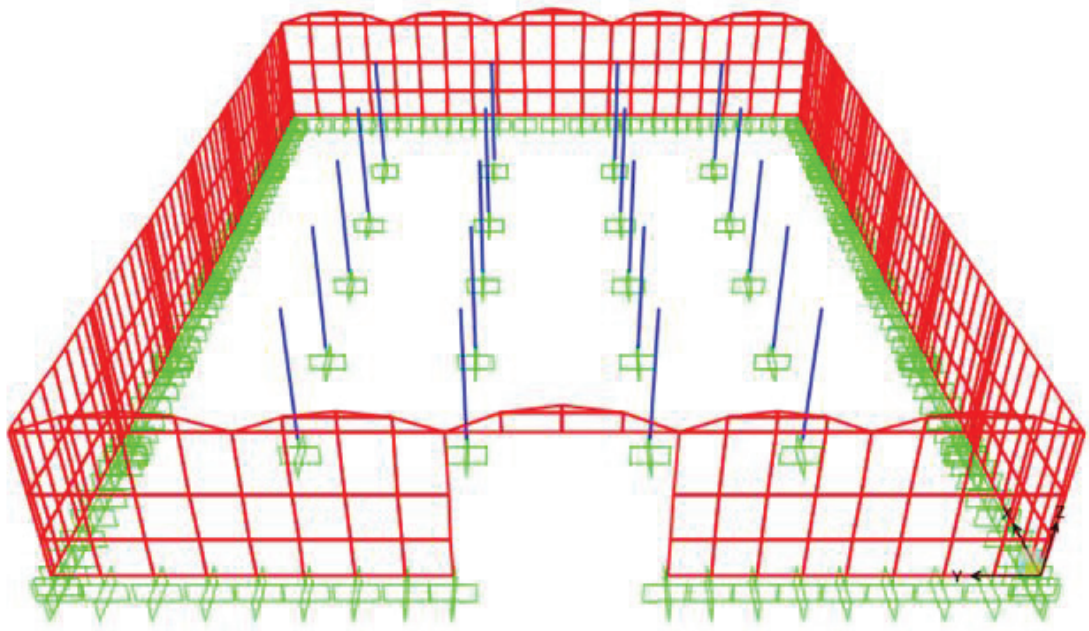


Figure 5.1. View of columns and external walls of the model

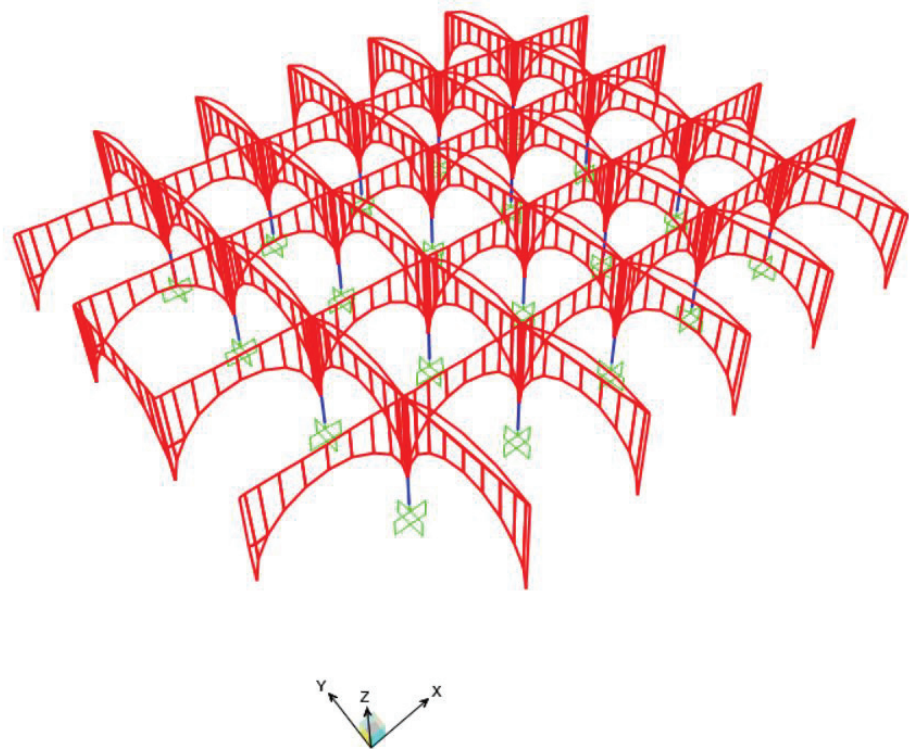


Figure 5.2. View of the model without external walls and roof

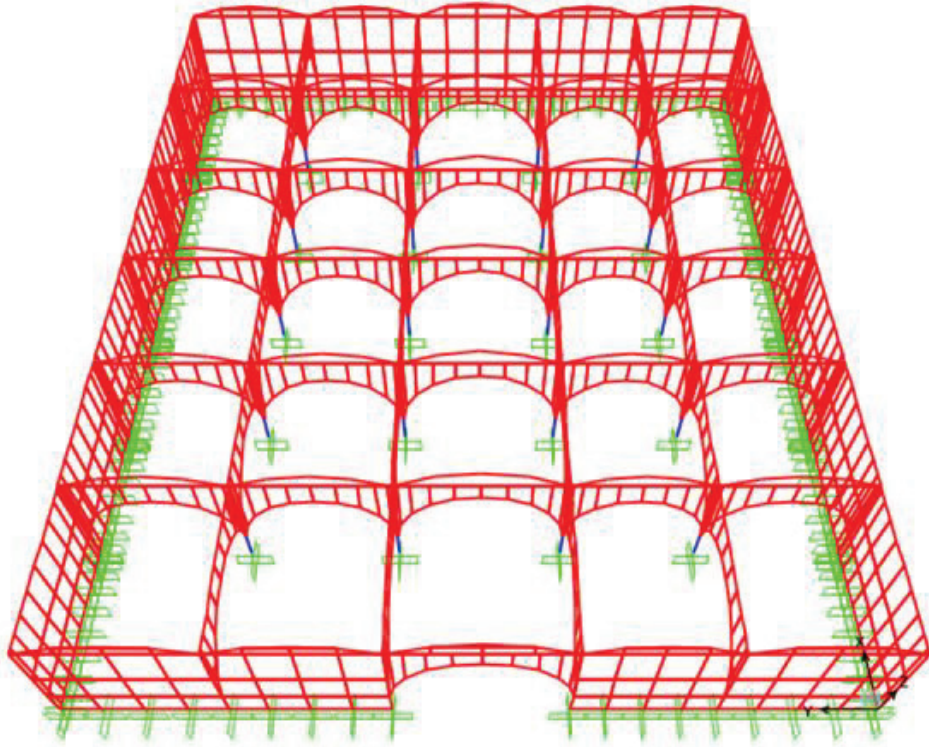


Figure 5.3. View of the model without roof

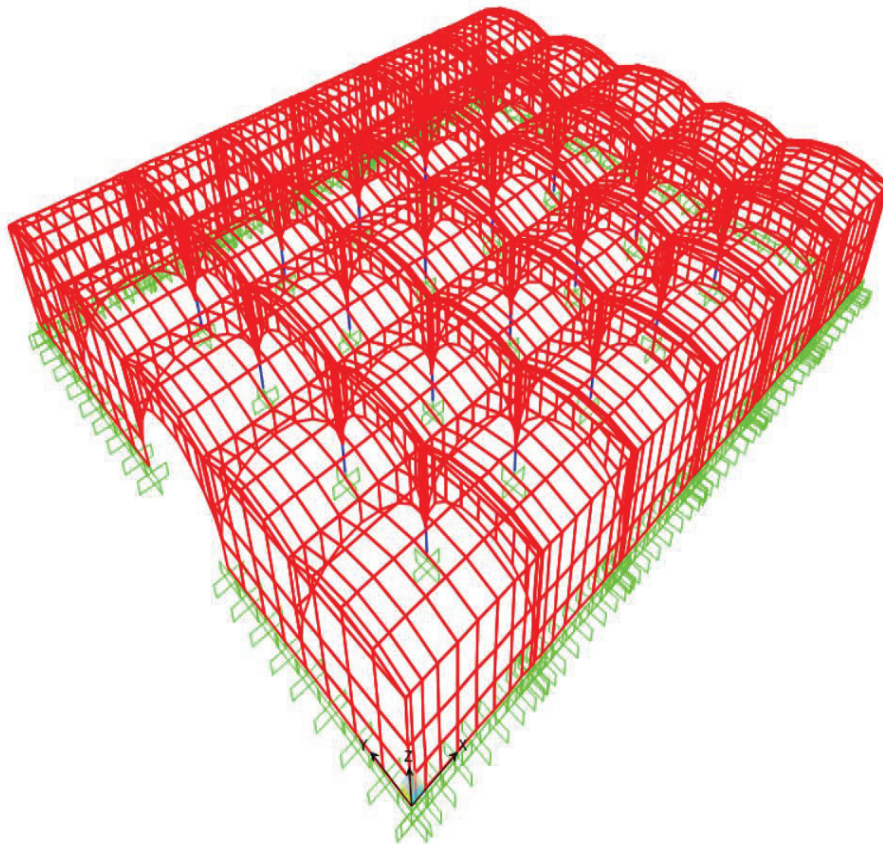


Figure 5.4. Front view of shell model of Çardak caravanserai

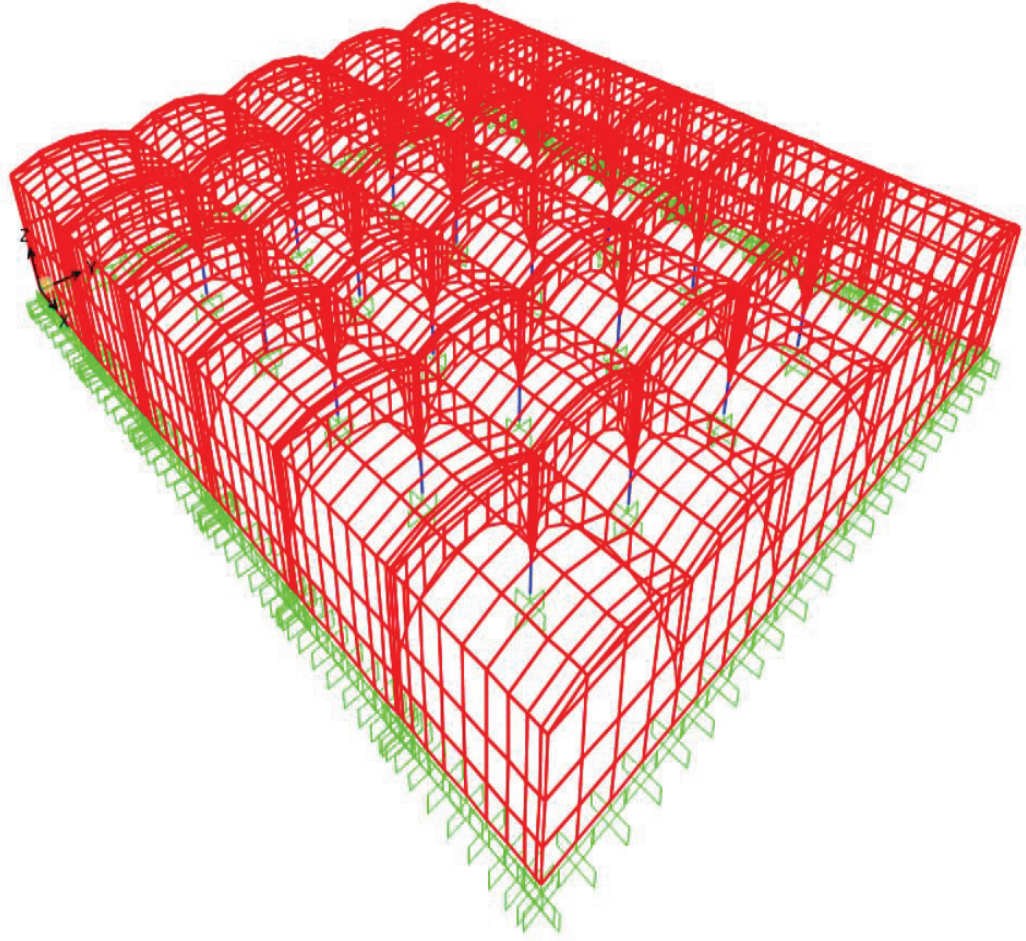


Figure 5.5. Back view of shell model of Çardak caravanserai

5.2. Determination of The Material Properties of The Structure

In the literature, according to TS EN 1952-1, the modulus of elasticity of the bearing walls can be determined by tests (TS EN 1952-1, 2000). The modulus of elasticity, E_{wall} , is found by $750f_k$ (f_k is characteristics compressive strength) when these tests are not performed. The wall shear modulus, G_{wall} , is taken as 40% of the modulus of elasticity (TSC, 2018: 247). In this case, the modulus of elasticity of the bearing wall can be calculated when the characteristics compressive strength, f_k , is found.

According to the management manual of earthquake risks for historical buildings in Turkey 2016, the mechanical properties of the material of the structures, being unavailable by tests, can be determined from Table 5.1 (VGM, 2016: 125). Mechanical characteristics of Çardak caravanserai were selected from the management manual of earthquake risks for historical buildings since material tests were not conducted.

Table 5.1. Mechanical characteristics of masonry wall materials

(Source: VGM, 2016: 125; Magenes and Penna, 2009: 190)

Masonry typology	f_m (MPa)	τ_o (kPa)	E (MPa)	G (MPa)	w (kN/m ³)
Irregular stone masonry	0.6~0.90	20~32	690~1050	115~175	19
Uncut stone masonry	1.1~1.6	35~51	1020~1440	170~240	20
Cut stone with good bonding	1.5~2.0	56~74	1500~1980	250~330	21
Soft stone masonry	0.8~1.2	28~42	900~1260	150~210	16
Dressed ashlar stone masonry	3.0~4.0	78~98	2340~2820	390~470	22
Solid brick masonry	1.8~2.8	60~92	1800~2400	300~400	18

According to table 5.1, the material of the masonry structure can be taken as cut stone and following properties are given below.

- E_{wall} (Modulus of Elasticity)= 1500 MPa (for cut stone)
- G_{wall} (Shear Modulus)= 600 MPa (0.40 E_{wall})
- γ (Poisson's Ratio)= 0.25

Compressive strength of the structure, f_c were taken as 1.5 MPa for other structure elements except vaults and 0.9 MPa for vaults, respectively (VGM, 2016: 125).

Tensile strength of masonry structure can be calculated as 10% of compressive strength of the structure (Koçak, 1999). So, tensile strengths, f_t were taken as 0.15 MPa and 0.09 MPa.

According to Turkish Seismic Design Code, the wall safety shear stress is calculated by Eq.5.1 below (TSC, 2018).

$$\tau_m = \tau_o + \mu\sigma \quad \text{Eq.5.1}$$

τ_m (the wall safety shear stress)= 0.40 MPa.

τ_0 (the wall cracking safety stress)= 0.10 MPa (TSC, 2018: 89).

μ (friction coefficient)= 0.4 (constant).

σ (the wall vertical stress)= 0.75 MPa.

Mass modeling is taken into account for the wall vertical stress. It can be calculated by using the average axial stress of the vertical load.

$\tau_m = 0.10 + 0.4 (1.5/2) = 0.40$ MPa (for stone masonry).

$\tau_m = 0.10 + 0.4 (0.9/2) = 0.28$ MPa (for vaults).

Specified strength values for material type of the structure are given in Table 5.2.

Table 5.2. Strength values for material type

Material Type	Compressive Strength (MPa)	Tensile Strength (MPa)	Shear Strength (MPa)
Stone Masonry	1.5	0.15	0.40
Vaults	0.9	0.09	0.28

5.3. Load Cases

The gravity loads are taken into account as dead load for the structure. Live loads are not considered since the the load bearing system is not affected by the live load. In load combinations, dead load and earthquake loads in x and y direction are considered only. Mass per unit volume of the bearing walls of masonry structure is taken as 21 kN/m³ (VGM, 2016: 125).

Also, there is a layer of fill on the vaults. It has a mass and vertical force applied to vault. The layer of fill is thin in the upper section of the vaults. Fill thickness increases in the end sections. In order to simplify and incorporate this difference in loads, each vault should be considered as divided into two areas. The equivalent vertical force should be distributed to these shell elements by finding the average fill thickness for blue and red sections in Figure 5.6. So, in each section, the multiplying of the average of the fill thicknesses at both ends of the section and fill unit weight gives load distributed over the area. Fill material was used as rubble stone. Its mass per unit volume is 19 kN/m³ (VGM, 2016: 125). Rubble fill is loaded under the dead load as area distributed load on the vaults.

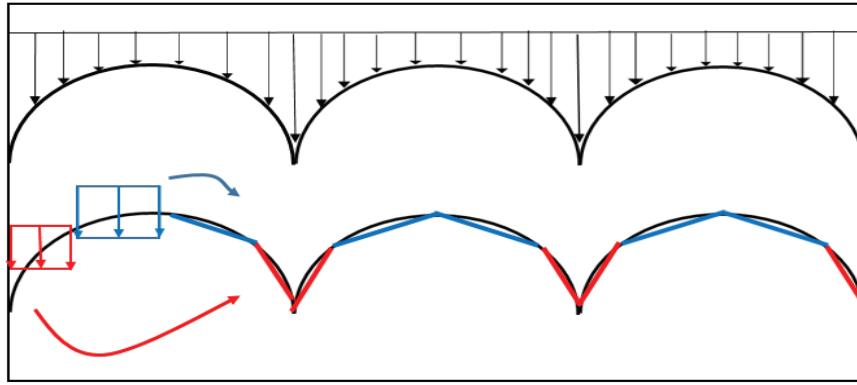


Figure 5.6. Determination of load distributed over the area

According to Turkish Seismic Design Code 2018, load combinations used for the stress controls of load bearing walls are indicated in Table 5.3.

Table 5.3. Load Combinations

Load Case	Dead	SpectX	SpectY
Load Type	Linear Static	Response Spectrum	Response spectrum
Load combinations	Combination Factors		
Dead+Ex+0.3Ey	1	1	0.3
Dead+Ex-0.3Ey	1	1	-0.3
Dead-Ex+0.3Ey	1	-1	0.3
Dead-Ex-0.3Ey	1	-1	-0.3
Dead+0.3Ex+Ey	1	0.3	1
Dead-0.3Ex+Ey	1	-0.3	1
Dead+0.3Ex-Ey	1	0.3	-1
Dead-0.3Ex-Ey	1	-0.3	-1

5.4. The Assessment and Results of Structural Analyses

The model consisting of shell and frame elements is analyzed with the SAP2000 software. The engineering comments are made depending on the results of the analysis. In this title, static under self-weight, modal and response spectrum analyses are presented. Also, the results of these analyses are evaluated.

5.4.1. Self-Weight Analysis

Static analyses under the structure self-weight are carried out to estimate the structure's current state of stress. According to these stress levels, the high stress locations are determined.

Shell stress definitions in SAP2000 are provided in Figure 5.7.

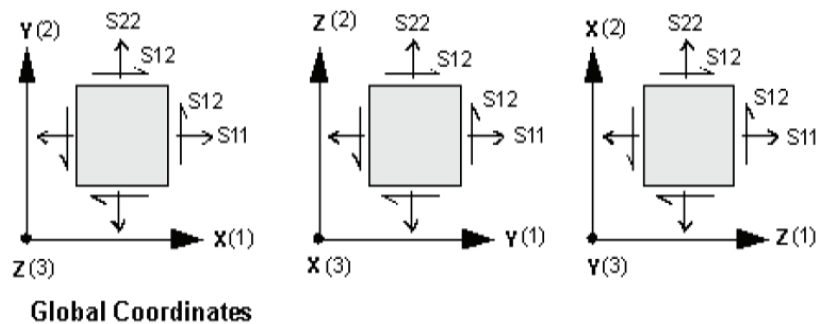


Figure 5.7. Normal and shear stresses on shell element

(Source: SAP2000)

In self-weight analysis, the displacements, normal and shear stresses of the caravanserai under dead load were evaluated. The global Z direction displacements are presented in Figure 5.8. The highest vertical displacements are 6.62 mm to the negative Z direction, in vaults. These displacements in the vaults are reduced up to 3.5 mm in the middle. Also, the displacements are seen up to 2.5 mm in the arches. The global Y direction displacements of the khan are shown in Figure 5.9. The maximum displacements are found as 1.61 mm to the positive Y direction, on the left side vaults and main exterior walls. The maximum negative Y direction displacements are also 1.61 mm on right side vaults and main exterior walls. In general, the structure is not at risk for displacement under its self weight.

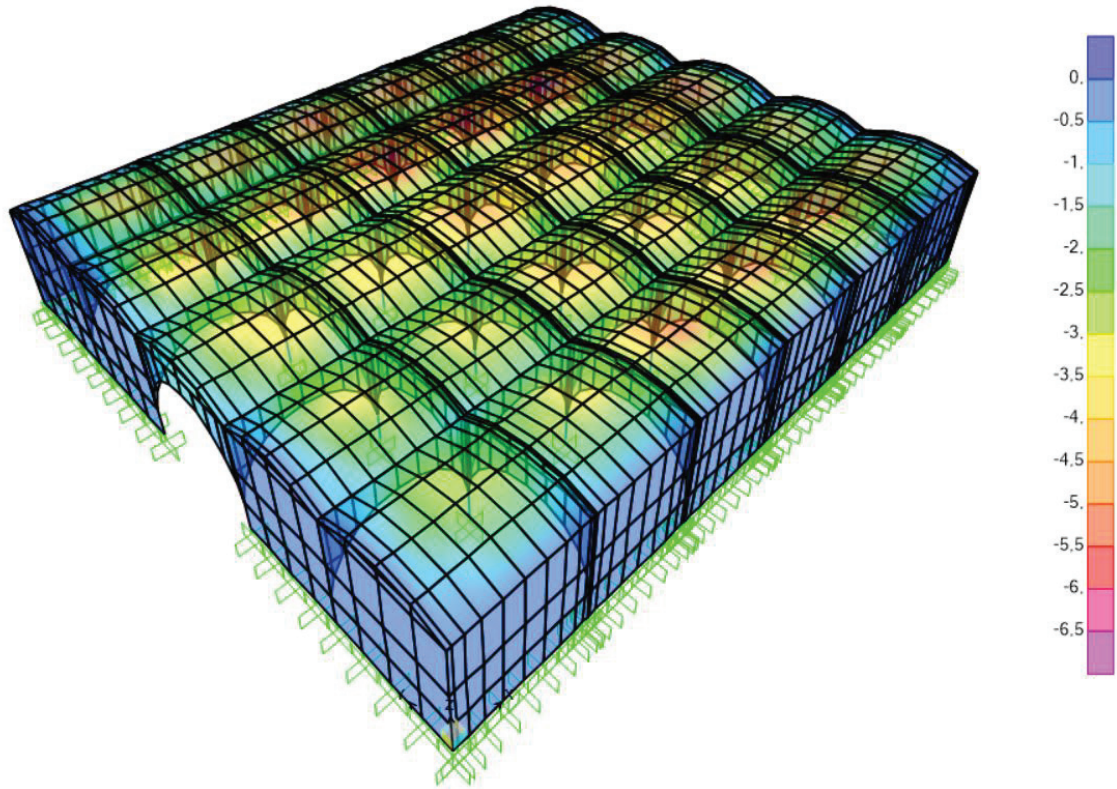


Figure 5.8. The displacement of Çardak khan in Z direction under self-weight (mm)

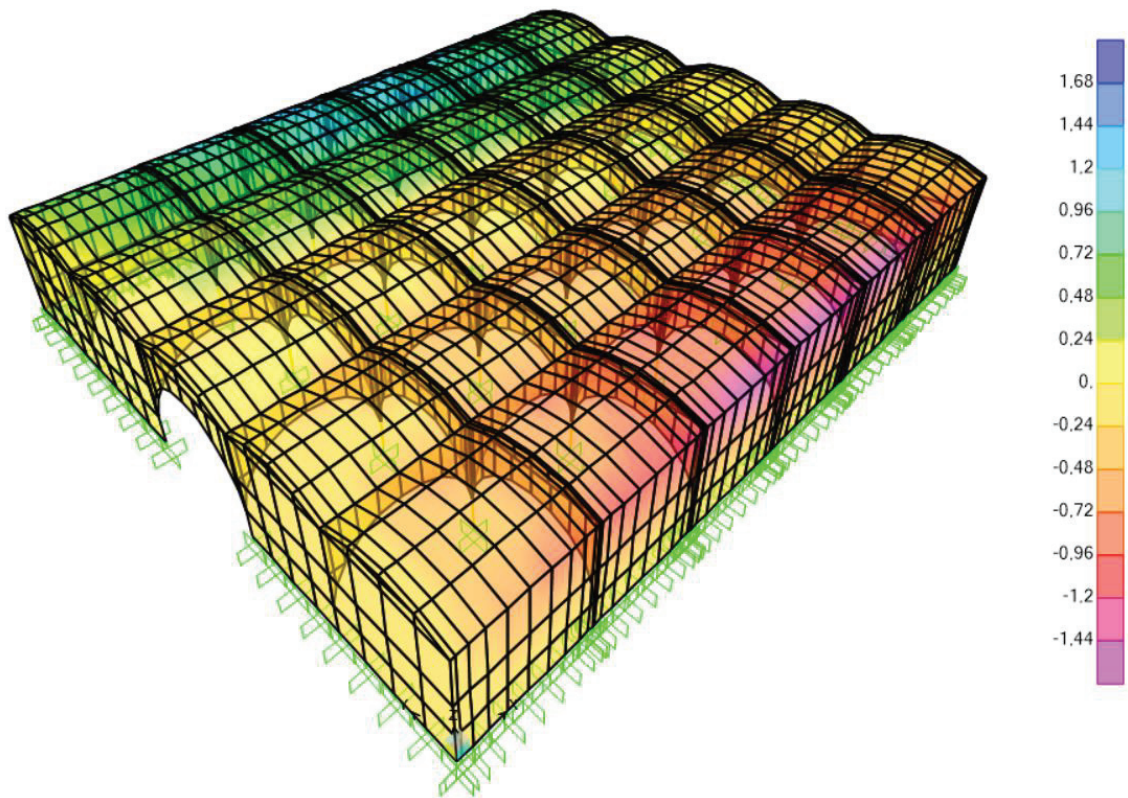


Figure 5.9. The displacemof Çardak khan in Y direction under self-weight (mm)

Normal stresses S11 under self weight are indicated in Figure 5.10, Figure 5.11 and Figure 5.12. The maximum normal stresses S11 are -0.88 MPa (compressive) and 0.064 MPa (tensile). The highest compressive stresses occur in arches, see Figure 5.14. Some tensile stresses are seen in main exterior walls, masonry columns, front and back of the vaults and in the middle section on the arches, see Figure 5.13 and Figure 5.14. The compressive and tensile strength of stone masonry and vaults are greater than the maximum normal stresses.

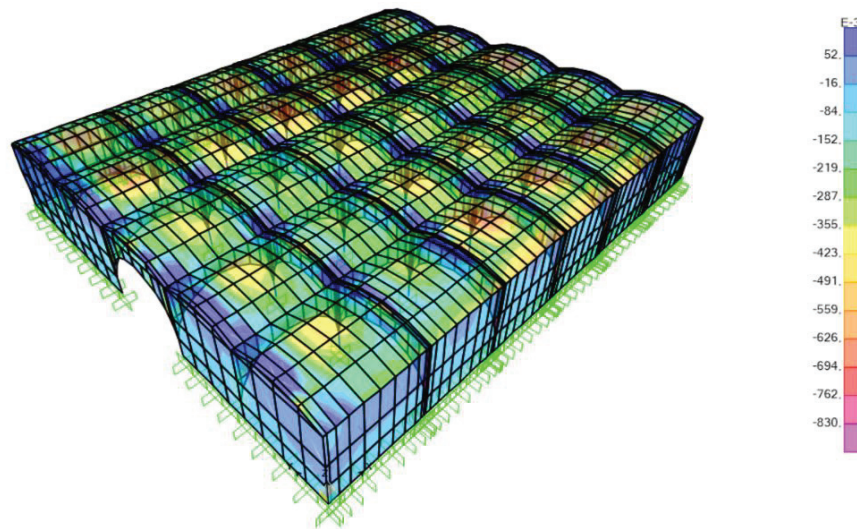


Figure 5.10. Normal stresses S11 developed under self-weight (10^{-3} MPa)

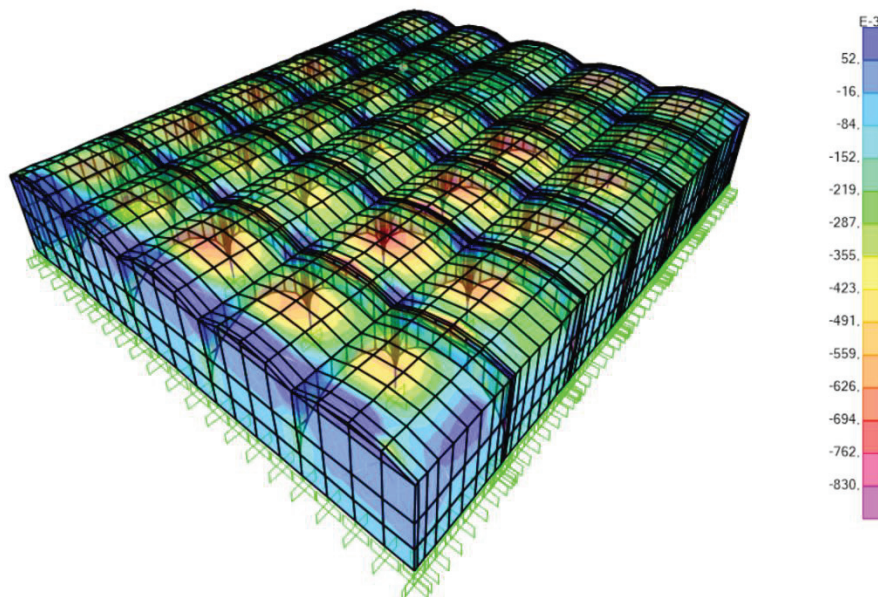


Figure 5.11. Back side of normal stresses S11 developed under self-weight (10^{-3} MPa)

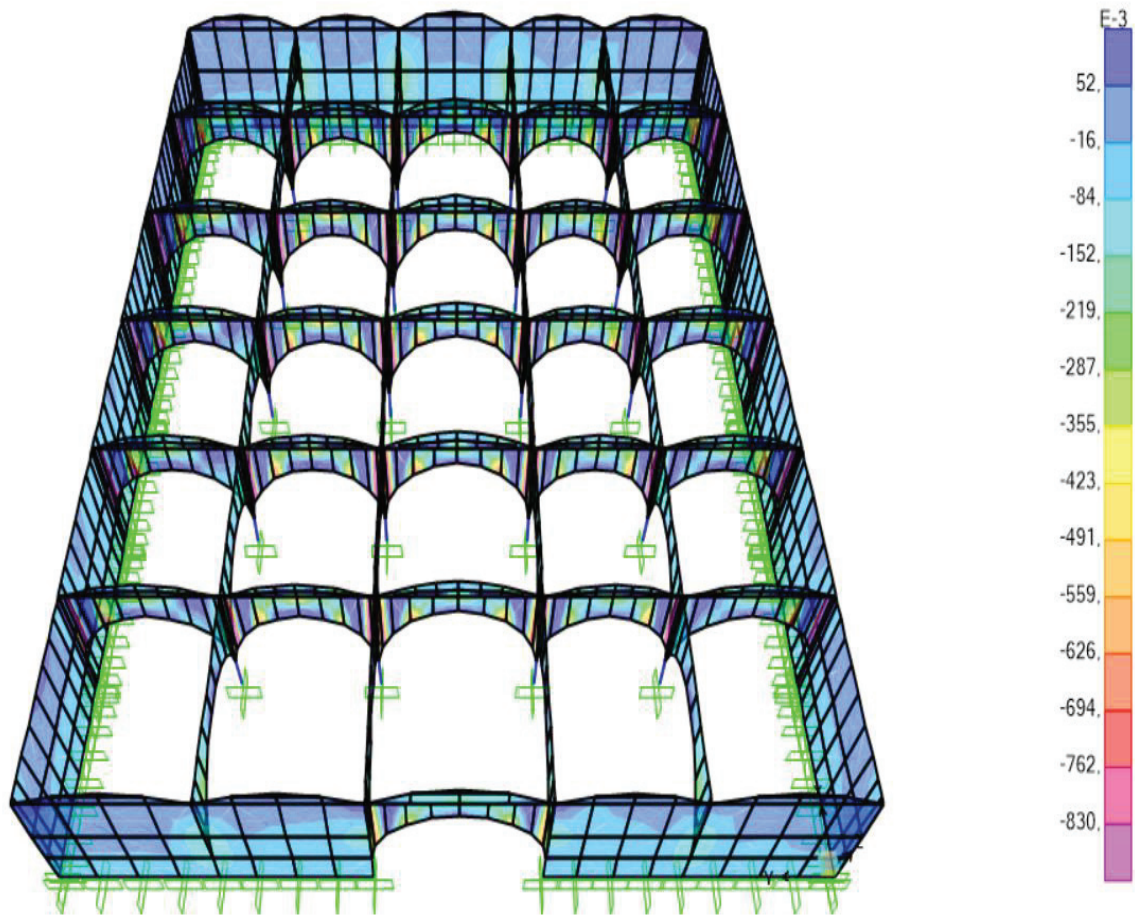


Figure 5.12. View of arches, columns and interior walls of normal stresses, S11 developed under self-weight (10^{-3} MPa)

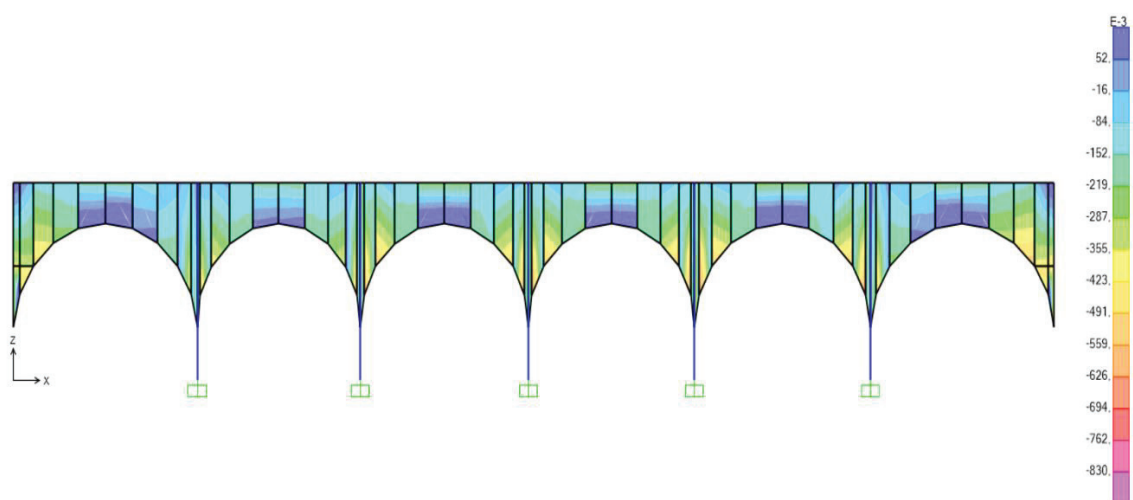


Figure 5.13. Detail of arches on xz plane at $y = +5$ m axis for normal stresses, S11 under self-weight

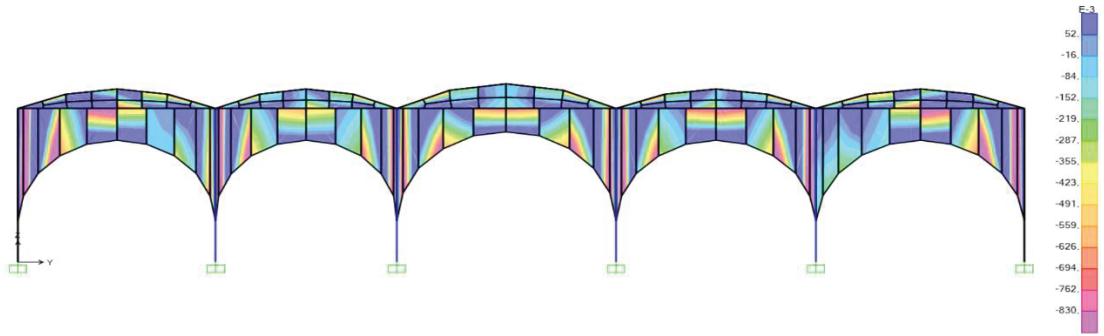


Figure 5.14. Detail of arches and vaults on yz plane at $x = +5$ m axis for normal stresses, S11 under self-weight

The maximum normal stresses S22 are -0.96 MPa (compressive) and 0.072 MPa (tensile), respectively, see Figure 5.17, Figure 5.18 and Figure 5.19. The highest compressive stresses are observed in the vaults. There are high compressive stresses in main exterior walls, interior walls and detail of the arches, see Figure 5.15 and Figure 5.16.

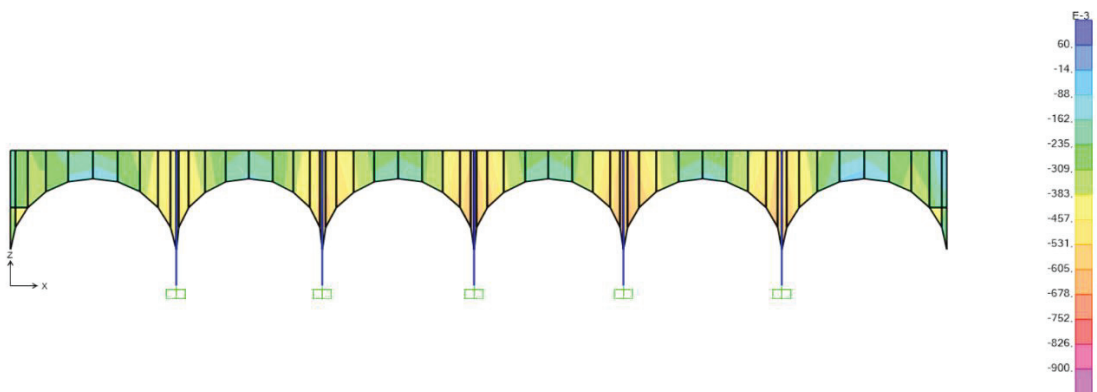


Figure 5.15. Detail of arches on xz plane at $y = +2.5$ m axis for normal stresses, S22 under self-weight

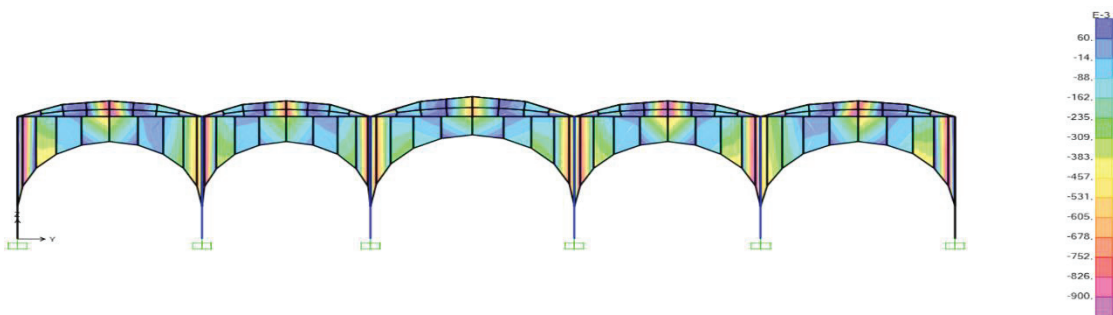


Figure 5.16. Detail of arches and vaults on yz plane at $x = +2.5$ m axis for normal stresses, S22 under self-weight

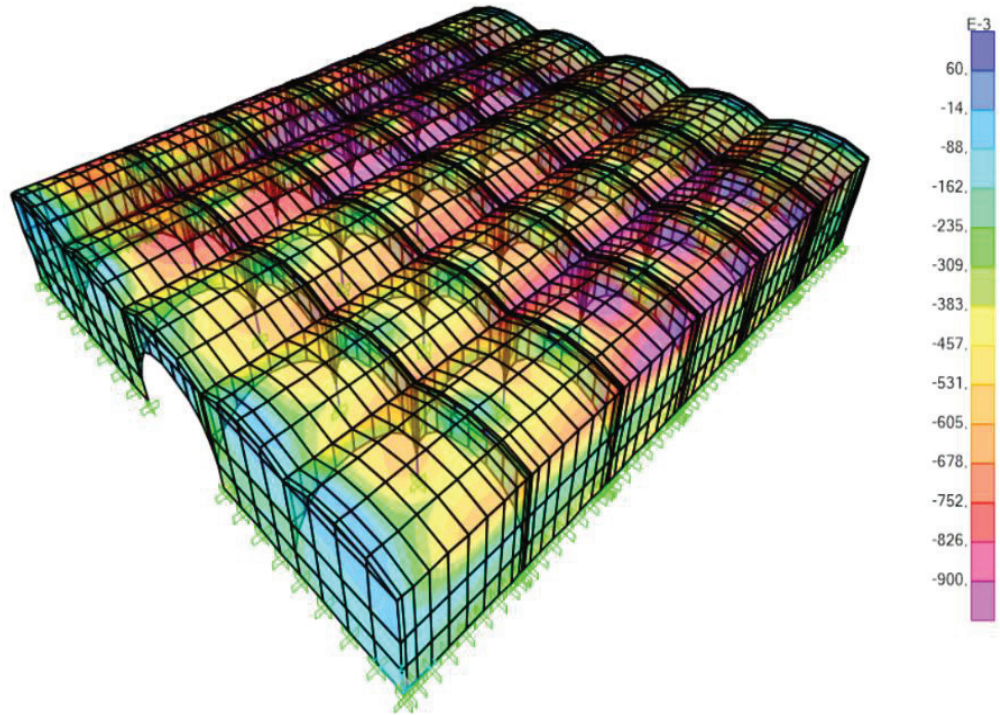


Figure 5.17. Normal stresses S22 developed under self-weight (10^{-3} MPa)

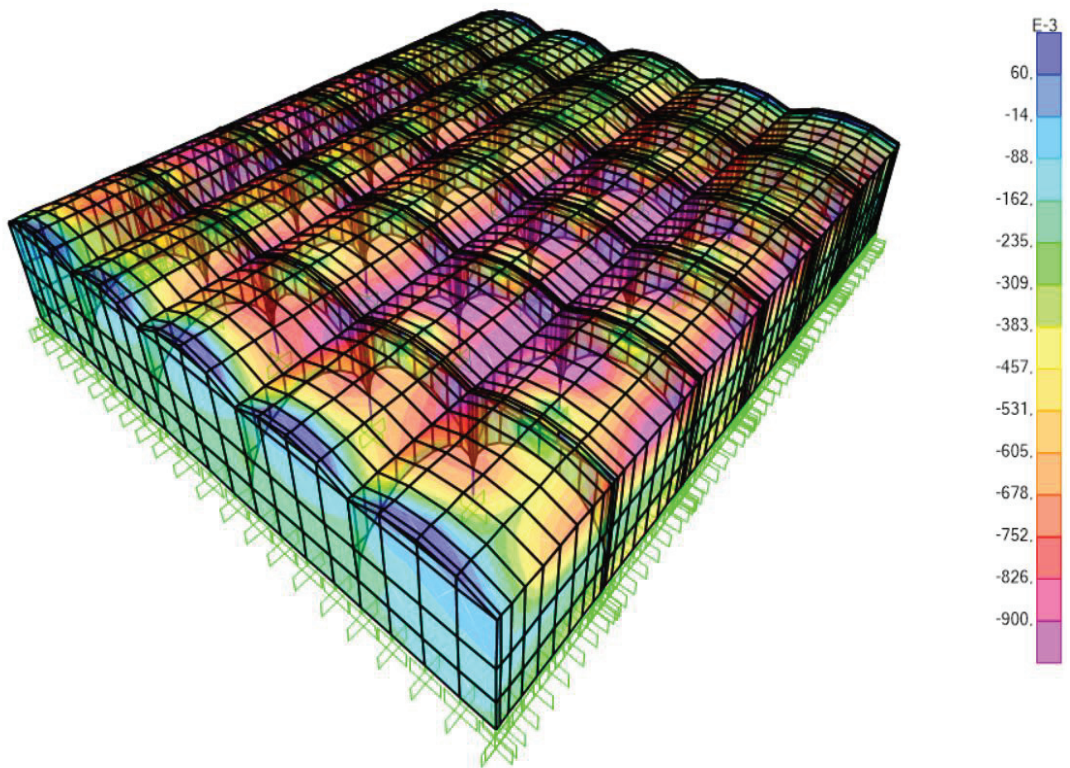


Figure 5.18. Back side of normal stresses S22 developed under self-weight (10^{-3} MPa)

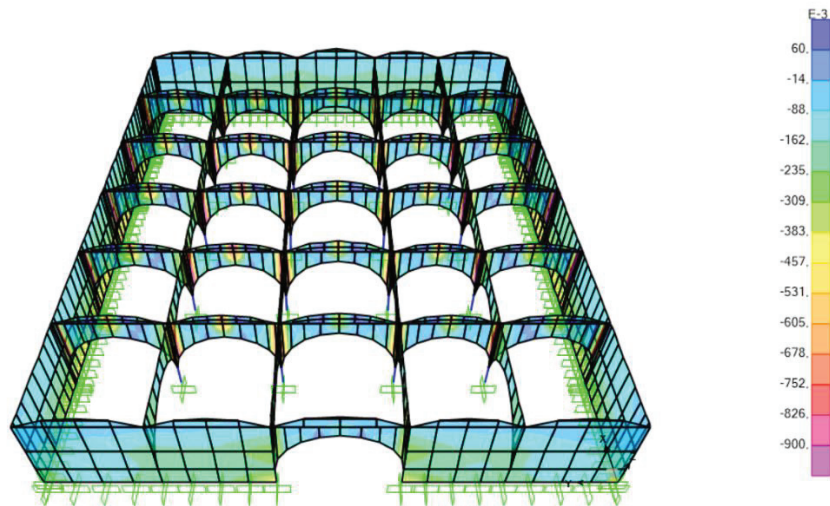


Figure 5.19. View of arches, columns and interior walls of normal stresses S22 developed under self-weight (10^{-3} MPa)

Shear stresses S12 under self-weight are clearly given in Figures 5.20, 5.21 and 5.22. The maximum shear stresses S12 are 0.27 MPa in masonry columns, interior walls, arches and some vault areas, see Figure 5.23 and Figure 5.24. These stresses occur at the top of arches in negative direction. The main exterior walls and the remaining vault areas have lower shear stress values. It seems that the maximum shear stresses do not exceed the shear strength in Table 5.2.

Consequently, Çardak caravanserai can be considered below the limits under its self-weight. The maximum normal and shear stress values, specified above, do not exceed the compressive, tensile and shear strength assumed in current structural case.

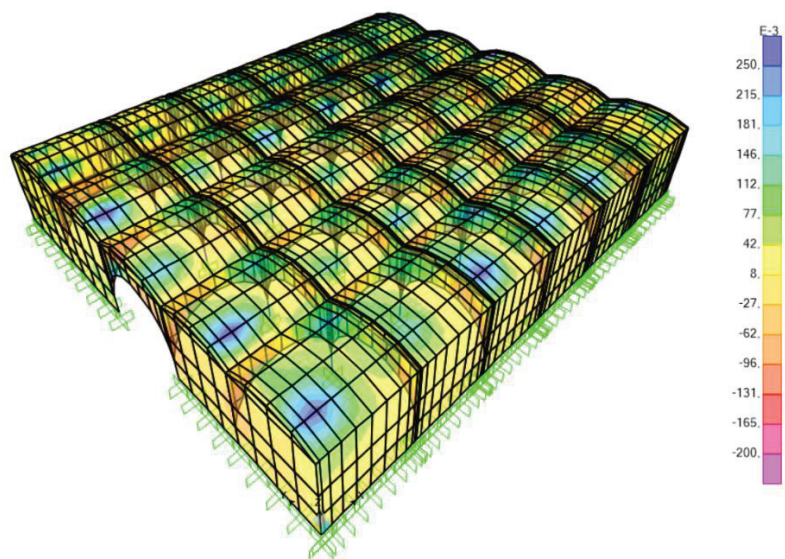


Figure 5.20. Shear stresses S12 developed under self-weight (10^{-3} MPa)

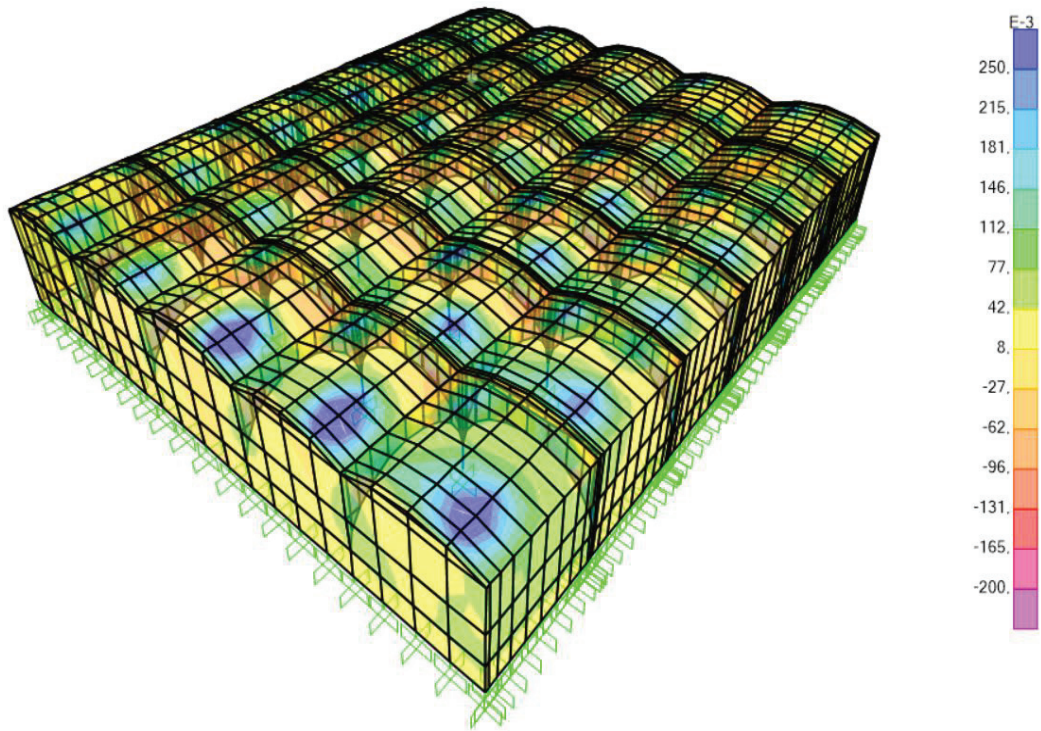


Figure 5.21. Back side of shear stresses S12 developed under self-weight (10^{-3} MPa)

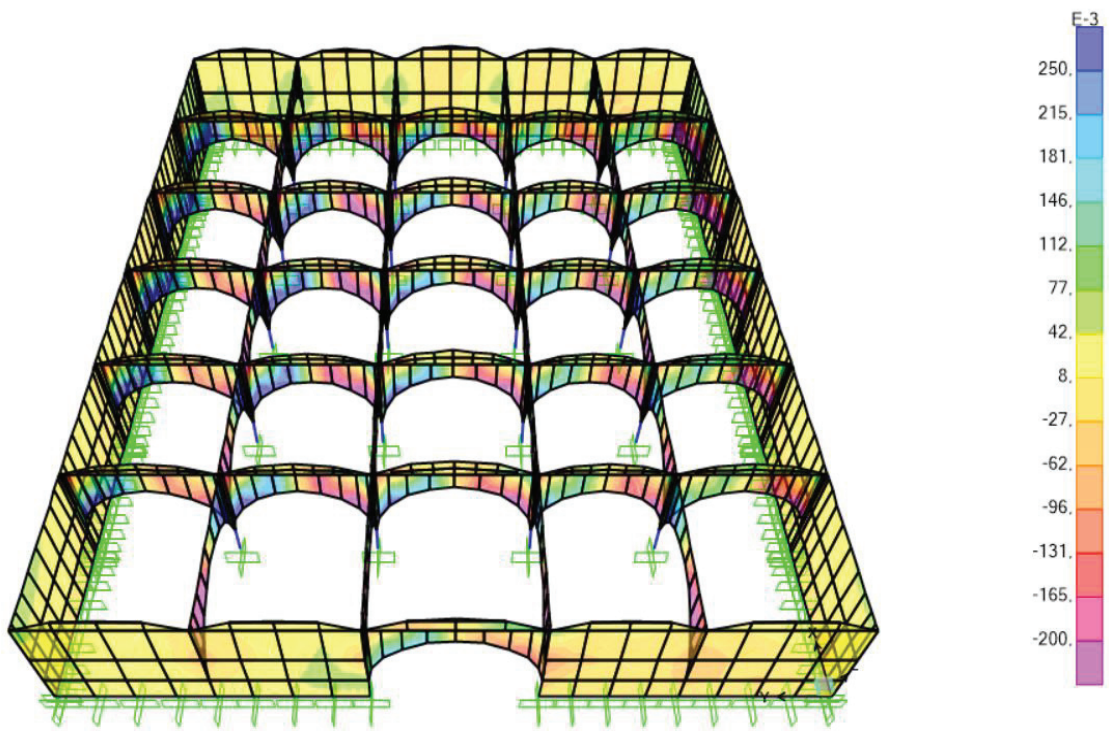


Figure 5.22. View of arches, columns and interior walls of shear stresses S12 developed under self-weight (10^{-3} MPa)

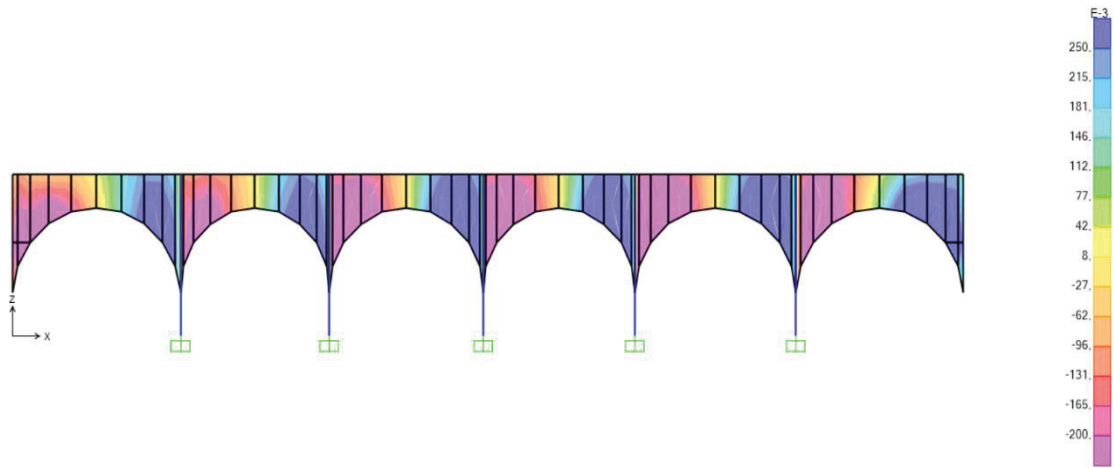


Figure 5.23. Detail of arches on xz plane at $y = +2.5$ m axis for shear stresses, S12 under self-weight

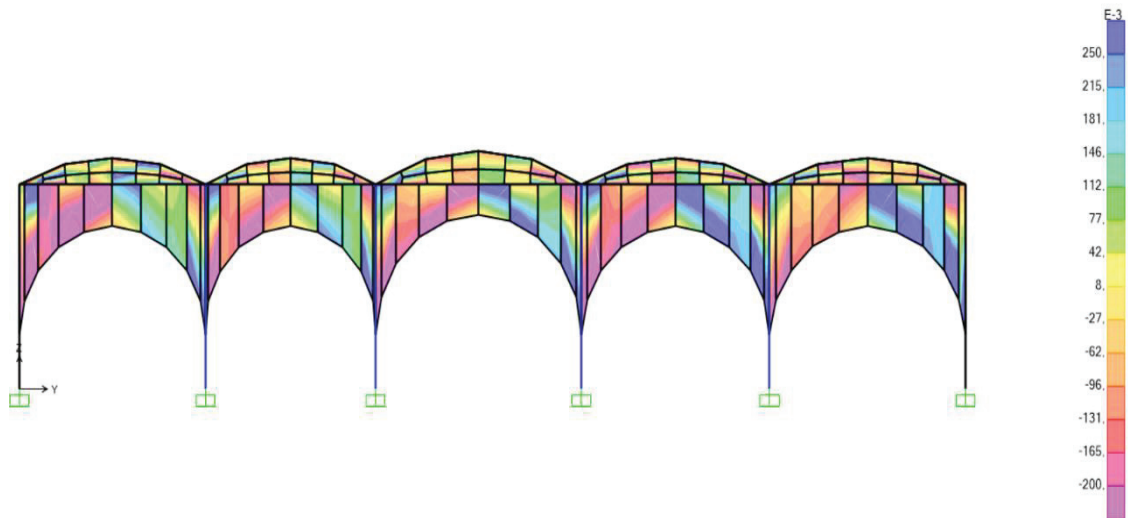


Figure 5.24. Detail of arches and vaults on yz plane at $x = +2.5$ m axis for shear stresses, S12 under self-weight

5.4.2. Modal Analysis

Modal analysis is a dynamic analysis method, which determines a structure's free vibration periods, mode shapes and mass participation ratios (Dadanlı, 2008: 86). Free vibration periods and modes can be determined by using mass and stiffness matrices of the building system. It is expressed by the mass participation ratio that the vibration in the mode shapes, which belongs to a free vibration rate, can affect the total mass of the structure and incorporate it into the oscillating movement (Uğuz, 2016: 78).

The shell model of Çardak Khan was subjected to modal analysis with SAP2000 software. Modal analysis was performed upto 100 modes to reach higher cumulative mass participation ratios.

According to Turkish Siesmic Design Code 2018, a lower limit is given for the sum of the modal masses. In modal calculation methods, the number of adequate vibration modes to be taken into account is to be determined that the sum of the effective masses calculated for each mode is never less than 95% of the building total mass, in each of x and y earthquake directions considered perpendicular to each other. However, all modes with a contribution of more than 3% are to be considered (TSC, 2018: 53).

As a results of the analysis, the mass participation ratios of the first 100 modes are 80% in the x and y directions. There is 67% mass participation ratio and reflects the displacement in y direction in the first mode. The second mode has 70% mass participation and reflects the displacement in x direction. In the first modes, lateral displacement movement is observed in x and y directions. After the fourth mode, the torsional modes are observed. The periods and mass participation ratios for the first ten modes are given below (Table 5.4).

Table 5.4. The periods and mass participation ratios for the first ten modes

Mode	Period (sec)	U_x	U_y	U_z	Total U_x	Total U_y	Total U_z	Total R_x	Total R_y	Total R_z
1	0.199	0.00	0.67	0.00	0.00	0.67	0.00	0.00	0.00	0.00
2	0.171	0.701	0.00	0.00	0.701	0.67	0.00	0.00	0.00	0.00
3	0.159	0.00	0.00	0.029	0.701	0.67	0.029	0.00	0.00	0.00
4	0.146	0.00	0.00	0.014	0.701	0.676	0.043	0.019	0.00	0.00
5	0.137	0.00	0.00	0.001	0.701	0.676	0.044	0.019	0.00	0.05
6	0.134	0.00	0.00	0.00	0.702	0.677	0.044	0.021	0.015	0.212
7	0.132	0.001	0.00	0.00	0.703	0.678	0.045	0.026	0.026	0.243
8	0.129	0.00	0.00	0.00	0.704	0.678	0.045	0.031	0.026	0.244
9	0.125	0.00	0.00	0.146	0.704	0.679	0.191	0.035	0.037	0.244
10	0.124	0.00	0.03	0.001	0.704	0.71	0.192	0.214	0.039	0.257

The mode shapes of the first ten of the caravanserai free vibration modes obtained by modal analysis are given below (Figure 5.25-5.34).

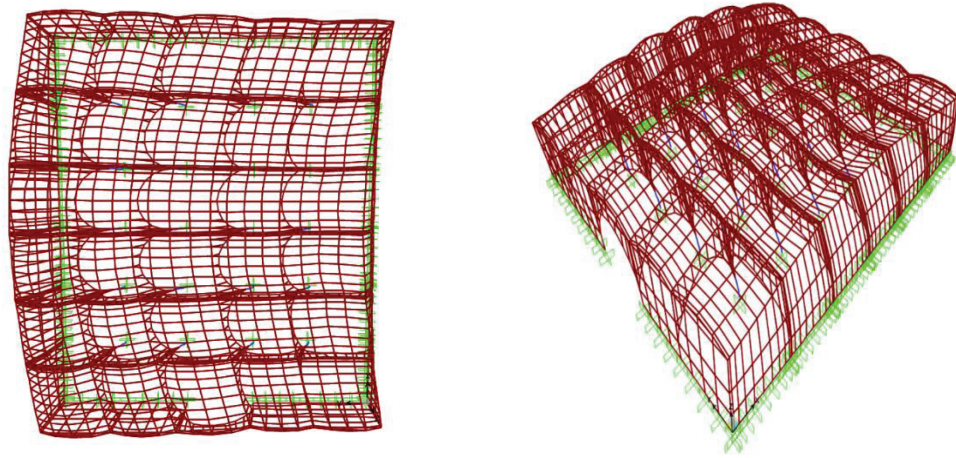


Figure 5.25. Deformed shape of 1. dominant mode ($T = 0.199$ sec.)

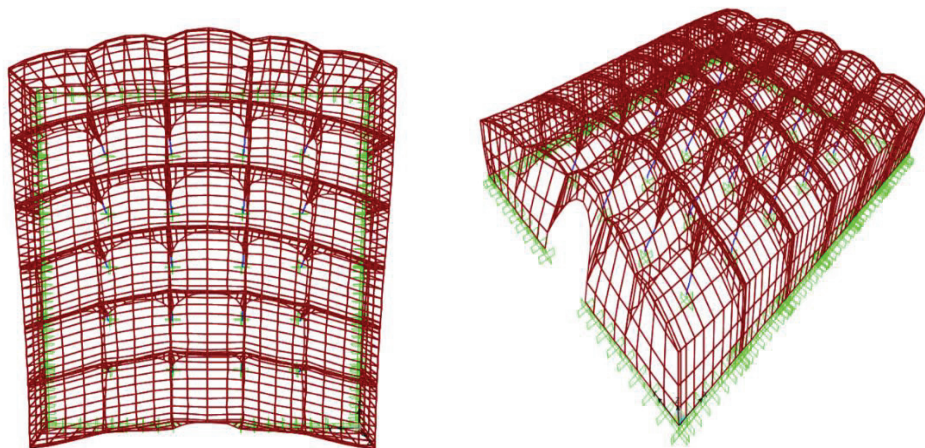


Figure 5.26. Deformed shape of 2. dominant mode ($T = 0.171$ sec.)

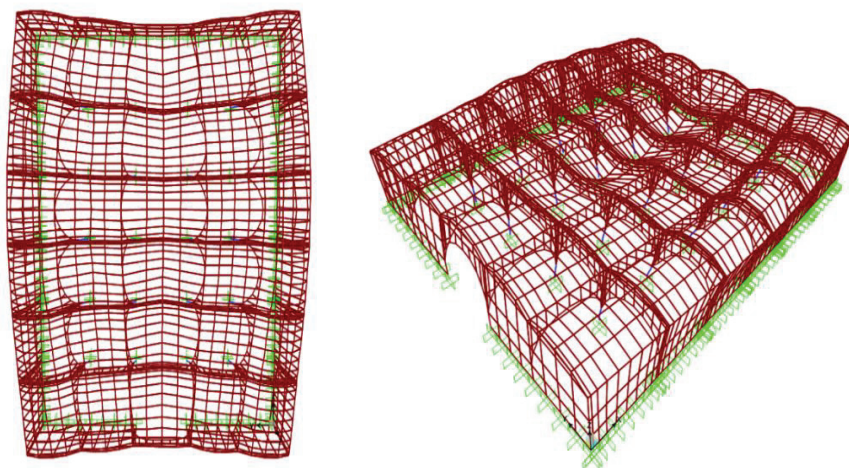


Figure 5.27. Deformed shape of 3. mode ($T = 0.159$ sec.)

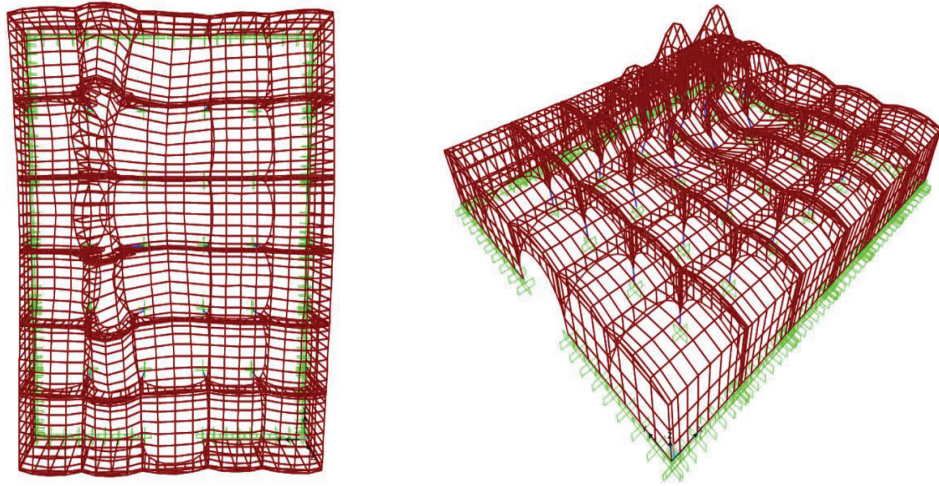


Figure 5.28. Deformed shape of 4. mode ($T = 0.146$ sec.)

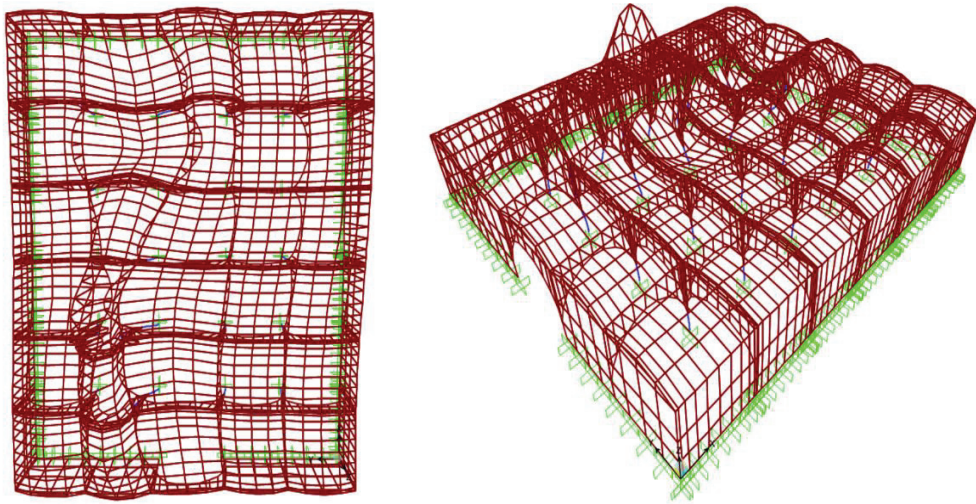


Figure 5.29. Deformed shape of 5. mode ($T = 0.137$ sec.)

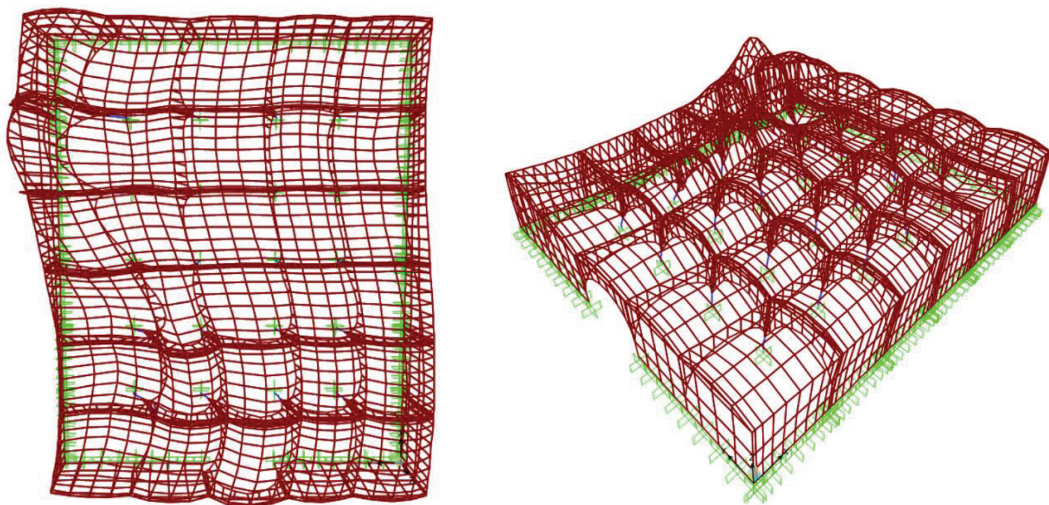


Figure 5.30. Deformed shape of 6. mode ($T = 0.134$ sec.)

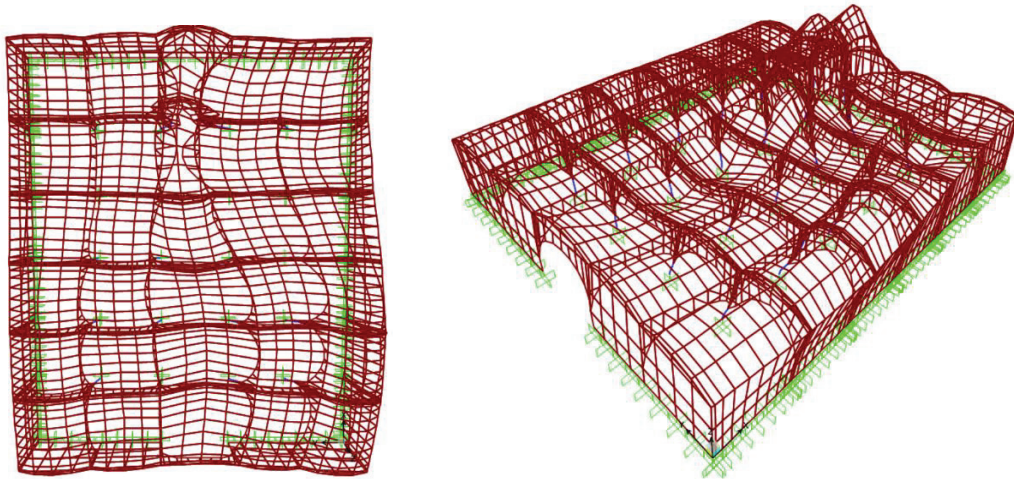


Figure 5.31. Deformed shape of 7. mode ($T = 0.132$ sec.)

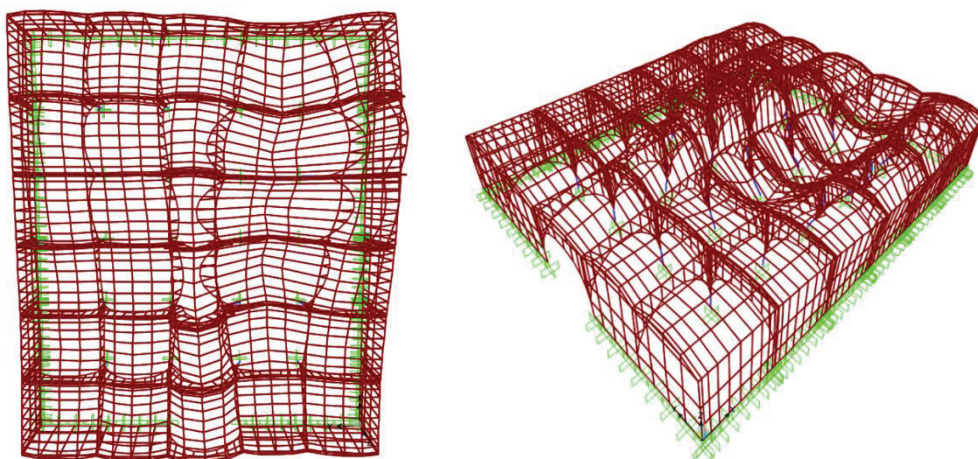


Figure 5.32. Deformed shape of 8. mode ($T = 0.129$ sec.)

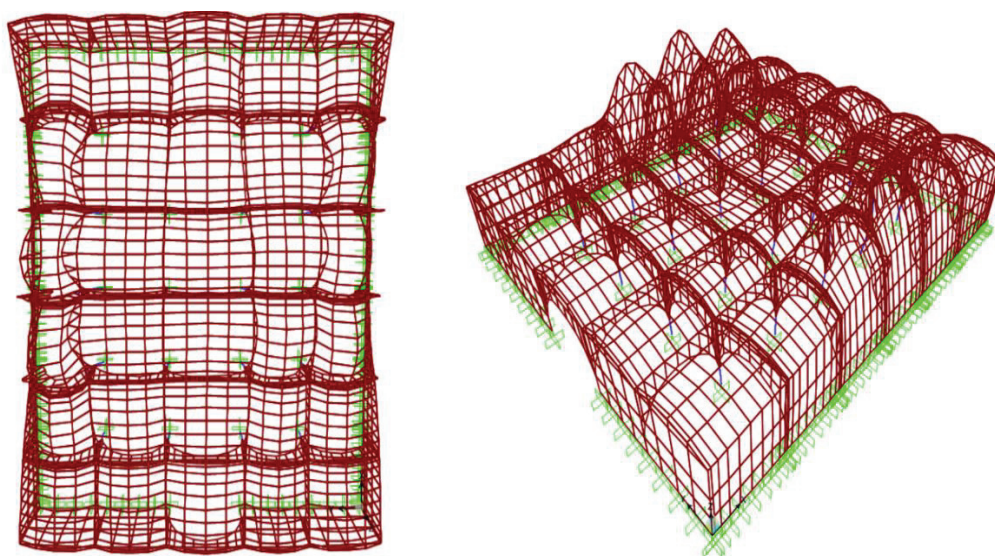


Figure 5.33. Deformed shape of 9. mode ($T = 0.125$ sec.)

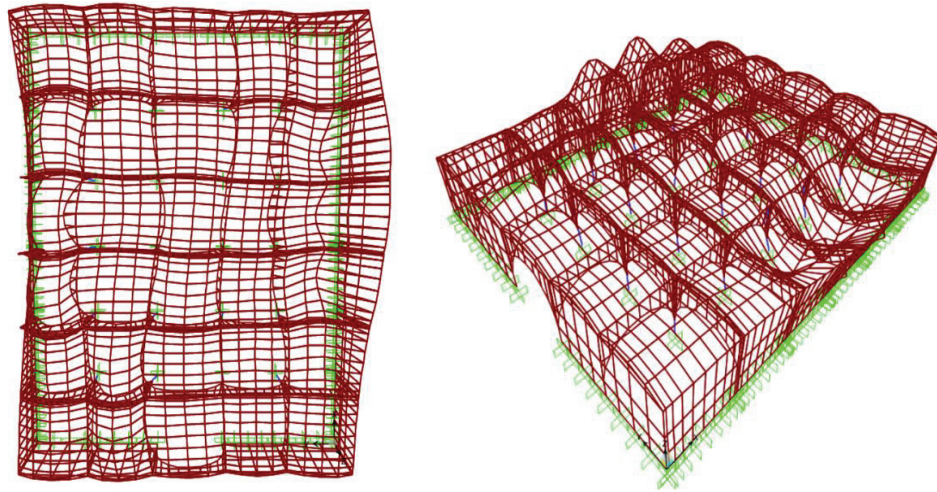


Figure 5.34. Deformed shape of 10. mode ($T = 0.124$ sec.)

5.4.3. Response Spectrum Analysis

Response spectrum analysis is based on the principle of mode superposition, which determines the dynamic behavior of the structure. In this method, the behavior of the structure is expressed depending on two translatory and a rotational motion, with the assumption that the structure mass is gathered at certain levels (Dadanlı, 2008: 87).

Turkish Seismic Design Code 2018 was used in order to analyze the behavior of the structure. Site parameters were taken from “AFAD” as the seismic code stated.

According to the earthquake ground motion level used for the analysis, the code defined design earthquake with an average recurrence interval of 475 years which corresponds to the probability of occurrence of 0.10 in 50 years (TSC, 2018: 7). Also, no field observation has been conducted on the soil properties of the location. According to soil properties in Denizli, the soil type is assumed as ZD which composes of dense sand, gravel or very dense clay layers (Akyol et al., 2007: 202; TSC, 2018: 343).

The parameters used in the calculation of earthquake forces are given below.

- I (Building Importance Factor) is taken as 1 (TSC, 2018: 15) (for other structures).
- R (Carrier System Behavior Coefficient) is taken as 2.5 (TSC, 2018: 38) (for unreinforced masonry buildings).
- D (System Overstrength) is taken as 1.5 (TSC, 2018: 38) (for unreinforced masonry buildings).
- Damping ratio is taken as 0.05 (TSC, 2018: 8).
- S_s (Short Period Spectral Acceleration Coefficient) is taken as 0.873 (Source: AFAD).

- S_1 (Spectral Acceleration Coefficient for 1 sec Period) is taken as 0.207 (Source: AFAD).
- PGA (Peak Ground Acceleration) is taken as 0.364 g (Source: AFAD).

As specified in Turkish Seismic Design Code, linear calculation methods are equivalent seismic load and modal calculation methods. Mode superposition method was used as modal calculation method in response spectrum analysis. The analyses are conducted for X and Y directions of the structure as separate load combinations.

In response spectrum analysis, Complete Quadratic Combination (CQC) is selected for modal combination. The square root of the sum of the squares (SRSS) is also used for directional combination.

Figures taken from AFAD and SAP2000 are presented below (Figure 5.35- 5.37).

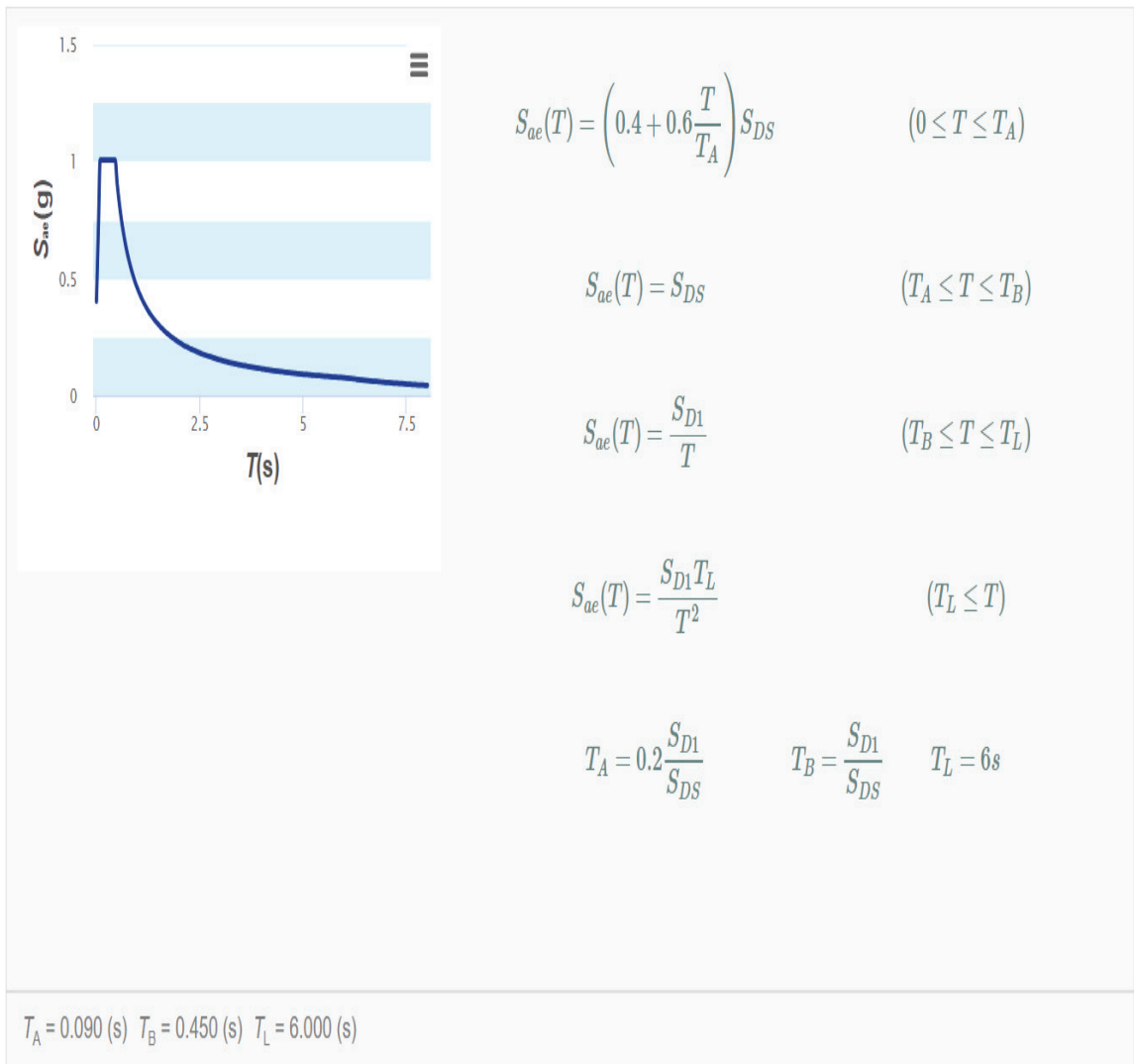


Figure 5.35. Horizontal elastic design spectrum

(Source: AFAD)

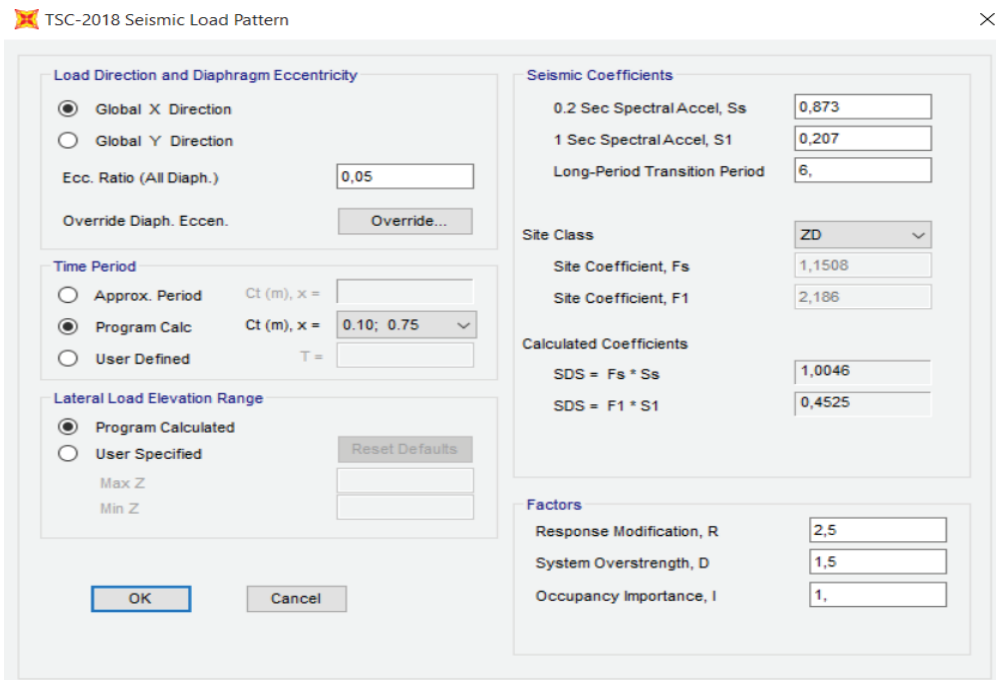


Figure 5.36. The seismic load pattern in x and y direction

(Source: SAP2000)

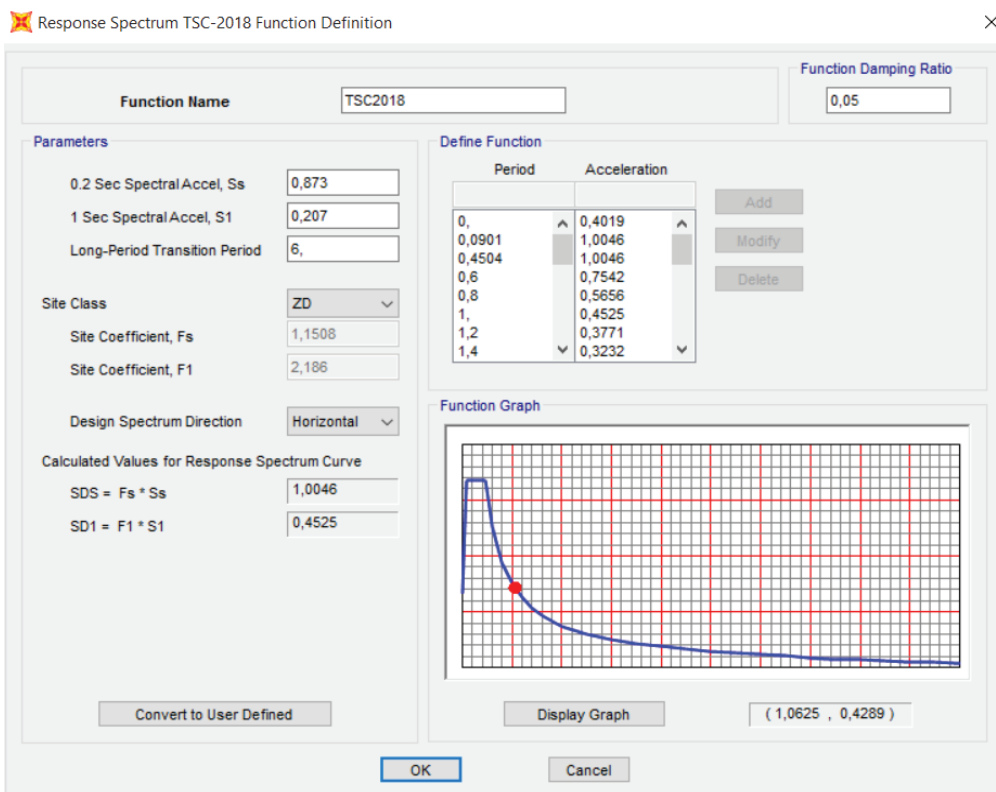


Figure 5.37. Response spectrum function

(Source: SAP2000)

5.4.3.1. Results of Response Spectrum Analysis

The structure should be assessed for 8 combinations given in Table 5.4. Assessment and results of the displacements, normal and shear stresses were presented for the analysis. The structure is symmetrical in two directions. Therefore, for the combinations of $Dead \pm Ex \pm 0.3Ey$, $Dead + Ex + 0.3Ey$ is selected as representative. Similarly for $Dead \pm Ey \pm 0.3Ex$, $Dead + Ey + 0.3Ex$ is selected as representative. These two load combinations are examined and presented below.

Under $Dead + Ex + 0.3Ey$ load combination, the maximum vertical displacement is 8.7 mm in the negative z direction on the right and left vaults, see Figure 5.38. Relatively higher vertical displacements are seen on vaults in other areas, in arches and interior walls, see Figures 5.38, 5.40 and 5.41. No displacements are found at the back side of the structure, see Figure 5.39. In addition, there are almost no displacements in exterior walls and columns or these vertical displacements are very low values there.

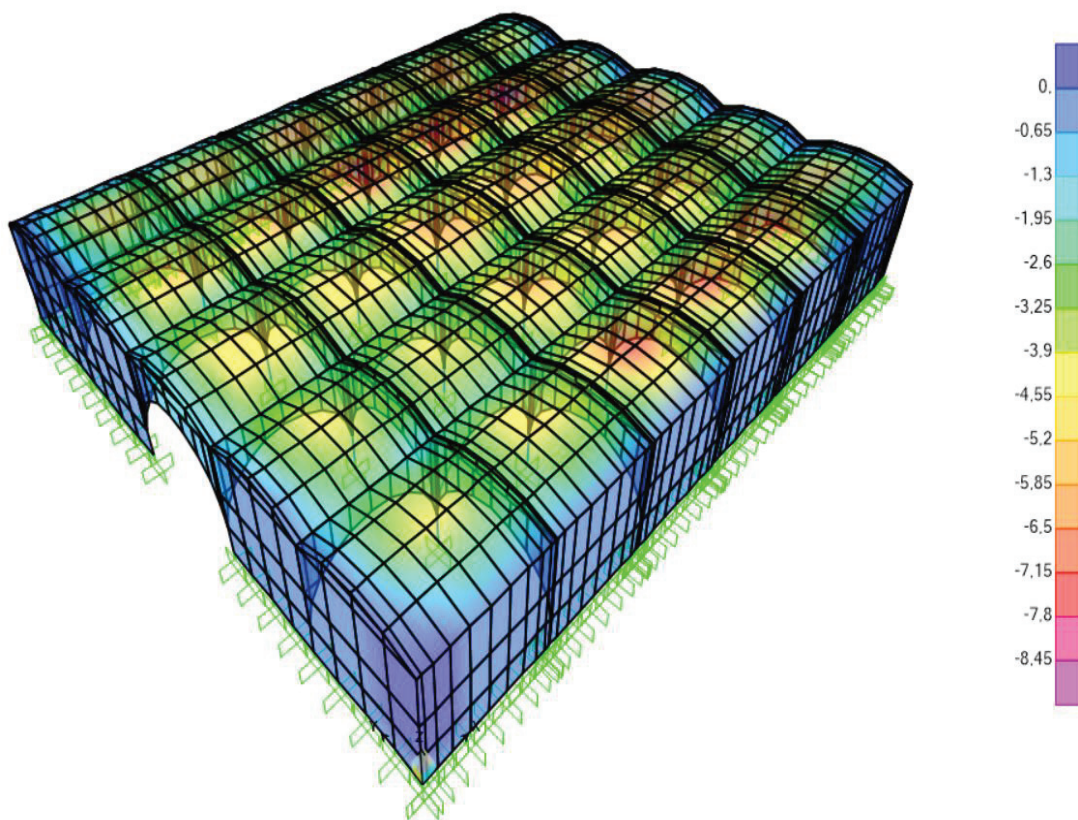


Figure 5.38. The vertical displacement in Z direction under $Dead + Ex + 0.3Ey$ load combination

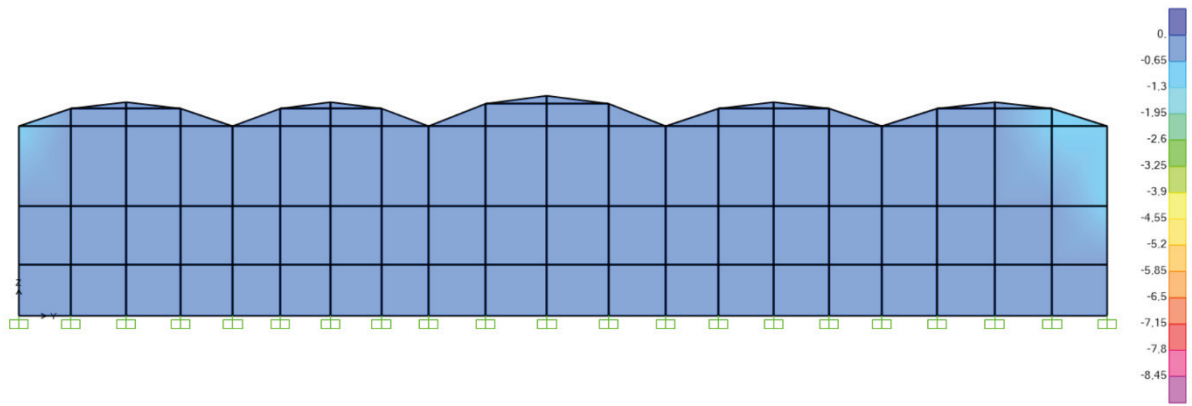


Figure 5.39. The vertical displacement of back side in Z direction on yz plane at $x = +15$ m axis under Dead+Ex+0.3Ey load combination

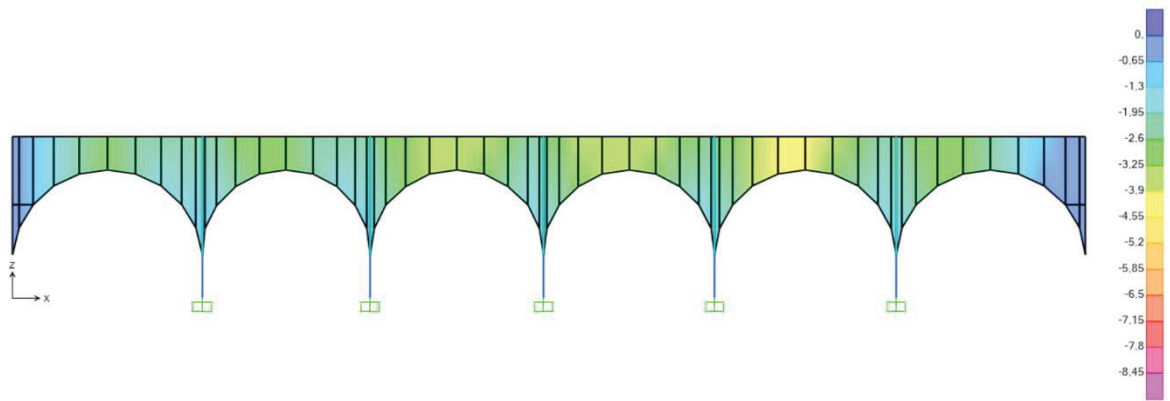


Figure 5.40. The vertical displacement of arches in Z direction on xz plane at $y = +2.5$ m axis under Dead+Ex+0.3Ey load combination

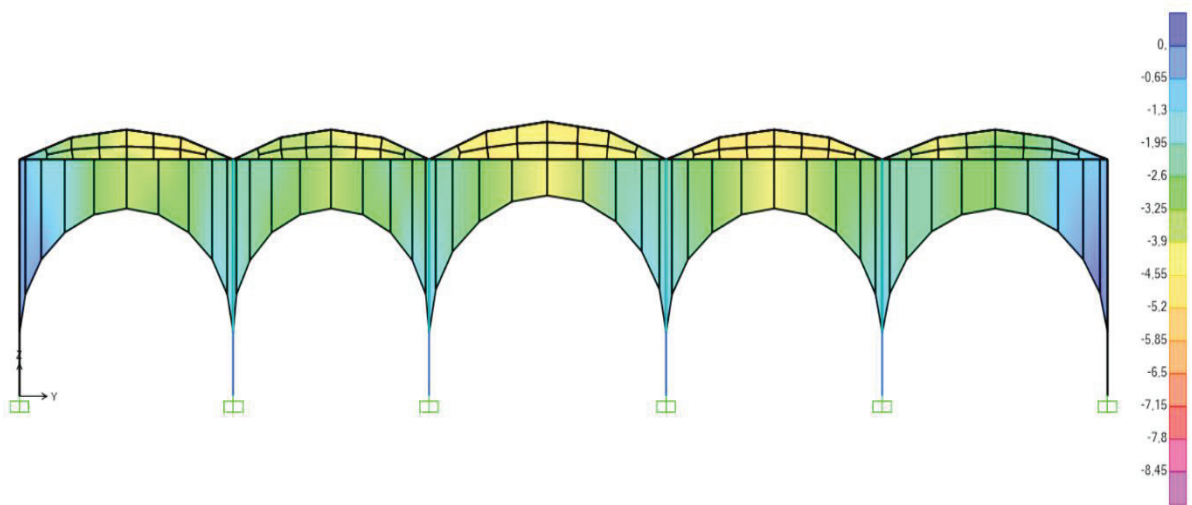


Figure 5.41. The vertical displacement of section in Z direction on yz plane at $x = +2.5$ m axis under Dead+Ex+0.3Ey load combination

Under Dead+Ex+0.3Ey load combination, the maximum displacement is 10.46 mm in the front and middle of vaults and this displacement is 10.6 mm at the back of vaults, see Figure 5.42 and Figure 5.41. Displacements vary from -3 to 3 mm, with the exception of the vaults at the back of the structure, see Figure 5.43. The displacement levels on arches and vaults has been presented in Figures 5.44-5.45. Also, the displacements are not significant in exterior walls and columns.

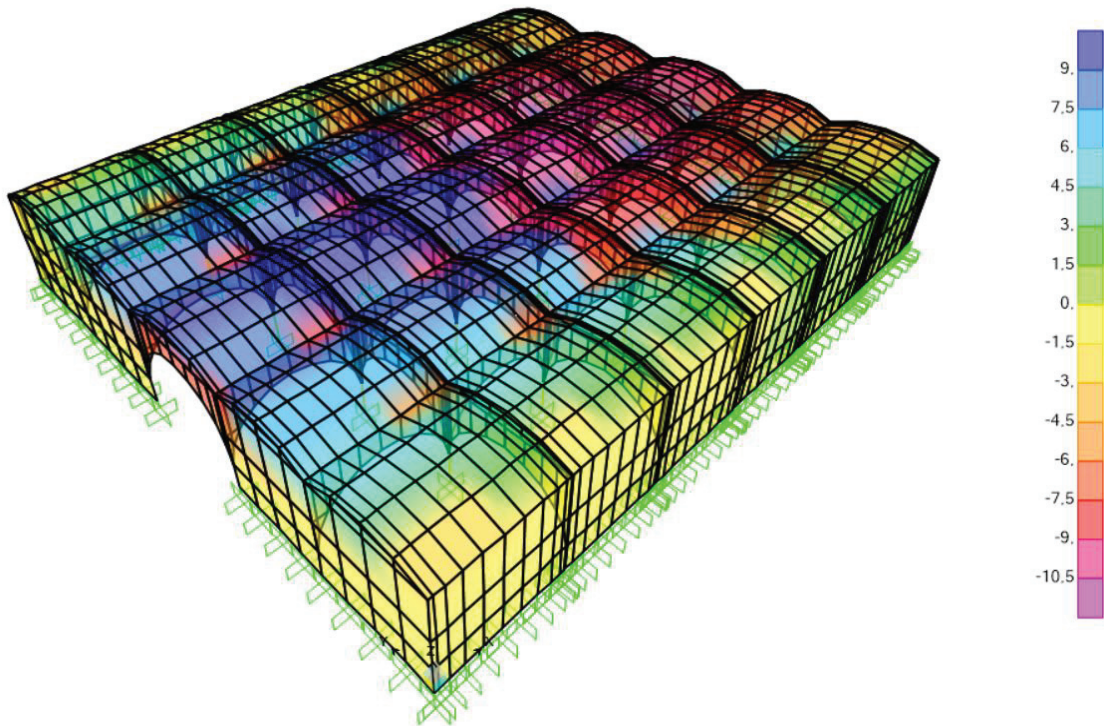


Figure 5.42. The displacement in X direction under Dead+Ex+0.3Ey load combination

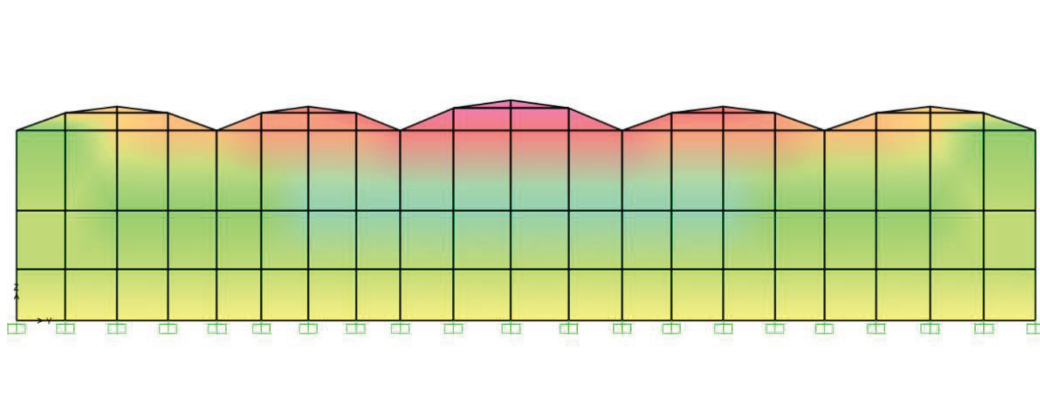


Figure 5.43. The displacement of back side in X direction of the section on yz plane at x = +15 m axis under Dead+Ex+0.3Ey load combination

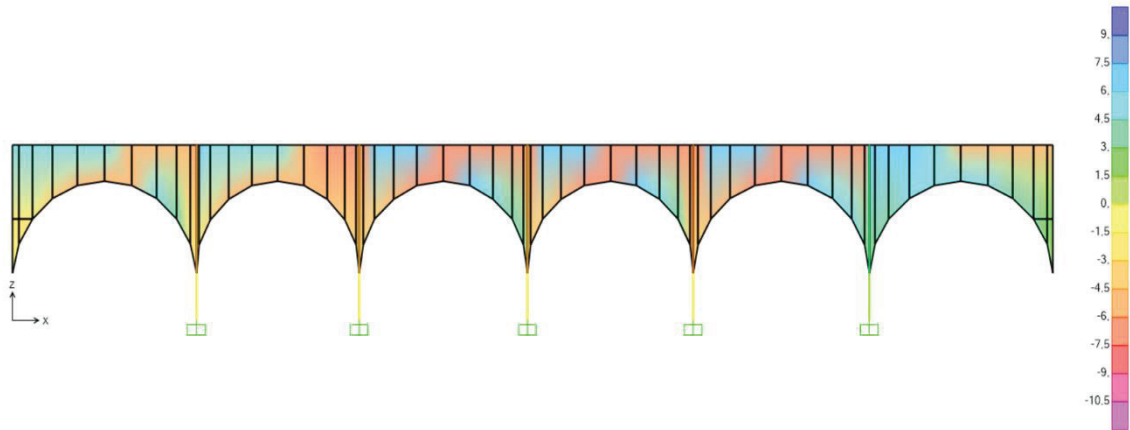


Figure 5.44. The displacement of arches in X direction on xz plane at $y = +2.5$ m axis under Dead+Ex+0.3Ey load combination

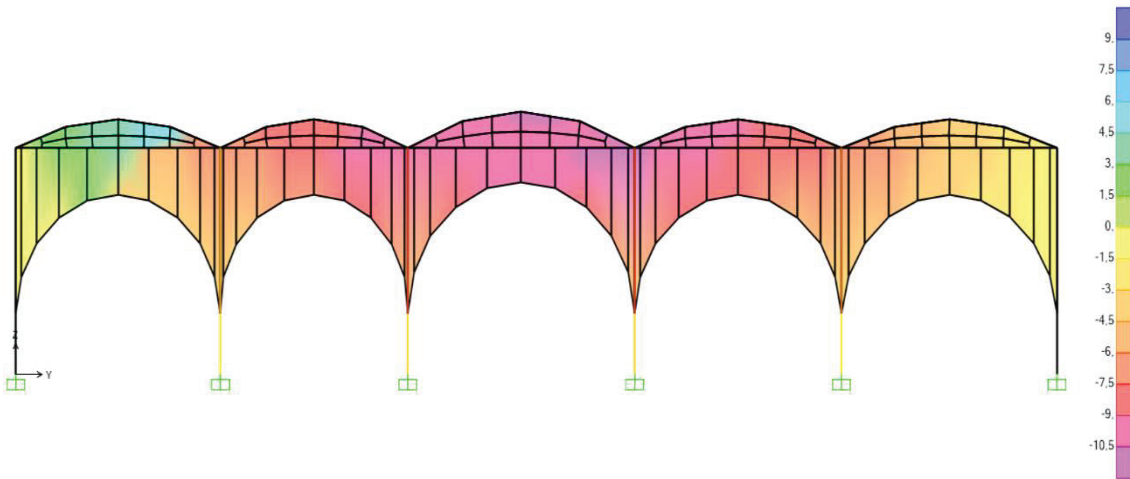


Figure 5.45. The displacement of section in X direction on yz plane at $x = +2.5$ m axis under Dead+Ex+0.3Ey load combination

According to the Dead+Ex+0.3Ey load combination, the maximum compressive and tensile stresses S_{11} are -1.05 MPa and 0.90 MPa, respectively. The highest tensile stress values are observed at the vault connections, in columns and at the top of arches, see Figures 5.46, 5.49 and 5.50. These values are larger than tensile strength. This is most probably due to the connection issues in the model for the vault shell to supporting wall or pier shell. The high tensile stresses are almost found in interior walls and in some parts of back of the structure, see Figures 5.47 and 5.48. Structural elements with high tensile stresses may need to be looked with extra care. Main exterior walls are below the limits for both tensile and compressive stresses. Also, the maximum

compressive stresses are seen at the back of vaults and the top of arches, see Figures 5.46, 5.49 and 5.50.

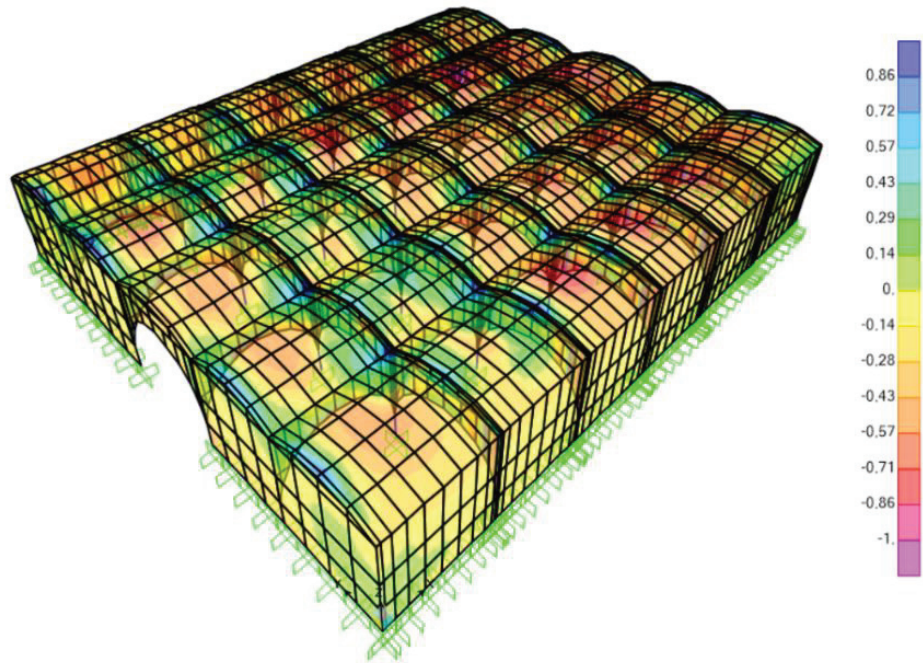


Figure 5.46. Normal stresses S11 due to spectral excitation under Dead+Ex+0.3Ey load combination (MPa)

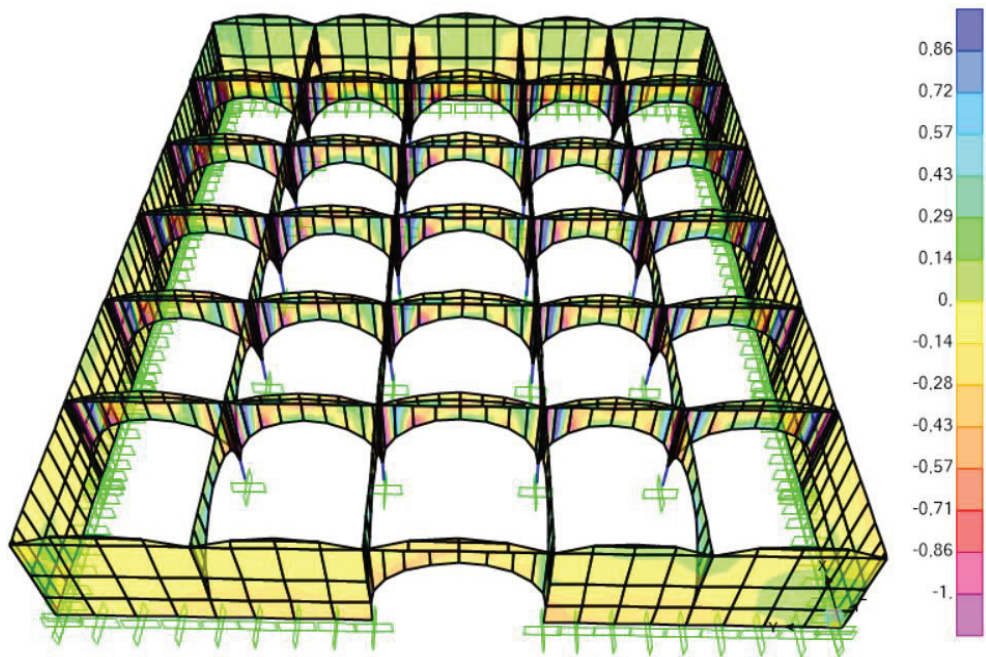


Figure 5.47. Normal stresses S11 except vaults due to spectral excitation under Dead+Ex+0.3Ey load combination (MPa)

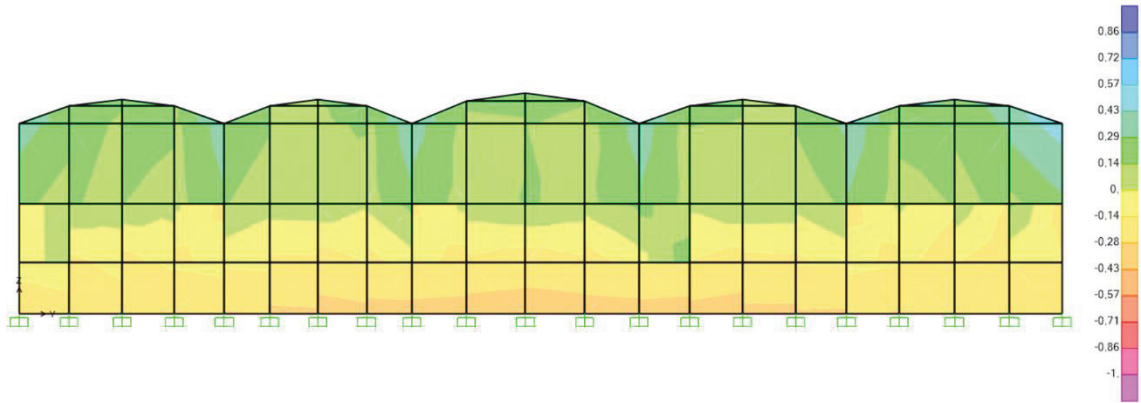


Figure 5.48. Normal stresses S11 of back side on yz plane at $x = +15$ m axis under Dead+Ex+0.3Ey load combination

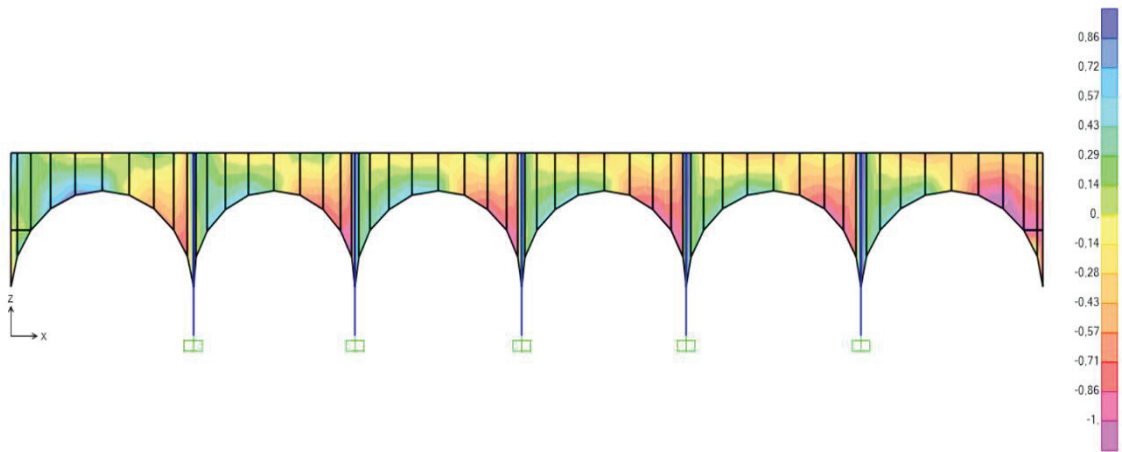


Figure 5.49. Normal stresses S11 of arches on xz plane at $y = +2.5$ m axis under Dead+Ex+0.3Ey load combination

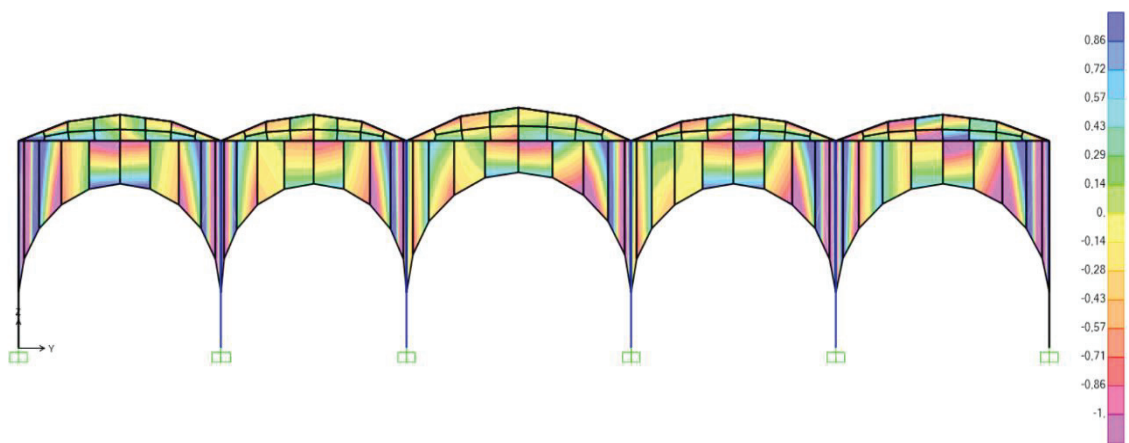


Figure 5.50. Normal stresses S11 of section on yz plane at $x = +2.5$ m axis under Dead+Ex+0.3Ey load combination

For normal stresses S22, the highest compressive and tensile stresses are -0.95 MPa and 0.18 MPa, respectively, see Figures 5.51 and 5.52. The maximum tensile stresses are formed at the junctures of main exterior wall and on the vault in front of the structure and in columns, see Figures 5.51 and 5.55. Also, the maximum compressive stresses are seen on vaults, at the edges of the arches and interior walls, on both sides of the portal and under the back of the structure, see Figures 5.53 and 5.54. The compressive stresses are high in main exterior walls and on other vaults. These stresses are not at risk since the compressive stress values are suitable.

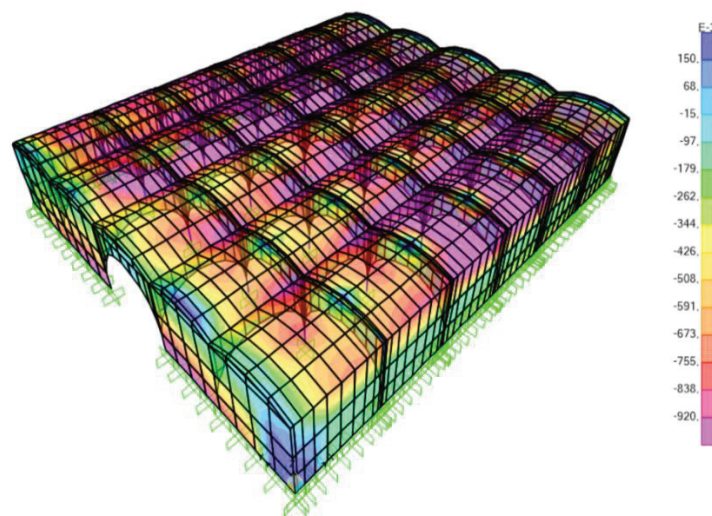


Figure 5.51. Normal stresses S22 under Dead+Ex+0.3Ey load combination (10^{-3} MPa)

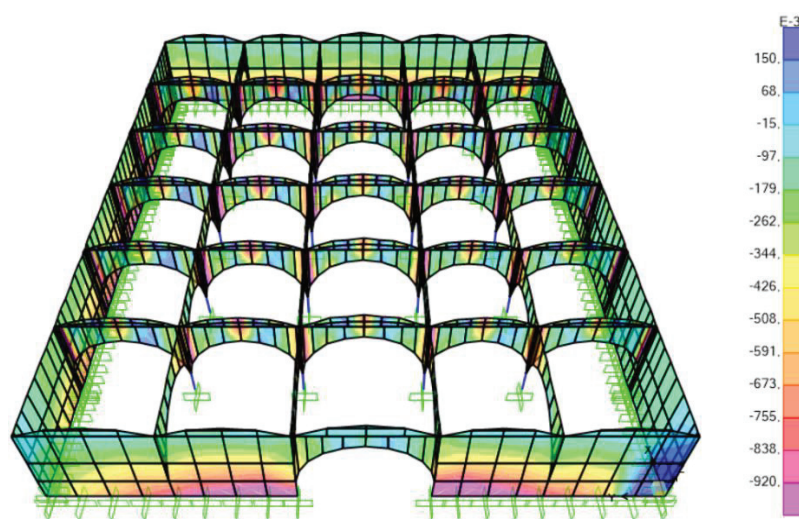


Figure 5.52. Normal stresses S22 except vaults under Dead+Ex+0.3Ey load combination (10^{-3} MPa)

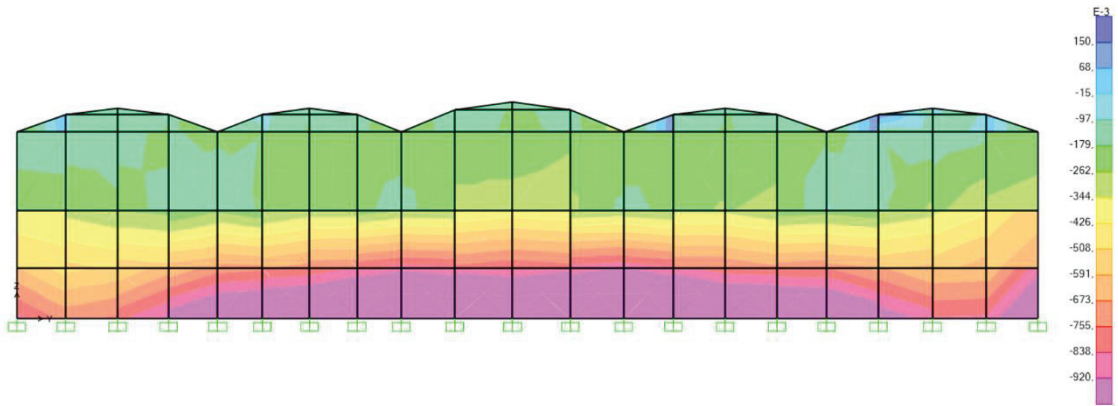


Figure 5.53. Normal stresses S22 of back side on yz plane at $x = +15$ m axis under Dead+Ex+0.3Ey load combination

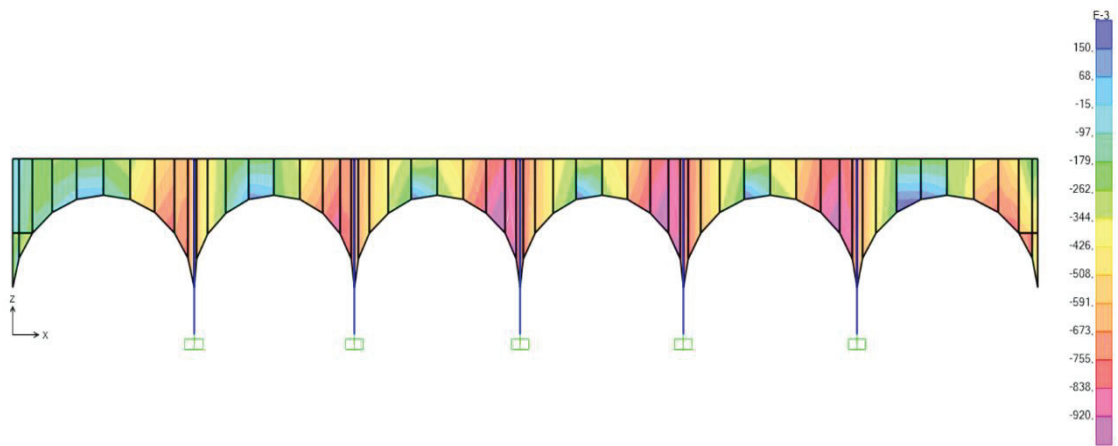


Figure 5.54. Normal stresses S22 of arches on xz plane at $y = +2.5$ m axis under Dead+Ex+0.3Ey load combination

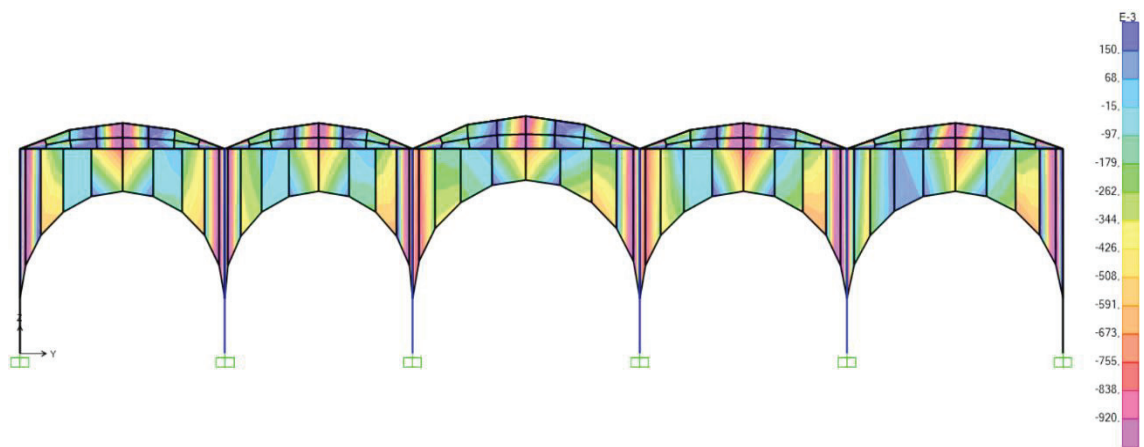


Figure 5.55. Normal stresses S22 of section on yz plane at $x = +2.5$ m axis under Dead+Ex+0.3Ey load combination

For the Dead+Ex+0.3Ey load combination, The maximum shear stresses S12 are 0.56 MPa on vaults, at the top of the arches and in columns, see Figures 5.56, 5.59 and 5.60. There are relatively higher shear stresses on the interior walls and in the structural elements close to the maximum shear stresses, see Figures 5.57 and 5.60. These stresses are critical since they exceed the limit value. In addition, main exterior walls and the back side of the structure have low shear stress values, see Figure 5.58.

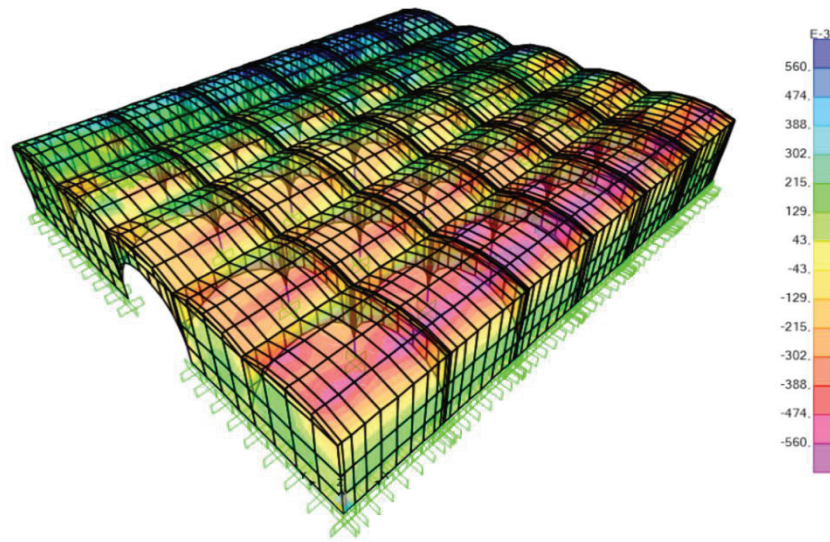


Figure 5.56. Shear stresses S12 under Dead+Ex+0.3Ey load combination (10^{-3} MPa)

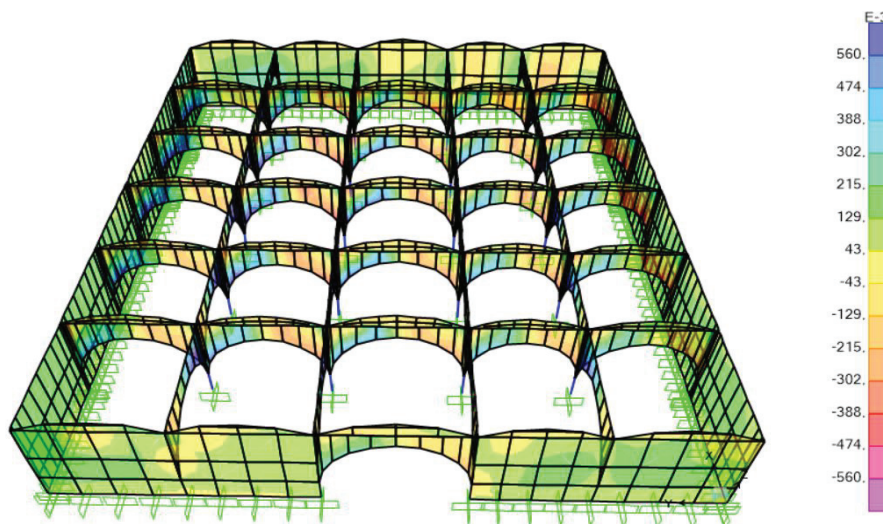


Figure 5.57. Shear stresses S12 except vaults under Dead+Ex+0.3Ey load combination (10^{-3} MPa)

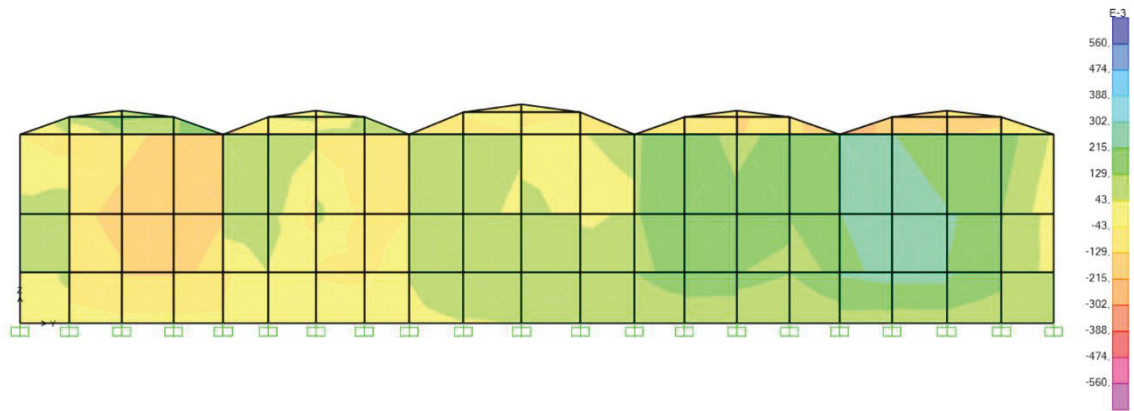


Figure 5.58. Shear stresses S12 of back side on yz plane at $x = +15$ m axis under Dead+Ex+0.3Ey load combination

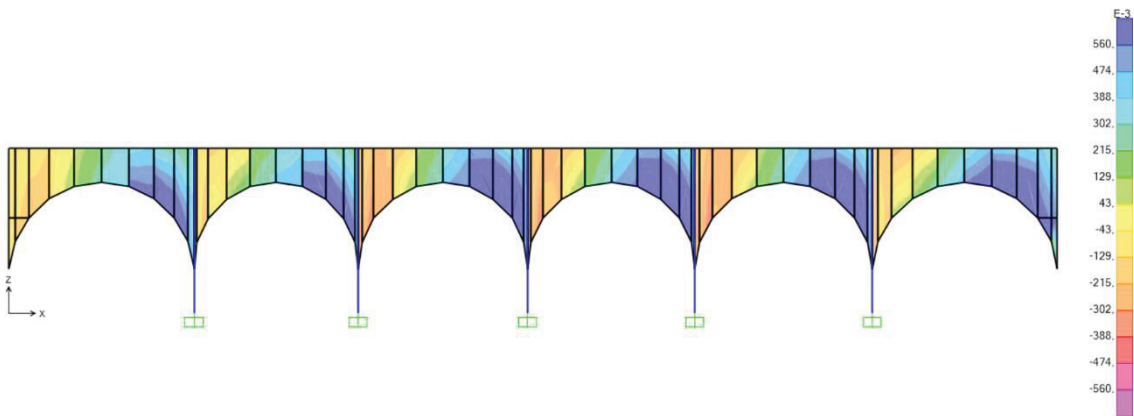


Figure 5.59. Shear stresses S12 of arches on xz plane at $y = +2.5$ m axis under Dead+Ex+0.3Ey load combination

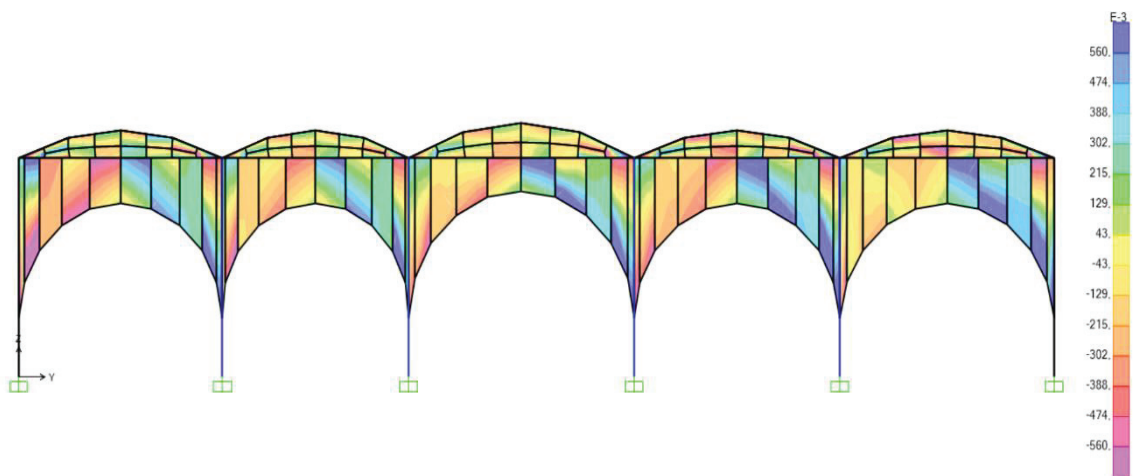


Figure 5.60. Shear stresses S12 of section on yz plane at $x = +2.5$ m axis under Dead+Ex+0.3Ey load combination

According to the Dead+Ey+0.3Ex load combination, the maximum vertical displacements in the negative z direction are seen as 13.02 mm on the vaults, see Figure 5.61. The vertical displacements in high value are found on other vaults and in some areas in the arches, see Figures 5.61, 5.62, 5.63 and 5.64.

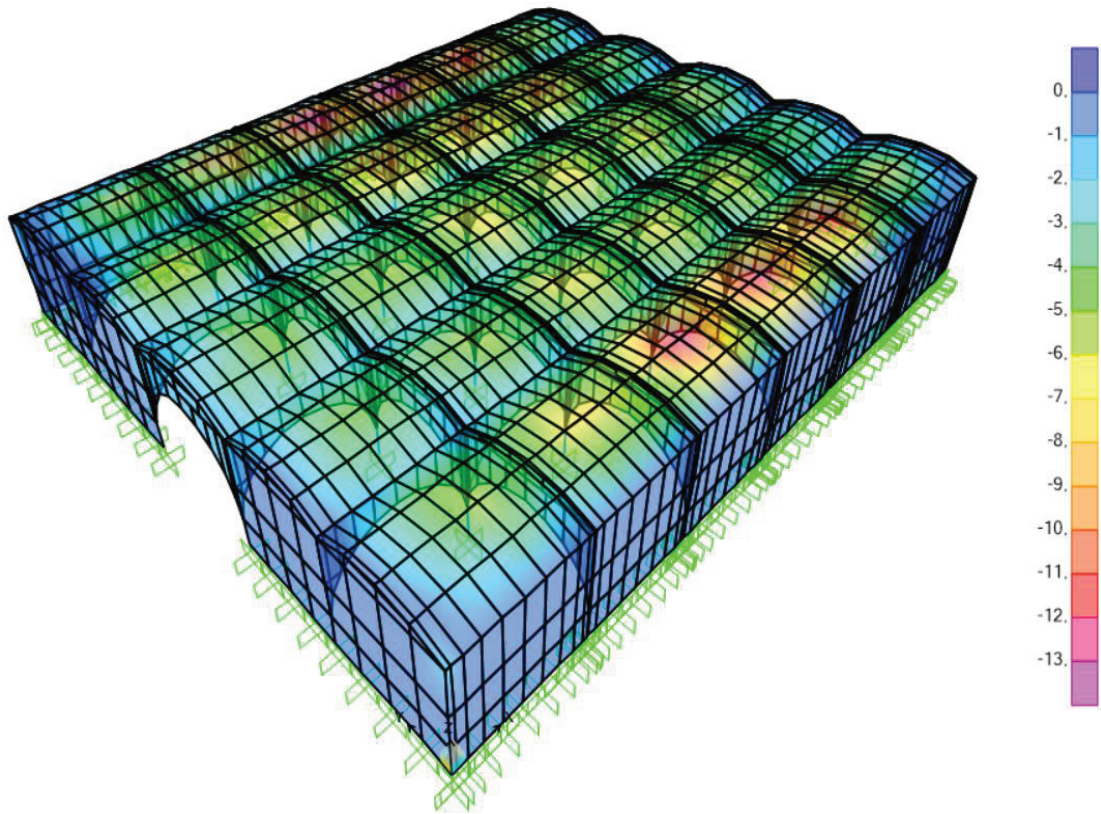


Figure 5.61. The vertical displacement in Z direction under Dead+Ey+0.3Ex load combination

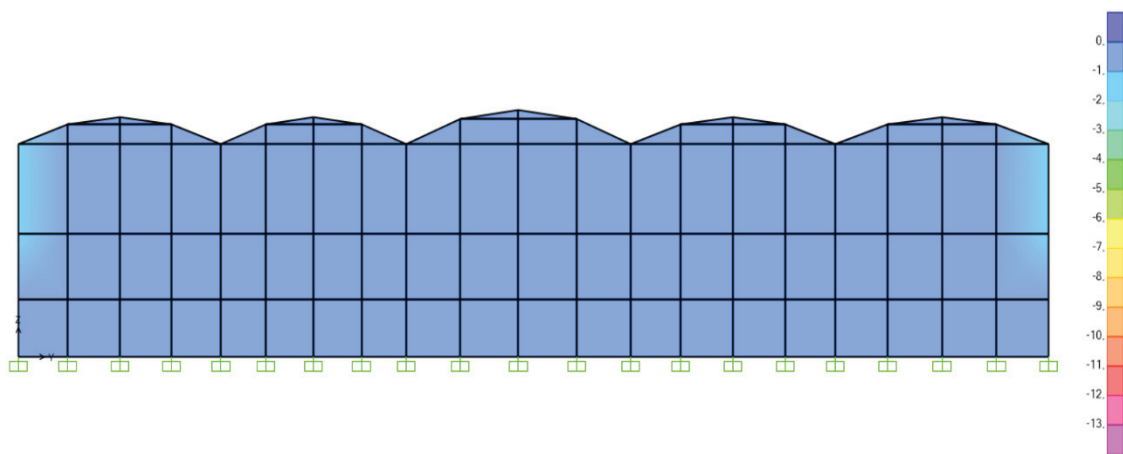


Figure 5.62. The vertical displacement in Z direction of back side on yz plane under Dead+Ey+0.3Ex load combination

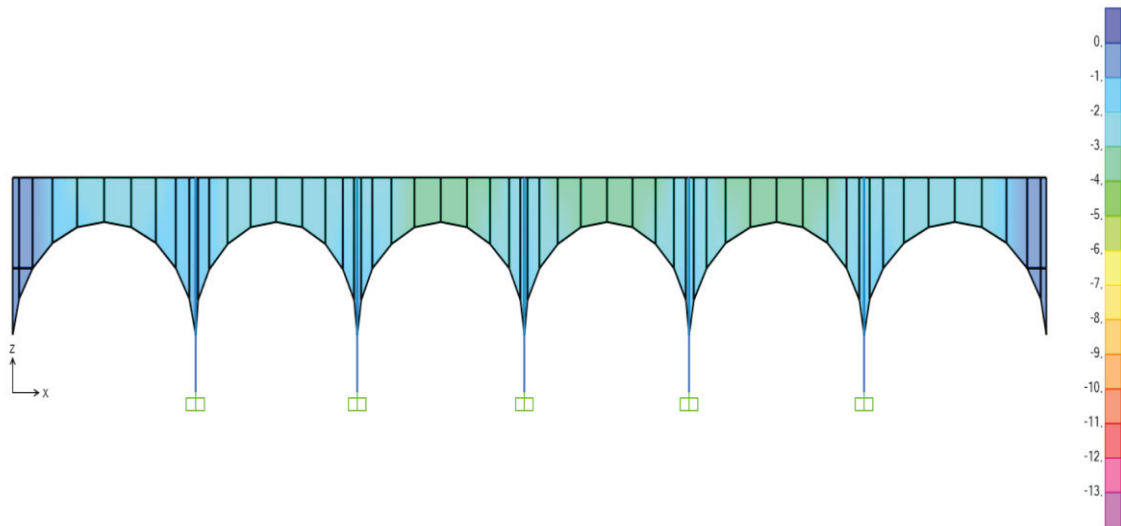


Figure 5.63. The vertical displacement in Z direction of arches on xz plane at $y = +2.5$ m axis Dead+Ey+0.3Ex load combination

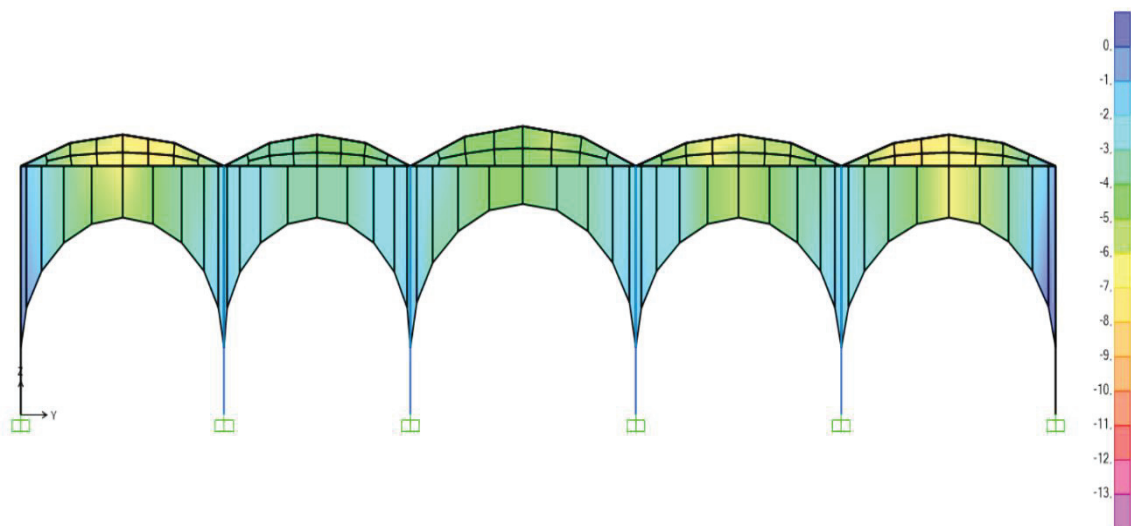


Figure 5.64. The vertical displacement in Z direction of section on yz plane at $x = +2.5$ m Plane axis under Dead+Ey+0.3Ex load combination

For the Dead+Ey+0.3Ex load combination, as shown in Figures 5.65 and 5.67, the maximum displacements are approximately 15 mm in the negative y direction on the vaults and at the top of the arches. The maximum ones in the positive y direction are 14.95 mm in the vaults to the left of the structure, see Figure 5.65. Moreover, the vaults in the middle of the building, the arches and interior walls have high, see Figures 5.65, 5.67 and 5.68. However, the displacements are lower in main exterior walls, in columns and at the back of the khan, see Figure 5.66.

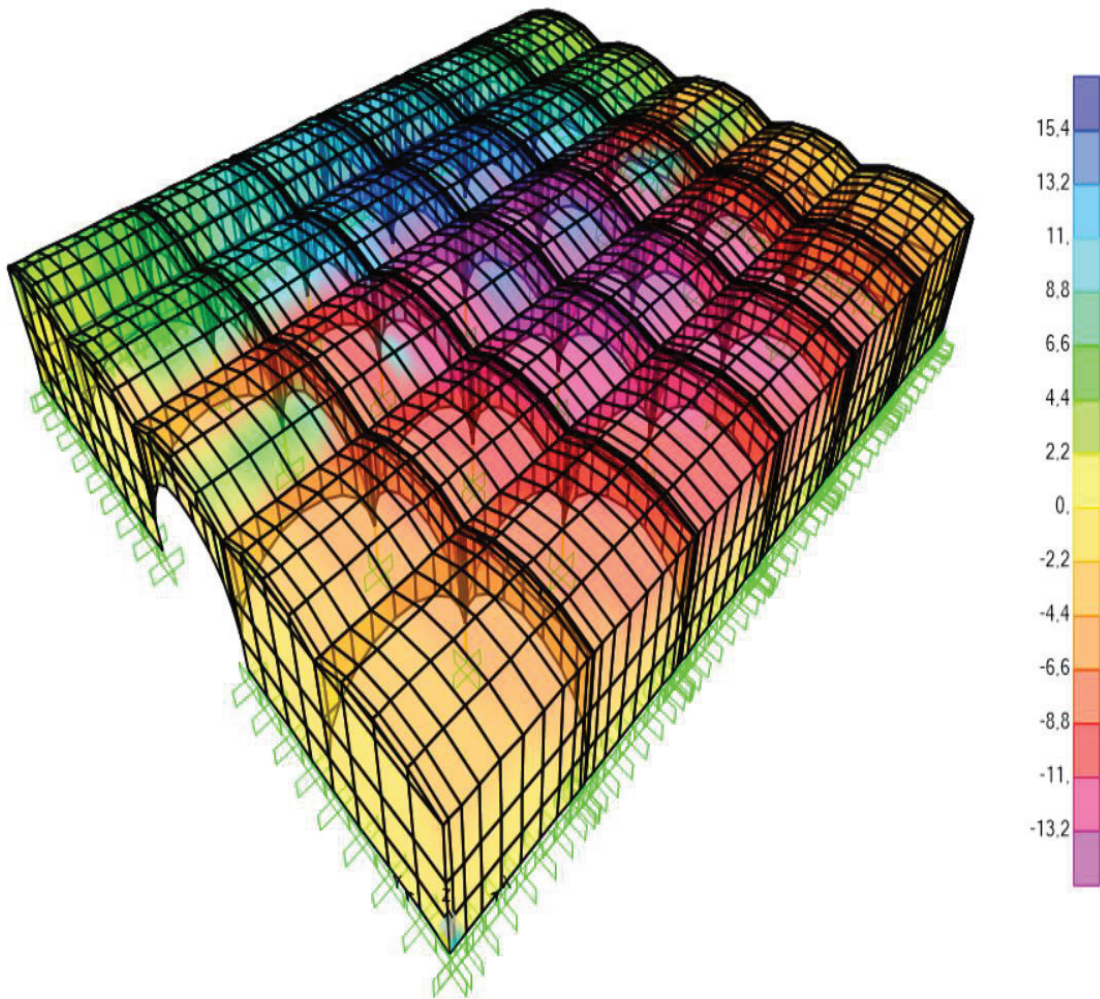


Figure 5.65. The displacement in Y direction under Dead+Ey+0.3Ex load combination

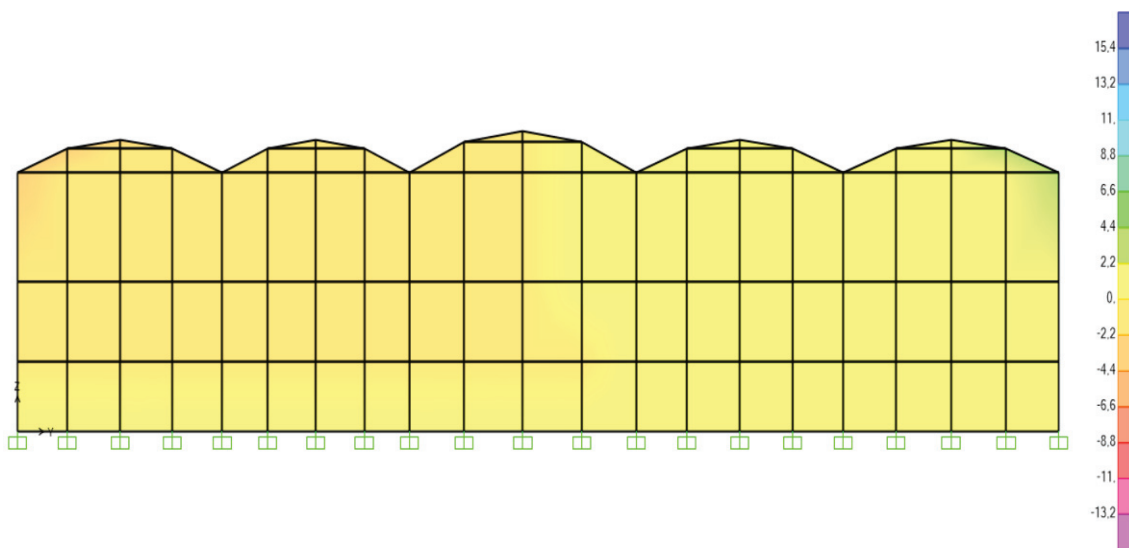


Figure 5.66. The displacement of back side in Y direction on yz plane under Dead+Ey+0.3Ex load combination

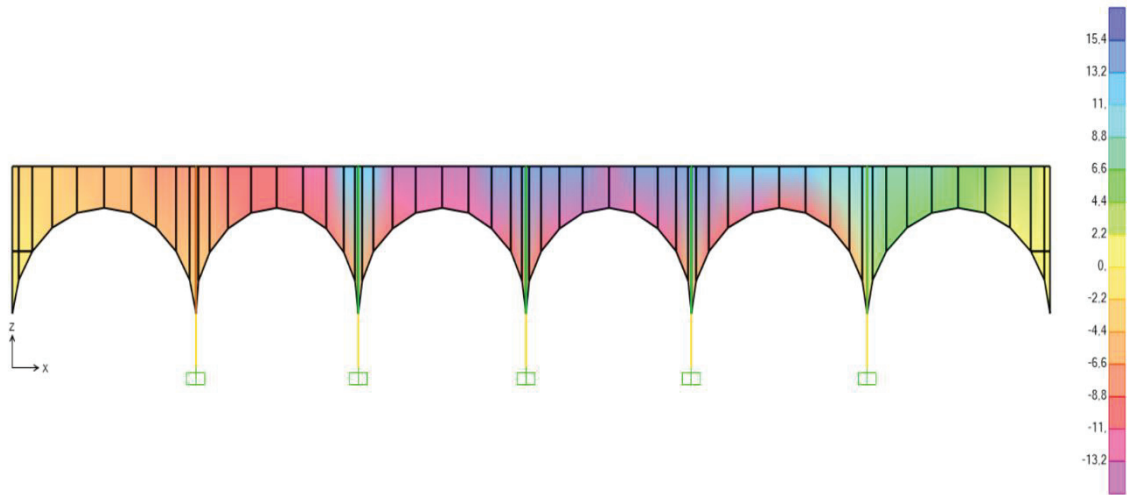


Figure 5.67. The displacement of arches in Y direction on xz plane at $y = +2.5$ m axis under Dead+Ey+0.3Ex load combination

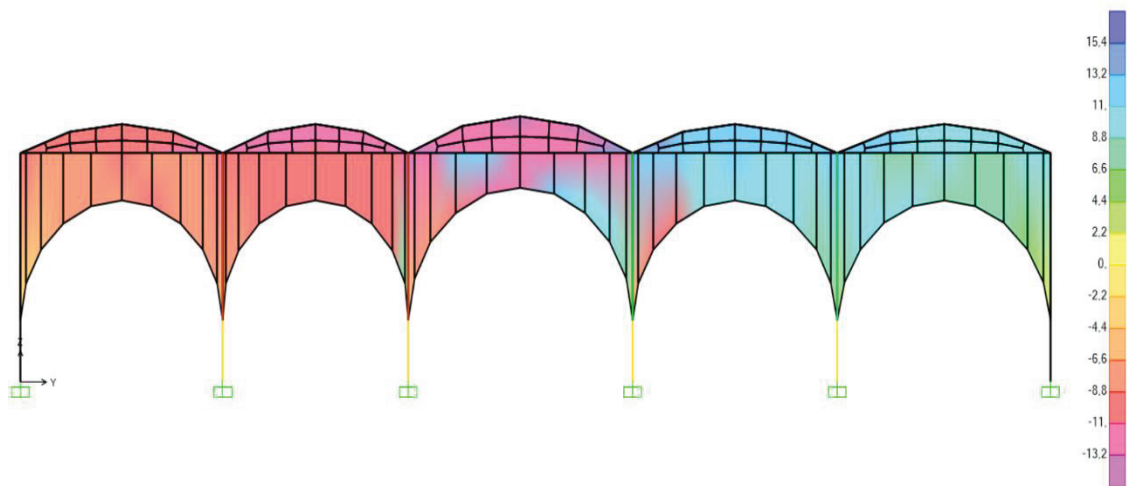


Figure 5.68. The displacement in Y direction of the section on yz plane at $x = +2.5$ m axis Dead+Ey+0.3Ex load combination

Under Dead+Ey+0.3Ex load combination, the maximum tensile stresses S11 are 0.25 MPa, see Figure 5.69. The stresses exceed tensile strength. These tensile stresses in the portal of the structure, in the buttresses of the entrance section, at the top of the arches, on the vaults, in main exterior walls, at the back of the structure and in the column indicates the vulnerable regions of the structure, see Figures 5.70, 5.71, 5.72 and 5.73. The highest compressive stresses S11 are 0.98 MPa on some vaults to the right of the structure and in interior walls, see Figure 5.69. The compressive stresses do not exceed the compressive strength except in areas where the vaults have maximum compressive stress.

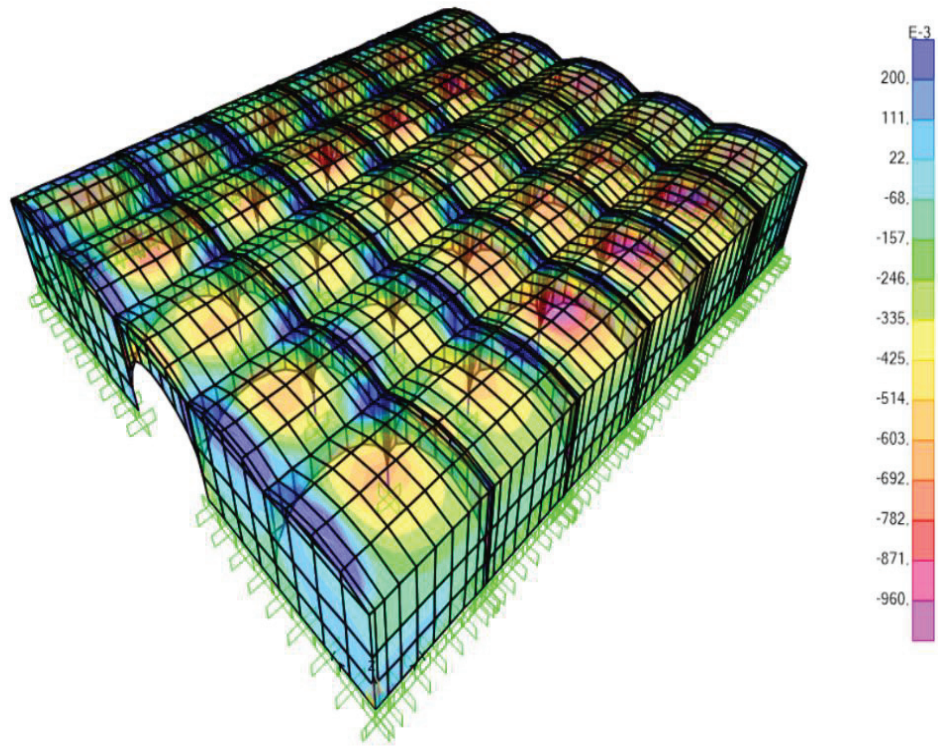


Figure 5.69. Normal stresses S11 under Dead+Ey+0.3Ex load combination (10^{-3} MPa)

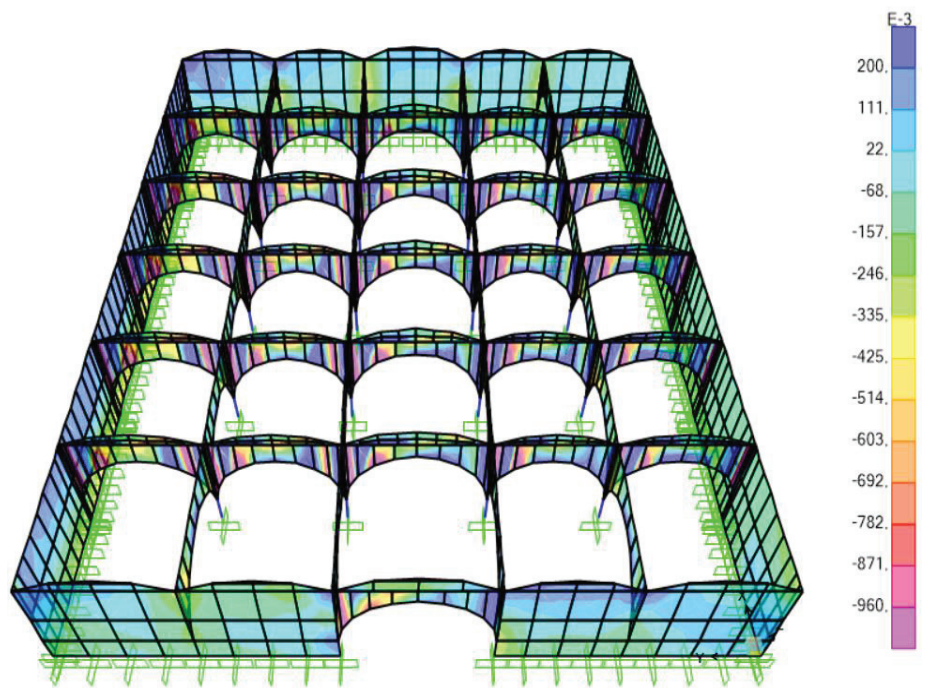


Figure 5.70. Normal stresses S11 except vaults under Dead+Ey+0.3Ex load combination (10^{-3} MPa)

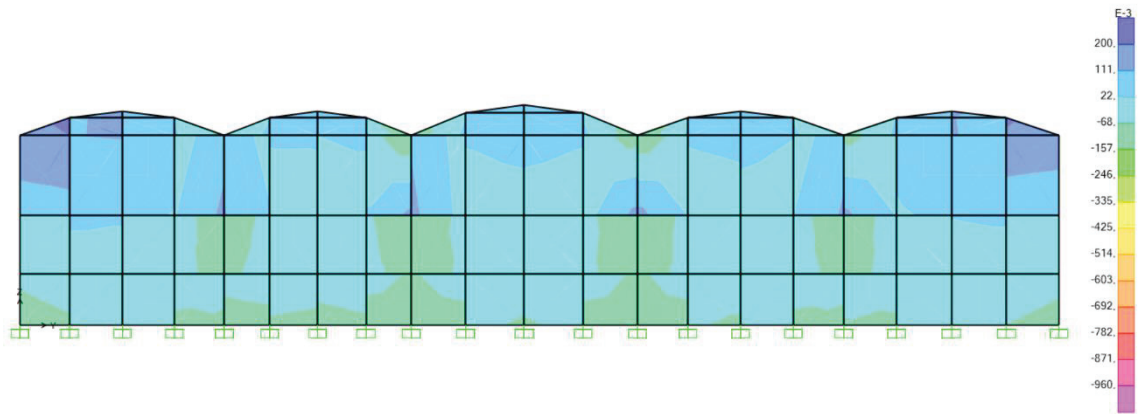


Figure 5.71. Normal stresses, S11 of back side on yz plane under Dead+Ey+0.3Ex load combination

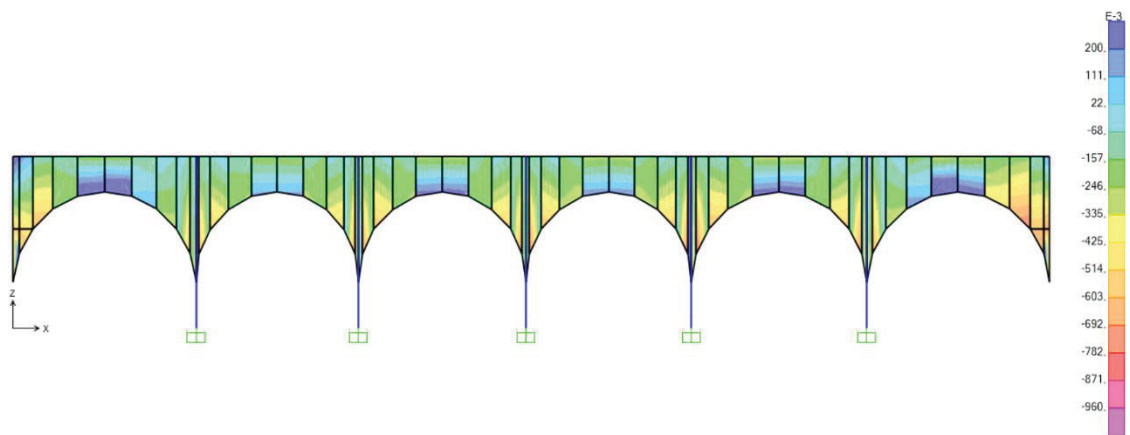


Figure 5.72. Normal stresses, S11 of arches on xz plane at $y = +5$ m under Dead+Ey+0.3Ex load combination

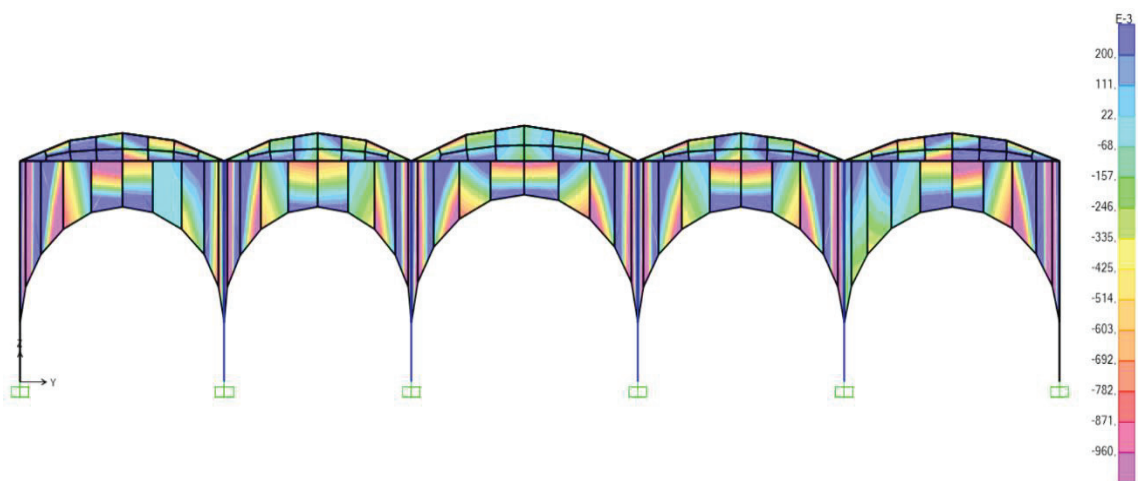


Figure 5.73. Normal stresses, S11 of section on yz plane at $x = +5$ m axis under Dead+Ey+0.3Ex load combination

The highest compressive and tensile stresses S_{22} under $\text{Dead} + E_y + 0.3E_x$ load combination in y direction are -1.95 MPa and 0.84 MPa , respectively, see Figures 5.74 and 5.75. High tensile stresses are found on the vaults, arches, columns at the right of the exterior main walls and in some areas at the back of the structure, see Figures 5.74-5.78. It is evident that both compressive and tensile stresses exceed the limits in above-mentioned structural elements.

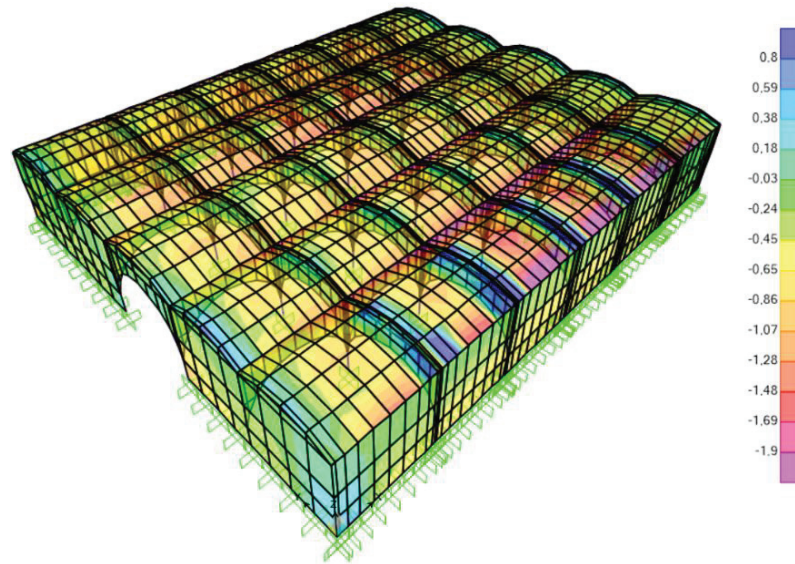


Figure 5.74. Normal stresses, S_{22} under $\text{Dead} + E_y + 0.3E_x$ load combination (MPa)

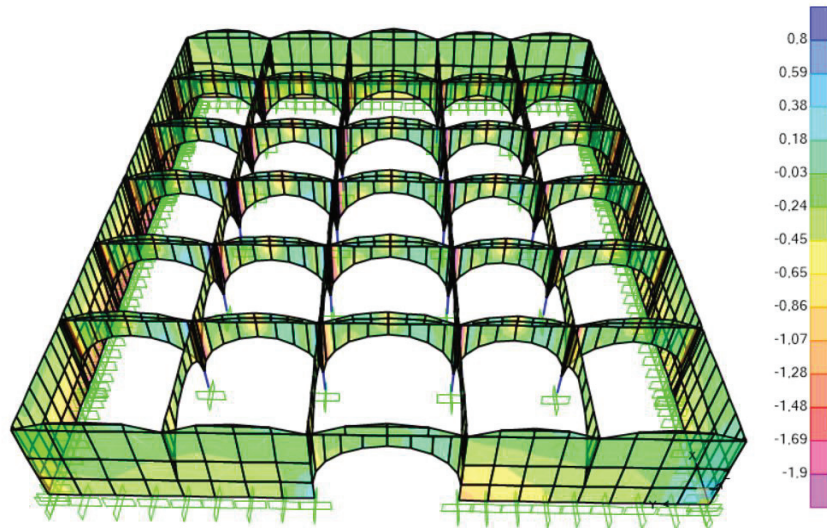


Figure 5.75. Normal stresses, S_{22} except vaults under $\text{Dead} + E_y + 0.3E_x$ load combination (MPa)

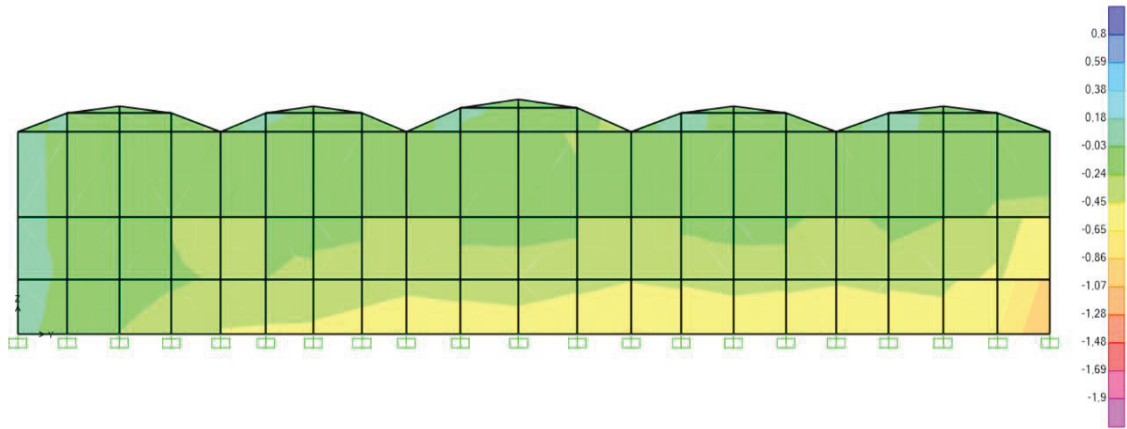


Figure 5.76. Normal stresses S22 of back side on yz plane under Dead+Ey+0.3Ex load combination

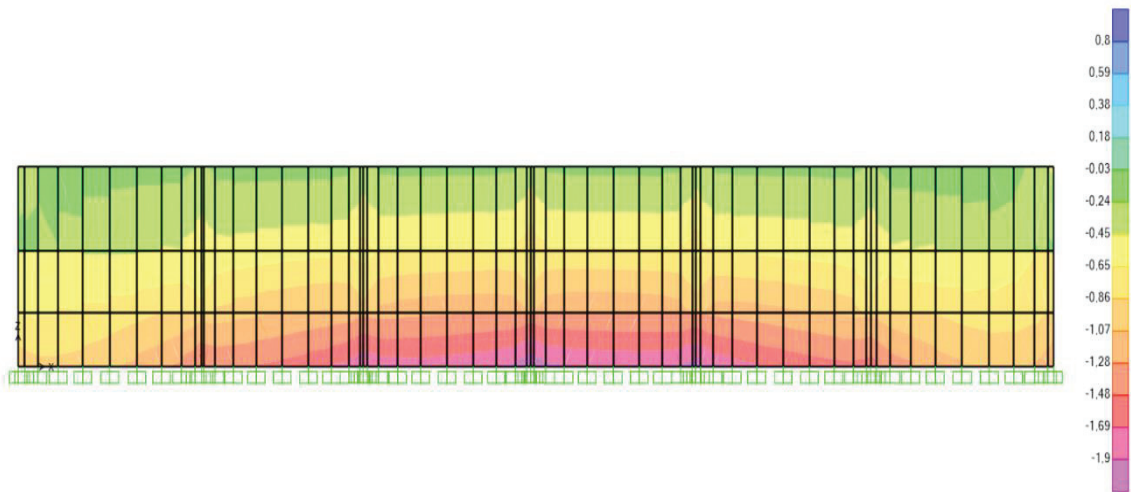


Figure 5.77. Normal stresses, S22 of main exterior wall on xz plane at y = +12.5 m axis under Dead+Ey+0.3Ex load combination

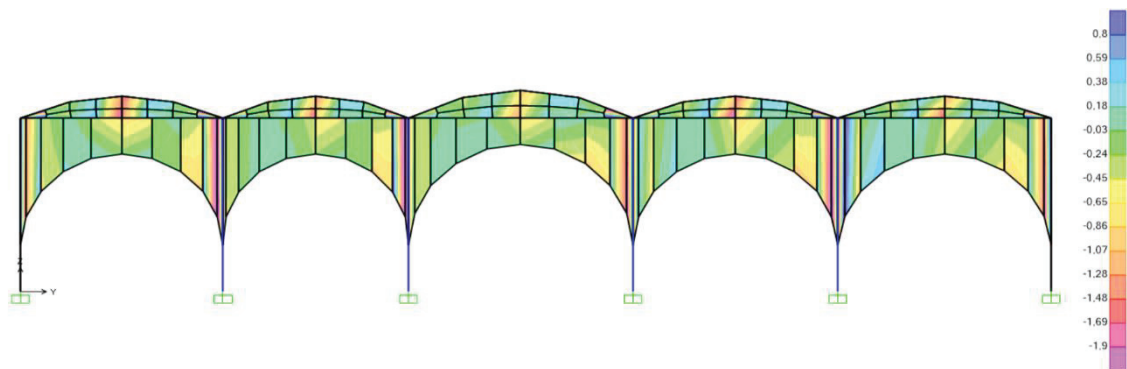


Figure 5.78. Normal stresses, S22 of section on yz plane at x = +5 m axis under Dead+Ey+0.3Ex load combination

According to dead and spectral excitation in y direction, the highest shear stresses, S12 are 0.66 MPa at the back and front vaults, on arches and in columns, see Figures 5.79-5.83. Also, it is seen that these stresses exceed the shear strength which is indicating the vulnerable zones. In addition, the bearing interior and exterior walls are safe in accordance with shear stresses, see Figures 5.80 and 5.81.

As a result, under Dead+Ey+0.3Ex load combination some structural elements exceed the strength limits in terms of the compressive, tensile and shear stresses which should be investigated extensively.

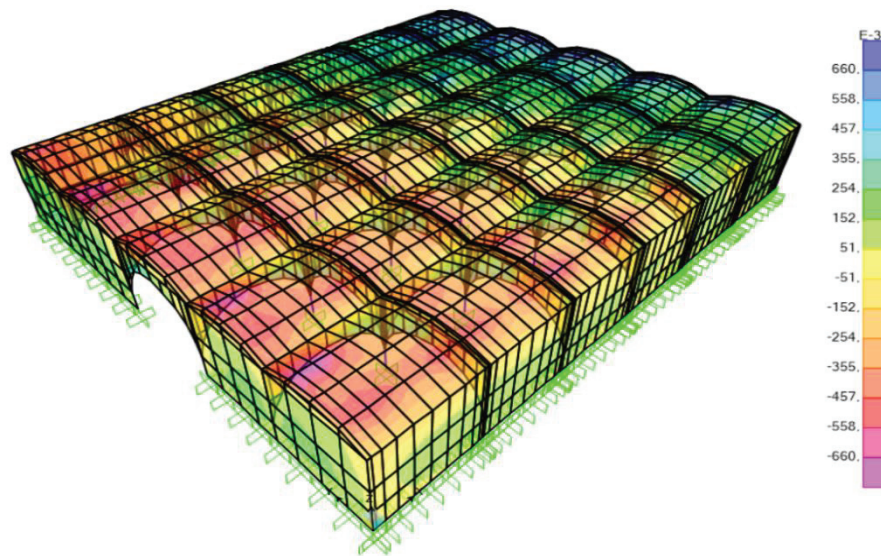


Figure 5.79. Shear stresses, S12 under Dead+Ey+0.3Ex load combination (10^{-3} MPa)

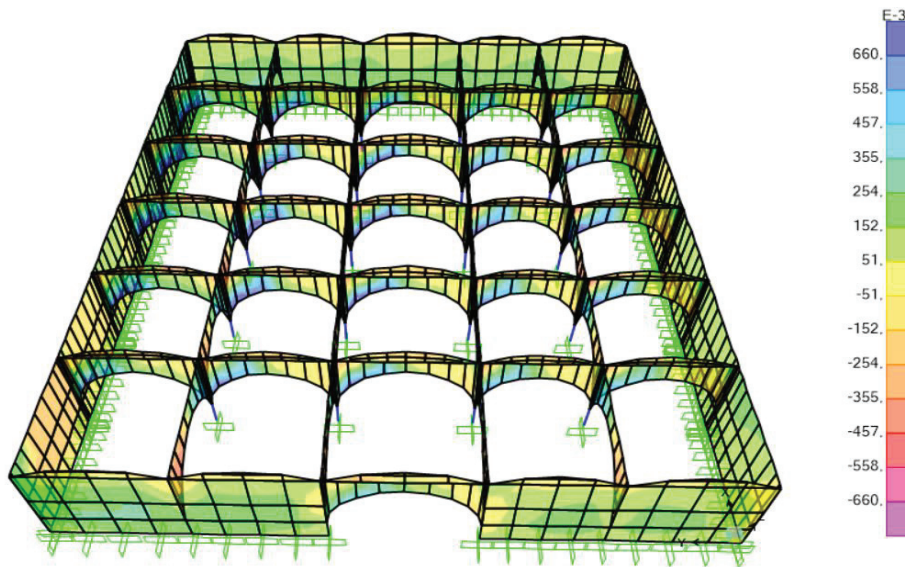


Figure 5.80. Shear stresses, S12 except vaults under Dead+Ey+0.3Ex load combination (10^{-3} MPa)

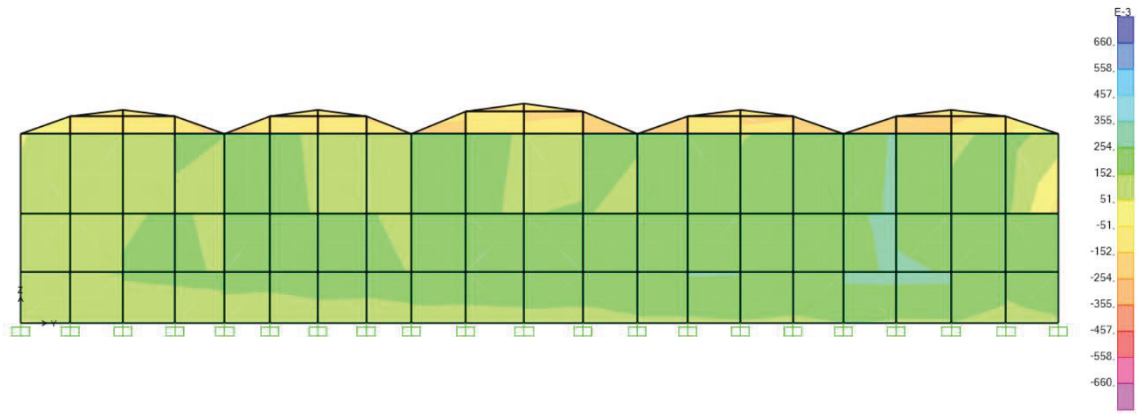


Figure 5.81. Shear stresses, S12 of back side on yz plane under Dead+Ey+0.3Ex load combination

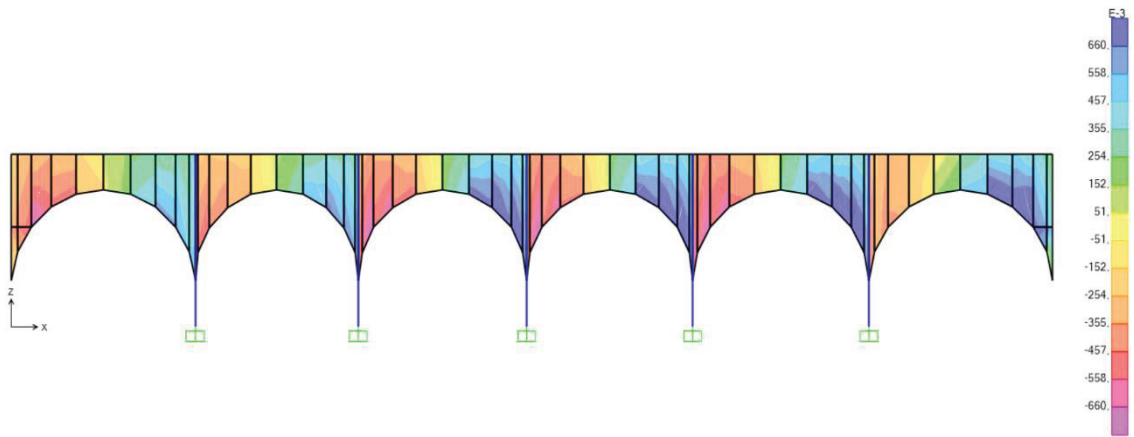


Figure 5.82. Shear stresses, S12 of arches on xz plane at $y = +5$ m axis under Dead+Ey+0.3Ex load combination

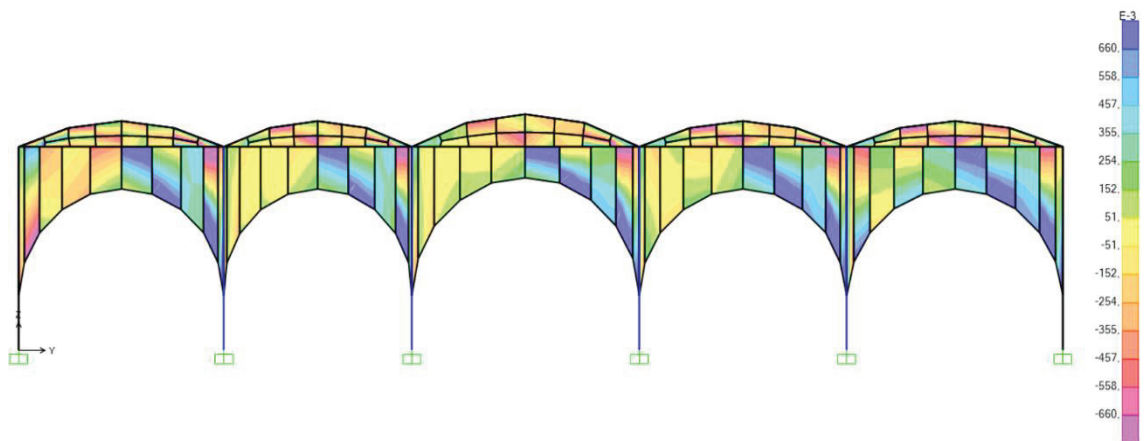


Figure 5.83. Shear stresses, S12 of section on yz plane at $x = +5$ m axis under Dead+Ey+0.3Ex load combination

CHAPTER 6

CONCLUSIONS AND RECOMMENDATIONS

In this study, the analyses and assessment of a historical masonry structure is investigated. The study is presented as a case study, Çardak Caravanserai in Denizli, built in 13th century. Firstly, general informations about masonry structures and the modeling techniques are explained. After that, the architectural and structural characteristics of Çardak caravanserai are explained and a historical research is conducted. Finally, the three dimensional shell model of the caravanserai is created by using macro modeling approach in SAP2000 software and self-weight analysis, modal and response spectrum analyses are conducted. The structure has been evaluated using the assumed material properties taken from the literature.

The outcomes are as follows:

1. Çardak khan is a document reflecting the structural characteristics of Seljuk period. It repeats majority of the widespread characteristics, but there are a few peculiarities such as the two rectangular platforms, variation in the form of the buttresses, and masonry stairs providing access to the terrace roof.
2. As a result of self-weight analysis, it is seems that the stress levels are below the capacity and at the current situation of structure there is no structural concerns.
3. Under the seismic actions, high tensile and shear stresses observed on the vaults and at the top of the arches. These elements need further investigation since at some points the strength values are exceeded.
4. Consequently, it seems that the current state of the caravanserai under dead loads does not pose any critical issue as expected . Under earthquake loads in both directions, the tensile and shear stresses exceed the strength limits of the material at some locations and further investigation should be conducted focusing these loacations before any intervention decisions are made.

Recommendations:

1. In order to check for the validity of the finite element model operational modal analysis might be run and a calibration to the FEM model can be processed.
2. The soil conditions need to be investigated as well to better assess the current

situation.

3. Material characterization and property estimation should be carried out in order to better represent them in the FEM model. In-situ and laboratory testing would be quite instrumental.
4. Consolidation would be the first choice for preventive conservation. This would aim to restating the capacity with techniques such as injection of repair grout, and restating any loose units and completion of minor material losses.
5. Structure requires more detailed analyses such as the field research, detailed tests of masonry structural material, non-linear static and seismic analyses and then a decision should be made whether or not strengthening is required.
6. If the capacity provided seems to be lower than the demanded capacity under any loading conditions, further detailed analysis needs to be carried out to make the before retrofitting decision available to reduce the consequences.
7. The historical structures should be conserved for generations. This would require to well maintain these structures after rehabilitating them. Monitoring these structures after rehabilitation and conducting regular inspections would be very instrumental in preserving them.

REFERENCES

- AFAD. 2019, “Deprem Bölgeleri Haritası”, <https://deprem.afad.gov.tr/deprem-bolgeleri-haritasi>, 03.05.2019.
- Akalın Şebnem. (2002), “Kervansaray” Türkiye Diyanet Vakfı İslam Ansiklopedisi, İstanbul: Türkiye Diyanet Vakfı.
- Akyol Erdal, Kaya Ali, Taşdelen Suat, Beyaz Turgay and Şen Gulmustafa. (2007), “Denizli Yerleşim Alanının Jeolojik-Jeoteknik Özellikleri”, Selçuk Üniversitesi Mühendislik-Mimarlık Fakültesi Dergisi, c.23, s.1-2, Pamukkale Üniversitesi Mühendislik Fakültesi Jeoloji Mühendisliği, Denizli.
- Aslanapa Oktay. (1960), Ribat İ.A. CI, MEB Yayınları, İstanbul.
- Bakırer Ömür. (1996), “Anadolu Selçuklu Dönemi Yapı Kitabeleri”, V. Milli Selçuklu Kültür ve Medeniyeti Semineri Bildirileri, Konya.
- Bathe Klaus Jürgen. (1982), “Finite Element Procedures in Engineering Analysis”, Prentice Hall, Inc., Englewood Cliffs, New Jersey 07632, First Edition, Massachusetts Institute of Technology, Boston, USA.
- Baykara Tuncer. (1969), Denizli Tarihi, İkinci Kısım (1070-1429), İstanbul; Fakülteler Matbaası.
- Bayram Ayşe, Nalça Canan, Keke Begüm, Özel Ebru, Özdemir Emre, Yönetken Ece, Eken Esra, Durmuşlar Feyza, Şener İdil, Ergin Merve, Birgin Özüm, Yönder Mustafa (2017), Restoration Project of Çardak Khan Denizli, Design in Architectural Restoration II, 2016-2017 Spring Semester, Supervisors: M. Hamamcıoğlu Turan and K. Çelik, Izmir Institute of Technology (IZTECH), Department of Architectural Restoration, Izmir.
- Bektaş Cengiz. (1999), Selçuklu Kervansarayları Korumaları Üzerine Bir Öneri, İstanbul, Yem Yayınları.
- Berto Luisa, Saetta Anna, Scotta Roberto and Vitaliani Renato. (2005), “Failure Mechanism of Masonry Prism Loaded in Axial Compression”, Computer Aspects, 38(2), 249-256, Italy.

- Betti Michele and Vignoli Andrea. (2007), “Modeling and Analysis of a Romanesque Church under Earthquake Loading: Assessment of Seismic Resistance”, Department of Civil and Environmental Engineering, University of Florence, I- 50139 Florence, Italy.
- Beyazıt Mustafa. (2002), “Denizli’de Çardak Han ve Ak Han”, Master’s Thesis, Pamukkale Üniversitesi, Denizli.
- Binda Luigia, Saisi Antonella and Tiraboschi Claudia. (2000), “Investigation Procedures for The Diagnosis of Historic Masonries”, Construction and Building Materials, Italy.
- Calderoni Bruno, Ghersi Aurelio, and Lenza Pietro. (1994), Seismic Behavior of Masonry Buildings, Proceeding of the 10th International Brick and Block Masonry Conference, Canada.
- Casollo Siro and Milani Gabriele. (2013), Simplified out-of-plane Modeling of There Leaf Masonry Walls Accounting for The Material Texture, Construction and Building Materials, Italy, 40(0): 330-351.
- Cecchi Antonella and Karam Sab. (2002), Out of Plane Model for Heterogeneous Periodic Materials: The Case of Masonry, European Journal of Mechanics, Italy, A/Solids (21)5: 715-746.
- Chaimoon Krit and Attard Mario M. (2006), “Modeling of Unreinforced Masonry Walls Under Shear and Compression”, Engineering Structures, 29(9), 2056-2068, Civil and Environmental Engineering, University of New South Wales, Sydney, Australia.
- Chandrupatla Tirupathi R. and Belegundu Ashok D. (1991), “Introduction to Finite Elements in Engineering”, First Edition, Prentice Hall International Editions, UK.
- Croci Giorgio. (1998), “The Conservation and Structural Restoration of Architectural Heritage”, Computational Mechanics Publications, Boston.
- Dabanlı Ömer. (2008), Tarihi Yığma Yapılarının Deprem Performansının Belirlenmesi, Yüksek Lisans Tezi, İstanbul Teknik Üniversitesi, İstanbul.
- Devellioğlu Ferit. (2001), Osmanlıca Türkçe Ansiklopedik Lugat, Ankara; Aydın Kitapevi Yayınları.

Erdmann Kurt. (1961), Das Anatalische Karavansaray, Catalog, Text, pp. 21-24.

Fersan Nur A., (1974), “The Çardak Kervansarayı in Denizli”, Unpublished Master’s Thesis, Middle East Technical University, Ankara.

Gedik Yaşar Hanifi. (2008), Analysis, Repair and Strengthening of Historical Masonry Structures; Case Study: Mehmet Aga Mosque, MSc. Thesis, Istanbul Technical University, Istanbul.

Google Maps. <https://www.google.com/maps>. 21/02/2019.

Guillaud Hubert, Joffroy Thierry and Odul Pascal. (1985), Compressed Earth Blocks: Manual of Design and Construction, Volume II, p.22.

Hendry Arnold, Sinha Braj and Davies Richard. (2004), Design of Masonry Structures, Third edition of Load Bearing Brickwork Design, Department of Civil Engineering University of Edinburgh, UK.

Kocaman İrfan, Kazaz İlker ve Okuyucu Dilek. (2018), Tarihi Erzurum Yakutiye Medresesi’nin Yapısal Davranışının İncelenmesi, Erzurum Teknik Üniversitesi, Mimarlık ve Mühendislik Fakültesi, İnşaat Mühendisliği Bölümü, 25050, Erzurum. Yayınlanma: Dokuz Eylül Üniversitesi- Mühendislik Fakültesi Fen ve Mühendislik Dergisi, Cilt 20, Sayı 58.

Koçak Ali. (1999), Linear and Nonlinear Analysis of Historical Masonry Structures under Static and Dynamic Loads Case Study: Küçük Aya Sofya Mosque, PhD Thesis, Yıldız Technical University, Istanbul.

Kömürcü Sedat. (2017), Analysis and Modelling of The In-Plane Behavior of Masonry Walls, MSc. Thesis, Istanbul Technical University, İstanbul.

Köprülü Fuat. (1942), “Ribat”, Vakıflar Dergisi, Vakıflar Müdürlüğü Meşriyatı, Sayı:2, Ankara.

Kuban Doğan, Yavuz Ayşıl Tükel. (2002), “Selçuklu Çağında Anadolu Sanatı”, Yapı Kredi Yayınları – 1567, İstanbul, 274-281.

Kuruşcu Ali Osman. (2005), “Yığma Yapıların Analizi”, Yüksek Lisans Tezi, Yıldız Teknik Üniversitesi, İstanbul.

- Kutlu Mehmet. (2009), Seljuk Caravanserais in The Vicinity of Denizli; Han-Abad (ÇardakHan) and Akhan, MSc. Thesis, Bilkent University, Ankara.
- Lourenco Paulo B., (1996), Computational Strategies for Masonry Structures, Delft University of Technology, Netherlands.
- Lourenco Paulo B., (2002), Computations on Historic Masonry Structures, Progress in Structural Engineering and Materials, 4(3): 301-319.
- Magenes Guido and Penna Andrea. (2009), “Existing Masonry Buildings: General Code Issues and Methods of Analysis and Assessment”, E. Cosenza (ed), Eurocode 8 Perspectives from the Italian Standpoint Workshop, 185-198, Doppiavoce, Napoli, Italy.
- Mandirola Martina, Penna Andrea, Rota Maria and Magenes Guido. (2012), “Experimental Assessment of The Shear Response of Autoclaved Aerated Concrete Masonry with Flat Truss Bed-Joint Reinforcement”, Proceeding of the 15th International Brick and Block Masonry Conference, Florianopolis, Brazil.
- Milani Gabriele, Pizzolato Marta, and Tralli Antonio. (2013), Simple Numerical Model with Second Order Effects for out-of-plane Loaded Masonry Walls, Engineering Structures, Italy, 48(0): 98-120.
- Müller Kurt. (1920), Die Karawanseraim im Vorderen Orient, Der Zirkel Architectur Verlag GMBH, Berlin.
- O’Sullivan T., (2016), Construction Design Masonry Available, from <http://masonrycontractors.com>. 26/11/2018.
- Özdemir Habibe. (2018), “Tarihi Yapıların Bilgisayar Destekli Analizi: Patara Antik Kent Tiyatrosu Sahne Yapısı Örneği”, Yüksek Lisans Tezi, Akdeniz Üniversitesi, Antalya.
- Pektaş Kutlu. (2007), “Çardak Han”, Anadolu Selçuklu Dönemi Kervansarayları, Ankara, 161-173.
- Roca Pere, Cervera Miguel, Gariup Giuseppe and Pela Luca. (2010), “Structural Analysis of Masonry Historical Constructions, Classical and Advanced Approaches”, Arch Comput Methods Eng 17: 299-325 DOI 10.1007/s11831-010-9046-1, Barcelona, Spain.

- SAP2000, (2018). CSI Analysis Reference Manual For SAP2000®, ETABS®, SAFE® and CSiBridge. CSI Computers & Structures, Inc. Berkeley, California, USA.
- Saraç Mahmut Murat. (2003), Tarihi Yığma Kargir Yapıların Güçlendirilmesi, Yüksek Lisans Tezi, İstanbul Teknik Üniversitesi, İstanbul.
- Satongar Şule. (1994), İstanbul Şehir Surları Horasan Harçları Üzerine Bir Araştırma, Yüksek Lisans Tezi, İstanbul Teknik Üniversitesi, İstanbul.
- Sattar Siamak. (2013), “Influence of Masonry Infill Walls and Other Building Characteristics on Seismic Collapse of Concrete Frame Buildings”, PhD Thesis, University of Colorado, Colorado, USA.
- Saygılı Özden. (2014), Use of Distinct Element Method in The Assessment of Earthquake Behavior of Masonry Structures, Graduate Program in Earthquake Engineering, Boğaziçi University, İstanbul.
- Schimmel Annemarie. (1975), Mystical Dimensions of Islam, University of North Carolina Press, Berlin, pp. 231-232.
- Şen Betül. (2006), Modeling and Analysis of The Historical Masonry Structures, MSc. Thesis, Boğaziçi University, İstanbul.
- Teomete Egemen. (2004), Finite Element Modeling of Historical Masonry Structures, Case Study: Urla Kamanlı Mosque, MSc. Thesis, Izmir Institute of Technology, Izmir.
- TS EN 1052-1, (2000). Methods of Test for Masonry – Part 1: Determination of Compressive Strength, Ankara.
- Turan Osman. (1964), Selçuklu Kervansarayları T.T.K. Belleteri, X/39 İstanbul.
- Turkish Seismic Design Code, (2018). Specification for Structures to be Built in Disaster Areas, Ministry of Public Works and Settlement Government of Republic of Turkey.
- Uğuz Seyit. (2016), Earthquake Safety Analysis of a Historical Masonry Building: Historical Gazi High School Case, MSc. Thesis, Selçuk University, Konya.

- UNI EN 16096, (2002), Conservation of Cultural Property – Condition Survey and Report of Built Cultural Heritage.
- Ural Ali and Doğangün Adem. (2007), “Evaluating The Seismic Performance of Masonry Structures Using with Micro Modeling Strategy”, Proceeding of The International Earthquake Symposium, Kocaeli.
- Ural Ali and Doğangün Adem. (2009), “Parameter Effects on Shear Capacity of Masonry Walls”, e-J. New World Sciences Academy 4(3), 340-350, Karadeniz Technical University, Trabzon.
- Usamentiaga Ruben, Venegas Pablo, Guerediaga Jon, Molleda Julio and Bulnes Francisco G. (2014), “Infrared Thermography for Temperature Measurement and Non-Destructive Testing”, Sensors 2014, 14, 12305-12348, doi:10.3390/s140712305, University of Oviedo, Spain.
- Uzunçarşılı İsmail Hakkı. (1929), Kitabeler 2, İstanbul.
- Ünay Ali İhsan. (2002), Tarihi Yapıların Depreme Dayanımı, O.D.T.Ü. Mimarlık Fakültesi, Ankara.
- Vakıflar Genel Müdürlüğü, 2016, “Tarihi Yapılar İçin Deprem Risklerinin Yönetimi Kılavuzu”<https://www.vgm.gov.tr/organizasyonlar/Documents/Sablon+pdf/25/04/2019>.
- Weck Olivier de and Kim Il Yong. (2004), Engineering Design and Rapid Prototyping, Finite Element Method, Massachusetts Institute of Technology, U.S.A.
- Whittow Mark. (1995), “Survey of Medieval Castles of Anatolia: Çardak Kalesi”, Anatolian Archaeology.
- Yalçiner Uğur G., (1997), “Caravanserai”, Arts Encyclopedia, İstanbul.
- Yavuz Ayşıl Tükel. (2007), Akhan’ın Uluslararası Denizli ve Çevresi Tarih ve Kültür Sempozyumu Bildiriler A. Özçelik, M.Y. Ertaş, Y. Kılıç, Y. Avcı, S. İnan, S. Parlaz, Isparta; Fakülte Kitapevi.

Yavuz Aşıl Tükel. (1992), “Anadolu Selçuklu Kervansaraylarında Mekan – İşlev İlişkisi İçinde Savunma ve Barınma”, in IX. Vakıf Haftası Kitabı. eds. İ. Ateş, S. Bayram and M. Narince, Ankara: Vakıflar Genel Müdürlüğü Yayınları, 253-284.

Yavuz Aşıl Tükel. (1997), “The Concepts That Shape Anatolian Seljuk Caravanserais” in Muqarnas.

Yılmaz Pelin. (2006), Tarihi Yapıların Modellenmesi ve Deprem Güvenliklerinin Belirlenmesi, Yüksek Lisans Tezi, Sakarya Üniversitesi, Sakarya.

Zienkiewicz Olgierd Cecil and Taylor Robert Leroy. (1987), “Finite Element Method: Basic Concepts and Linear Applications”, McGraw Hill Book Company; Fourth Edition, Barcelona, Spain.